Chapter 1—Introduction

1.1 Motivation

Consolidation is a phenomenon in, which defines the gradual settlement of soil over a time at a variable rate, under some amount of load. Such settlement is very apparent in clays and sands saturated with water. Consolidation test is performing by applying different load to soil specimen and measuring the deformation corresponds to load. The result of the test is used to predict the soil settlement in the field due to change in effective stress.

Consolidation test are design to analysis the 1-D deformation and drainage condition experience in field. Rigid confining rings are used to prevent lateral displacement. For the purpose of drainage in vertical direction porous stones are provided at top and bottom of sample.

The term "consolidation" was first used by **Thomas Telform** in 1809. Consolidation test were first carried by **Frontard** in 1910. For that purpose he takes the thin soil sample having thickness 2 inch and diameter 14 inch. The sample was placed in metal container with a perforated base. Incremental load is applied by a piston, so that equilibrium will reach after each load increment. Test was performed in a room with high humidity, to prevent the drying of the sample.

Karl Von Terzaghi started his consolidated research at Rebert college (Istanbul) in1919. In 1925, Karl Terzaghi proposed the one-dimensional consolidation theory, where the excess pore water pressure (u), depth within the clay layer (z) and time (t) are related by the following governing differential equation

$$\frac{\partial u}{\partial t} = C_v \frac{\partial^2 u}{\partial z^2}$$

Where Cv is the coefficient of consolidation.

According to Terzaghi (1943), "a decrease in water content of a saturated soil without replacement of the water by air is called consolidation." When clayey soils, which have a low coefficient of permeability, are subjected to a compressive stress due to construction, the pore water pressure will immediately increase; however, because of the low permeability of the soil, there will be a time lag between the application of load and the expulsion of the pore water and thus, the settlement. This phenomenon is called consolidation which is the main theme of present study.

He explained that the grains or particles constituting the soil are more or less bound together by certain molecular forces and constitute a porous material with elastic properties. The voids of that elastic skeleton are filled with water. A load applied to this system will produce a gradual settlement, depending on the rate at which the water is being squeezed out of the voids. Terzaghi applied these concepts to the analysis of the settlement of a column of soil under a constant load and prevented the sample from lateral expansion. This made it a One-Dimensional experiment with only vertical drainage.

However, despite increased interest on the behaviour of soil, little is yet known about the magnitude and characteristics of secondary compression of these deposits. Evaluation of clay layer secondary compression of marshy land is required for estimation of expected total settlement of permanent structure. Moreover, preloading technique through surcharge has been employed with some success as a mean of insitu improvement of engineering properties of clay layer. However, for this technique to be effective the compressibility of the clay layer complex needs to be thoroughly investigated.

In saturated clay, during undrained conditions the applied load at time t = 0 is resisted completely by the pore water. If a drainage conditions exists, then initial pore water pressure dissipates with time leaving the soil, again in a fully saturated state, the consequent reduction in the volume of the soil is approximately equal to the volume of water entering to the free drainage boundaries. The continuous increase in the effective stress at any given time equals to the decrease in the excess pore pressure.

The assumption, along with the continuity conditions of water movement, enables the creation of the necessary equation based on Fourier series that express the development of the consolidation process.

The settlement due to consolidation is the major controlling factor in the design of footings and foundations, some errors had been encountered by assuming consolidation only occurs in vertical direction. Any immediate settlement that occurs on application of the load is estimated using elastic theory.

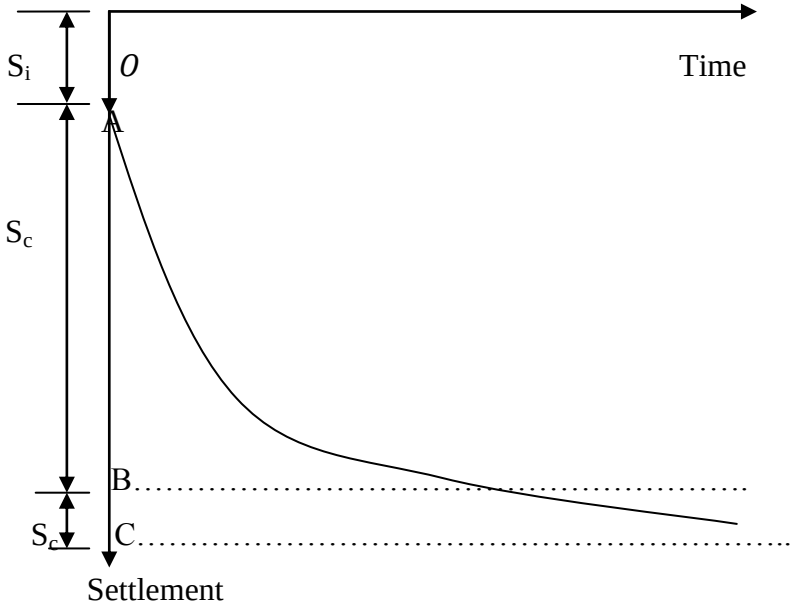

Figure 1.1: Time rate settlement curve for elastic loading

(Courtesy: Soil Mechanics basic concepts, Aysen A 2002 pp 214)

Where,

S_i = immediate settlement

S_c = consolidation settlement

S_g = secondary settlement

Above figure represents typical time settlement relationship for an element of saturated clay during a vertical load increment. The settlement or the vertical compressive deformation of the element is divided in to three segments S_i, S_c, S_g. The time-dependent deformation of saturated clayey soil best can be understood by considering a simple model that consists of a cylinder with a spring at its center.

Some soft soil occurs naturally in poor condition that cannot be worked upon. For example, sandy soils with high sand percentage experience immediate settlement where as soft clay life bentonite has low permeability, settlement is not instantaneous. Settlement will continue for long time period. Both the soil cannot be used for any purpose separately, but it may be useful when mixed in right proportion. When small size particle like bentonite is mixed up to certain limit with

sand in increases the compactness of soil mixture. Further causes increase in dry density of soil, therefore engineering properties of soil also improved.

As the percent of clay mineral increases in the rate of consolidation decreases and the overall settlement of the soil increases. The increase in clay mineral causes the increase in secondary settlement of soil.

The settlement estimation can be done by taking representative soil sample and performing consolidation test on the sample. This settlement analysis for the sample is carried by Fourier analysis. The analysis may also done by analytic method as well as numerical method.

1.2 Major scientists and their contribution

Table 1.1: Major Scientists & their Contribution

Scientists	**Contribution**
Terzaghi's Analysis, 1925	1-D Consolidation
Biot Theory, 1940	3-D Consolidation with restructuring of soil solids
Ji et al., 1948	Obtain quasi-dynamic solution for symmetric consolidation of isotropic soil.
Schiffman, 1958	1-D consolidation theory under time dependant loading where the permeability and coefficient of consolidation vary with time.
Geng et al., 1962	Use of Laplace transforms to obtain solution for non linear 1-D consolidation.
Davis & Raymond, 1965	Relation of permeability of soil with coefficient of consolidation.
Gibson & Hussey, 1967	Analysis of 'rate of consolidation' depending upon thickness of soil strata.
Mikasa et al., 1968	1-D Consolidation theory in terms of compressive strains instead of excess pore pressure..
Booker and Small, 1976	Finite layer analysis technique for 2-D and 3-D consolidation of multilayered soils.

Oslon.et al., 1977	Incorporate Ramp loading as mode of load application in 1-D consolidation.
Cai et al., 1981	Semi analytical 1-D consolidation solution with variation of cyclically loaded soil compressibility.
Senjuntichai and Rajapakse, 1989	Solution for consolidation of multilayered soils by an exact stiffness method in the cylindrical coordinate system.
Sridharan et al., 1995	Analysis of Time factor for secondary consolidation of extremely clayey soil.
Wang and Fang, 2001	Analysis of Biot consolidation problem for multilayerd porous media by a state space method in cylindrical coordinate system.
Trivedi et.al (2004)	Collapsible behaviour of coal ash.
Conte et al., 2006	Analysis of coupled consolidation of unsaturated soil under plain strain loading.
Rani et al., 2011	Consolidation of mechanically isotropic but hydraulically anisotropic clay layer incorporating compression of pore fluid and solid constituents.
Vinod et al., 2010	Cross section range of fast loading for radial consolidation.
Tewatia et al., 2012	Quick and fast loading methodology to guage/measure rate of consolidation of primary as well as secondary processes.
Trivedi et.al (2014)	Consolidation of clayey gouge amid permeating rock mass

1.3 Objective of study

The objective of the study is towards understanding of consolidation behaviour of bentonite sand mixture By increasing the percentage of bentonite deformation of sample increases and the rate of consolidation decreases. This study represents how the variation of consolidation behaviour increases by increasing the clay minerals

in soil. The sand bentonite mixture with different percentage of bentonite mix shows large variation in consolidation behaviour, which is helpful in a comparison analysis by different method.

These thin samples are consolidated to achieve final settlement either by Biot theory or by Terzaghi theory. When a soil layer is subjected to a compressive stress, such as during the construction of a structure, it will exhibit a certain amount of compression. The settlement due to consolidation is the major controlling factor in the design of footings and foundations.

The main objective is investigate the effect of compressibility on excess pore pressure, void ratio in sample, coefficient of consolidation, degree of consolidation, drainage boundary on bentonite sand mixture. The rate of consolidation is compared for different percentage of bentonite. The settlement of sample is compared for different loading and different percentage of bentonite content. The variation of void ratio with effective stress is compare for different percent of bentonite in mix. The variation of coefficient of consolidation with is studied for different loading condition and different bentonite percent. The variation of drainage characteristic with loading condition is also analysed.

The degree of consolidation is estimated by traditional Fourier solution. This solution is compared with numerical solution by explicit method. Degree of consolidation is also estimate by implicit method and compared for different time step. The Fourier solution of consolidation of soil is tedious and complex procedure, numerical solution gives simple and more accurate result.

1.4 Organisation of report

Chapter 1 It provides the introduction to the consolidation process, how it occurs and factors on which it depends. Chapter basically deals with the mechanism of the consolidation process and settlement that took place as a result of the same. It also gives the information about settlement of soil and its behaviour during load application. This chapter also gives idea about the objective of the project work.

Chapter 2 Describes about the literature reviews of various methods and techniques that are carried out by renowned researchers in past few decades for

determination of rate of consolidation. Various researches had been carried out in determination of 3-dimensional consolidation.

Chapter 3 It deals about Fourier anslyses and the numerical analyses that are to be used for determination of rate of consolidation. Precise and clear vision had been given about the applicability for numerical solution.

Chapter 4 Discussed about the experiments that has been conducted on different sets of sample, along with different engineering properties of soil that are determined in the laboratory. All the experiments are performed according to I.S. Codes.

Chapter 5 In this chapter result and validation are correlated at different condition. Numerical solutions (finite difference, explicit method) are compared with Fourier solution based on data obtained in laboratory. Implicit solution at different time step is also compared.

Chapter 6 This part includes the conclusion part of the project work along with limitations that arouses in numerical as well as experimental technique.

The last part contains an account of several research publications has been made, which we had referred during study.

Chapter 2—Literature Review

2.1 Literature review

Consolidation is likely to be linked to the changes in effective stress, which result from the changes in pore-water pressure as seepage flow progresses toward the drainage boundaries. Upon application of an external load, there is an initial increase in the pore-water pressure throughout the sample known as the initial excess pore water distribution. According to Darcy's law, the excess pore water pressures i.e., pressures in excess of hydrostatic are the driving force of seepage flow.

Consolidation studies for soil were first carried out by **Terzaghi**. According to Karl von **Terzaghi (1925**) "consolidation is any process which involves decrease in water content of a saturated soil without replacement of water by air. If the soil skeleton and the pore fluids in the soil pore space assumed incompressible, the total volume change in the soil due to load will occur due to squeezing of pore fluid out of soil skeleton known as consolidation. As squeezing proceeds, soil grains rearrange themselves into a more stable and denser configuration and decrease in volume and surface settlements results.

M. A. Boit (1940) introduced a general theory on Three-Dimensional consolidation, which considered forces acting on the soil from all directions and also settlement due to shear deformation. Consolidation theory was originally developed by Terzaghi for the one dimensional case, and therein, exclusively considered vertical stress and strain, and neglected horizontal effects. Biot later extended Terzaghi's theory to two- and three-dimensional saturated soils. Biot's reformalization of Terzaghi's theory is also contemporarily referred to as the true two- or three-dimensional consolidation theory, as it permits the total stress to be varied as a function of time during the consolidation process. Both theories assume that loading is instantaneously applied and maintained constant as a function of time; however, realistic loadings in construction are usually applied gradually as a function of time.

Gray (1945) presented solutions for a system of two contiguous clay layers with either permeable or impermeable external boundaries. The solution is obtained by applying Terzaghi's differential equation within each layer and formulating a continuity relation at the interface between the two layers. The solution requires that there be a single excess pore-water pressure at the interface and that the flow q from one layer must be equal to the flow into the other layer.

Mikasa (1963) derived a 1D consolidation equation for a saturated clay having homogeneous consolidation properties throughout its depth, one that is in terms of compression strain in place of excess pore pressure by the Terzaghi equation. In consideration of the various assumptions and limitations of the Terzaghi theory, a more advanced and generalized formulation had been presented for the case of finite strains, nonlinear consolidation parameters, and consideration of self-weight effects on consolidation.

Barden and Berry (1965) and Mesri and Rokhsar (1974) solved the consolidation problem for constant loading by means of the finite difference method; in which the commonly accepted e-log effective stress and e-log permeability laws were employed.

Studies of **Taylor and Merchant (1940), Hansen (1961), Christic (1965) and Martins and Lacerda (1985)** showed that the primary consolidation and secondary consolidation occur concurrently. However, **Mitchell (1993) and Naatan et al (1995**) reported that the secondary consolidation starts when 90-95% of primary consolidation has taken place.

Abid & Pyrah (1988) presented some guidelines for using the finite-element (FE) method to predict 1D consolidation behaviour using both diffusion and coupled approaches. First computer program for finite difference solution of consolidation was given by **Terry Howard** at the University of California, Berkeley in **1970**. The program was then modified by **Wong** from 1979 through 1983. The current version of the program **(CONSOL Version 3.0**), was developed by **Tan (2003).** There is a comprehensive literature on Eigen problems, **Hoffman (1992)** and many software programs exist to solve them. Eigen problems can be easily solved with MS Excel **Volpi (2005)** and FORTRAN, **Anderson et al., (1999).**

Wang et al (2002) presented an algorithm to solve Biot's consolidation problem using meshless method called RPIM. Two variables in Biot's consolidation theory, displacement and excess pore water pressure, were spatially approximated by the same shape functions through the radial PIM technique.

Jim et al (2008) used explicit and implicit techniques for computing 1D consolidation in layered soils. They stated that the explicit approach used gives accurate results in early stages of consolidation and implicit approach is accurate for later times.

Rujikiatkamjorn et al., (2008) conducted both two-dimensional and three-dimensional numerical analyses of a combined vacuum and surcharge preloading system, using the finite-element code ABAQUS and the modified Cam-clay model. A numerical model based on dual-Lagrangian framework was presented by **Fox and Lee, (2008)** for analysis of coupled large strain consolidation and solute transport in saturated porous media.

Julie Lovisa et. al (2010) estimate the consolidation behavior of a soil stratum subjected to various initial excess pore pressure distributions which occur under one-dimensional loading. He showed that analysis in terms of average degree of consolidation provides an incomplete representation of the consolidation behavior. While the average degree of consolidation curves for all uniform and linearly varying initial distributions are identical, the degree of consolidation isochrones for each distribution is unique. **Huang and Griffith (2010)** used the Finite element modelling for comparing 1-D consolidation in layered soils for coupled and uncoupled situations of pore water pressure and settlement.

Hyeong-Joo Kim et.al (**2011)** Numerical Analysis of One-Dimensional Consolidation in Layered Clay Using Interface Boundary Relations in Terms of Infinitesimal Strain The interface boundary relations are derived in this study for the numerical analysis of one dimensional consolidation in multilayered clay profiles. Numerical examples are presented for multilayer clay profiles under single

and double drainage conditions that validate the predicted excess pore pressures, strains, settlements, and rates of consolidation using interface boundary relations in terms of infinitesimal strains that are equivalent to those expressed in terms of excess pore pressures.

Rani (2011) studied the consolidation of a mechanically isotropic but hydraulically anisotropic clay layer subjected to axi-symmetric surface loads, allowing for compressibility of the pore fluid and solid constituents. Soil consolidation is often caused by external loadings, such as in building or embankment construction on clayey soil.

Robinson gives the approach for analysis of starting of secondary consolidation. **Sudhir et.al(2003)** analysed the beginning of secondary given by R. G. Robinson. They represent the secondary consolidation by hyperbolic model. They develop the method which separates the secondary from primary consolidation.

Trivedi et.al (2004) conducted extensive study on the collapsible behaviour of coal ash to examine the factors influencing the collapse settlement of compacted coal ash due to wetting. This study with proper assumptions can be used for collapsible soils as well.

Recently, **Trivedi et al (2014)** studied the effect of clayey gouge in a permeating rock mass. They derived an expression for 1-D consolidation in 2-D drainage. They introduced a dimensionless ration constant r, which is a function of shape factor and rock mass characteristics.

Chapter 3—General Theory and Application

3.1 Differential equation for one dimensional consolidation with vertical drainage

The one-dimensional consolidation theory was first proposed by Terzaghi (1925).In the case of one-dimensional consolidation the flow of water through soil occurs only in one direction. Considering the direction of flow of water through z direction only. Then q_x, q_y, dq_x and dq_y are equal to zero, and thus the rate of flow of water through soil element is given by:

$$(q_z + dq_z) - q_z = \text{rate of change of volume of soil element} = \frac{\partial V}{\partial t} \quad (1)$$

Here,

$$V = dx\, dy\, dz \quad (2)$$

Writing above equation in form of coefficient of permeability $[k = k_z]$ as

$$k \frac{\partial^2 h}{\partial z^2}\, dx\, dy\, dz = \frac{\partial V}{\partial t} \quad (3)$$

Also,

$$h = \frac{u}{\gamma_w} \quad (4)$$

$$\frac{k}{\gamma_w} \frac{\partial^2 u}{\partial z^2} = \frac{1}{dx\, dy\, dz} \frac{\partial V}{\partial t} \quad (5)$$

During consolidation the rate of change of volume is equal to the rate of change of the void volume. So,

$$\frac{\partial V}{\partial t} = \frac{\partial V_v}{\partial t} \quad (6)$$

Here, V_v represent volume of voids in the soil element and

$$V_v = eV_s \quad (7)$$

Here V_s represents volume of soil solids in the element, therefore

$$\frac{dV}{dt} = V_s \frac{\partial e}{\partial t} = \frac{V}{1+e}\frac{\partial e}{\partial t} = \frac{dx\, dy\, dz}{1+e}\frac{\partial e}{\partial t} \tag{8}$$

Substituting the above relation into equation (5), we get

$$\frac{k}{\gamma_w}\frac{\partial^2 u}{\partial z^2} = \frac{1}{1+e}\frac{\partial e}{\partial t} \tag{9}$$

The change in void ratio,∂e, is due to the increase of effective stress; assuming that these are linearly related, then

$$\partial e = -a_v \partial(\Delta\sigma') \tag{10}$$

Here a_v represents coefficient of compressibility, then

$$\partial e = a_v \partial u \tag{11}$$

Combining equations (9) and (11),

$$\frac{k}{\gamma_w}\frac{\partial^2 u}{\partial z^2} = \frac{a_v}{1+e}\frac{\partial u}{\partial t} = m_v \frac{\partial u}{\partial t} \tag{12}$$

Where,

$$m_v = \text{coefficient of volume compressibility} = \frac{\partial v}{1+e} \tag{13}$$

Or,

$$\frac{\partial u}{\partial t} = \frac{k}{m_v \gamma_w \partial z_2} = C_v \frac{\partial^2 u}{\partial z^2} \tag{14}$$

Where,

$$C_v = coefficient\ of\ consolidation = \frac{k}{m_v \gamma_w} \tag{15}$$

Equation (14) represent the basic differential equation of Terzaghi's consolidation theory here u is the product of a function of z and a function of t. Hence

$$u = F(z)G(t) \tag{16}$$

So,

$$\frac{\partial u}{\partial t} = F(z)\frac{\partial}{\partial t}G(t) = F(z)\ G'(t) \tag{17}$$

And,

$$\frac{\partial^2 u}{\partial z^2} = \frac{\partial^2}{\partial z^2}F(z)G(t) = F''(z)G(t) \tag{18}$$

From equations (14), (17), and (18),

$$F(z)\ G'(t) = C_v F''(z)G(t) \tag{19}$$

The right part of above equation is a function of z only and independent of t; the left part of equation is a function of t only and independent of z. Therefore,

$$F''(z) = -B^2\ F(z) \tag{20}$$

A solution to equation (20) can be given by

$$F(z) = A_1 \cos Bz + A_2 \sin Bz \tag{21}$$

Where $A_1$and A_2 are constants.

Also, the right-hand side of equation (19) can be written as

$$G'(t) = -B^2 C_v G(t) \tag{22}$$

The solution to equation (22) is given by

$$G(t) = A_3 \exp(-B^2 C_v t) \tag{23}$$

Where A_3 is a constant. Combining equations (16), (21), and (23),

$$u = (A_1 \cos Bz + A_2 \sin Bz)\ A_3 \exp(-B^2 C_v t)$$

$$= (A_4 \cos Bz + A_5 \sin Bz) \exp(-B^2 C_v t) \quad (24)$$

Where, $A_4 = A_1 A_3$ and $A_5 = A_2 A_3$

The constants in equation (24) may be obtain from the boundary condition can be evaluated from the boundary conditions, which are as follows:

1. At $t = 0, u = u_t$.
2. $u = 0$ at $z = 0$
3. $u = 0$ at $z = H_t = 2H$.

H is the length of the drainage path, then from third boundary condition

$$A_5 \sin 2BH = 0 \quad or \quad 2BH = n\pi$$

Where *n* is an integer. Then, a general solution of equation (24) can be in given as

$$u = \sum_{n=1}^{\infty} A_n \sin \frac{n\pi z}{2H} \exp\left(\frac{-n^2\pi^2 T_v}{4}\right) \quad (25)$$

Where $T_v = C_v t/H^2$ is the nondimensional time factor

To satisfy the first boundary condition, we must have the coefficients of A_n such that

$$u_t = \sum_{n=1}^{\infty} A_n \sin \frac{n\pi z}{2H} \quad (26)$$

Equation (26) is a Fourier sine series, and A_n can be given by

$$A_n = \frac{1}{H} \int_0^{2H} u_t \sin \frac{n\pi z}{2H} \, dz \quad (27)$$

Combining equations (25) and (27),

$$u = \sum_{n=1}^{\infty} \left(\frac{1}{H} \int_0^{2H} u_t \sin \frac{n\pi z}{2H} \, dz \right) \sin \frac{n\pi z}{2H} \exp\left(\frac{-n^2\pi^2 T_v}{4}\right) \quad (28)$$

So far we have not made any assumptions regarding the variation of u_t with the depth several possible types of variation for u_t may considered.

Constant u_t with depth. i.e., $u_t = u_0$ if (Figure 3.1) – referring to equation (28),

$\frac{1}{H}\int_0^{2H} u_t \sin\frac{n\pi z}{2H}\, dz = \frac{2u_0}{n\pi}(1-\cos n\pi)$ So,

$$u = \sum_{n=1}^{\infty} \frac{2u_0}{n\pi}(1-\cos n\pi)\sin\frac{n\pi z}{2H}\exp\left(\frac{-n^2\pi^2 T_v}{4}\right) \qquad (29)$$

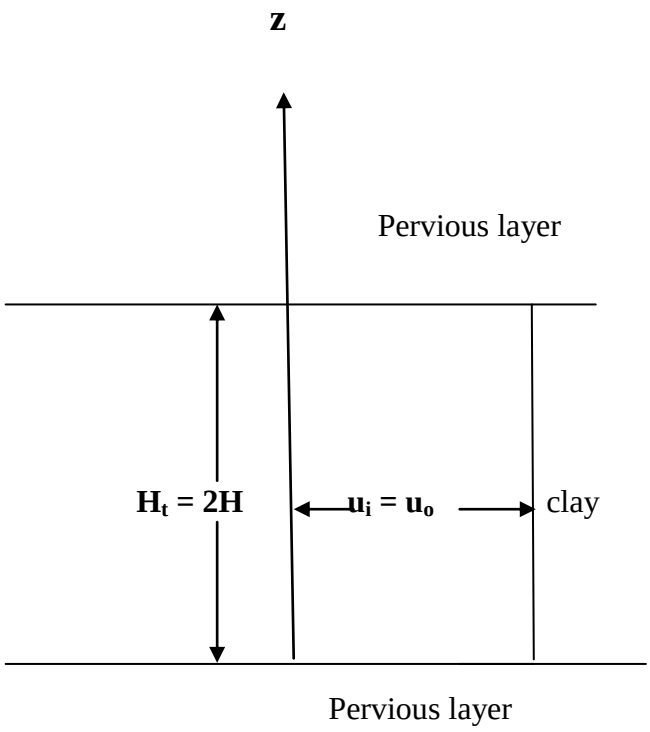

Figure 3.1: Constant excess pore water pressure with depth at time t=0 (double drainage)

If n is even, then $(1-\cos n\pi) = 0$. So, u is also zero. For the nonzero terms substituting $n = 2m+1$ where m is an integer. So equation (29) will be

$$u = \sum_{m=0}^{\infty} \frac{2u_0}{(2m+1)\pi}[1-\cos(2m+1)\pi]\sin\frac{(2m+1)\pi z}{2H}\exp\left[\frac{-(2m+1)^2\pi^2 T_v}{4}\right]$$

Or,

$$u = \sum_{m=0}^{\infty} \frac{u_0}{M}[1-\cos 2M]\sin\frac{M\pi z}{H}\exp(-M^2 T_v) \qquad (30)$$

Where M= $(2m+1)\pi/2$.

Now the degree of consolidation at any depth z is defined as

$$U_z = \frac{excess\ pore\ water\ pressure\ dissipated}{initial\ excess\ pore\ water\ pressure}$$

$$= \frac{u_0 - u}{u_0} = \frac{\sigma'}{u_0} \tag{31}$$

Where σ' is the increase of effective stress at a depth z due to consolidation. From equations (30) and (31),

$$U_z = 1 - \sum_{m=0}^{\infty} \frac{2}{M} \sin \frac{Mz}{H} \exp\left(-M^2 T_v\right) \tag{32}$$

Figure 3.2 shows the variation of U_z with depth for various values of the non-dimensional time factor, T_v; these curves are called isochrones.

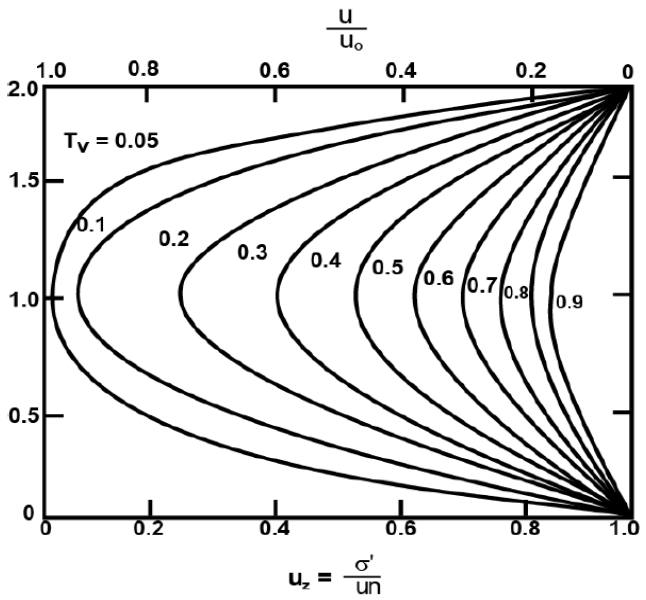

Figure 3.2: Variation of U_z with $^{z}/_{H}$ and T_v

(Courtesy: Soil Mechanics basic concepts, Aysen A 2002 pp 228)

In most cases, however, we need to obtain the average degree of consolidation for the entire layer. This is given by

$$U_{av} = \frac{(1/H_t)\int_0^{H_t} u_t dz - (1/H_t)\int_0^{H_t} u\, dz}{(1/H_t)\int_0^{H_t} u_t dz} \tag{33}$$

The average degree of consolidation is also the ratio of consolidation settlement at any time to maximum consolidation settlement. Note, in this case, that $H_t = 2H$ and $u_t = u_0$.

Combining equations (30) and (33),

$$U_{av} = 1 - \sum_{m=0}^{\infty} \frac{2}{M^2} \exp(-M^2 T_v) \qquad (34)$$

Fig 4 gives the variation of U_{av} vs. T_v

Terzaghi suggested the following equations for U_{av} to approximate the values obtained from equation (34):

$For,\ U_{av} = 0 - 53\%$:

$$T_v = \frac{\pi}{4}\left(\frac{U\%}{100}\right)^2 \qquad (35)$$

$For, \quad U_{av} = 53 - 100\%: \quad T_v$

$$= 1.78 - 0.933[\log (100 - U\%)] \qquad (36)$$

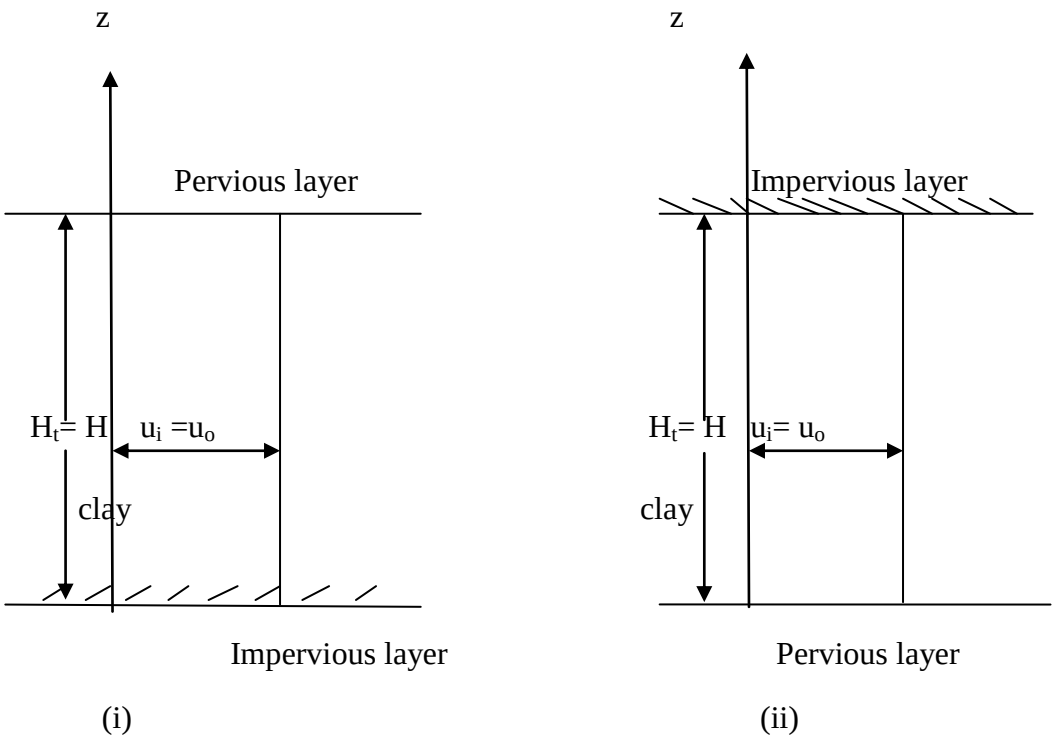

Figure 3.3: : Constant excess pore water pressure with depth at time t=0 (one way drainage)

Linear variation of u_i . The variation in initial excess pore water pressure, can be expressed as

$$u_t = u_1 - u_2 \frac{H - z}{H} \tag{37}$$

Substitution of u_t in equation (28)

$$u = \sum_{n=1}^{\infty} \left[\frac{1}{H} \int_0^{2H} \left(u_1 - u_2 \frac{H - z}{H} \right) \sin \frac{n\pi z}{2H} dz \right] \sin \frac{n\pi z}{2H} \exp \left(\frac{-n^2 \pi^2 T_v}{4} \right) \tag{38}$$

The average degree of consolidation can be obtained by solving equations (38) and 33):

$$U_{av} = 1 - \sum_{m=0}^{\infty} \frac{2}{M^2} \exp(-M^2 T_v) \tag{39}$$

Sinusoidal variation of u_t. Sinusoidal variation can be expressed in form of equation as:

$$u_t = u_3 \sin \frac{\pi z}{2H} \tag{40}$$

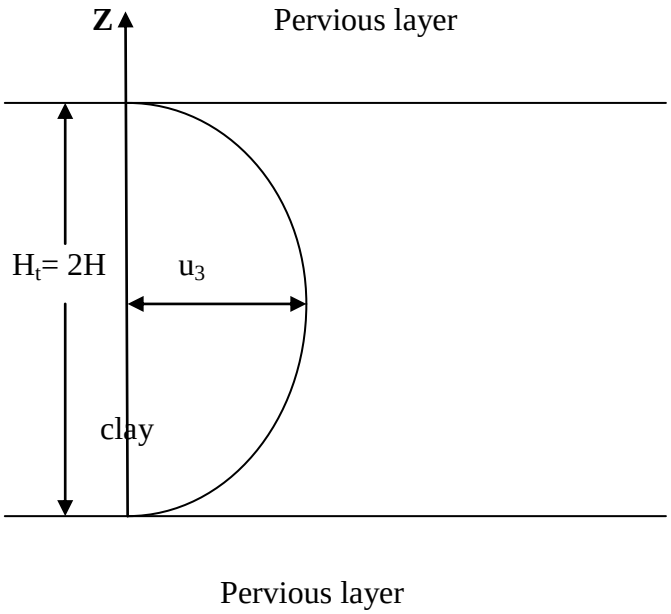

Figure 3.4: Sinusoidal variation of pore water pressure (two-way drainage)

The solution for the average degree of consolidation for this type of excess pore water pressure distribution is of the form

$$U_{av} = 11 - \exp\left(\frac{-\pi^2 T_v}{4}\right) \quad (41)$$

3.2 Finite difference method

For the time dependent problems, there is considerable development in finite difference method during the period of Second World War. But the application to practice problem possible only after the development of computer aid system. A major role was played by Von Neumann.

In numerical analysis, the **FTCS** (Forward-Time Central-Space) method is a finite difference method used for numerically solving the heat equation and similar parabolic partial differential equations. It is a first-order method in time, explicit in time, and is conditionally stable when applied to the parabolic equations.

The FTCS method is based on central difference in space and the forward Euler method in time, giving first-order convergence in time and second-order convergence in space. For example, in one dimension, if the partial differential equation is

$$\frac{\partial u}{\partial t} = F(u, x, t, \frac{\partial^2 u}{\partial x^2})$$

Therefore, $u(i\Delta x, n\Delta t) = u_i^n$, and forward Eular method is given as:

$$\frac{u_i^{n+1} - u_i^n}{t} = F_i^n(u, x, t, \frac{\partial^2 u}{\partial x^2})$$

The function *F* must be discretized spatially with a central difference scheme. This is an explicit method which means that, u_i^{n+1} can be explicitly computed (no need of solving a system of algebraic equations). FTCS method is computationally inexpensive since the method is explicit.

The FTCS method, for one-dimensional equations, is numerically stable if and only if the following condition is satisfied:

$$r = \frac{\alpha \Delta t}{\Delta x^2} \leq \frac{1}{2}$$

3.3 Solution of 1-d consolidation equation using finite difference method

Vertical consolidation is dictated by Terzaghi's 1D consolidation equation. A finite difference approach can be used to solve for the pore pressure.

If the problem domain is discretized in time and space as shown in Figure 3.2, equation for 1-D consolidation can be rewritten as: (Hazzard et al.)

$$\frac{\partial u}{\partial t} = \frac{u_{i,t+\Delta t} - u_{i,t}}{\Delta t} \qquad (42)$$

$$c_v \frac{\partial^2 y}{\partial x^2} = (1-\varnothing)\{ \frac{c_v}{(\Delta h)^2} [\, u_{i-1,t} - 2u_{i,t} + u_{i+1,t} \,]\} + \varnothing\{ \frac{c_v}{(\Delta h)^2} [\, u_{i-1,t+\Delta t} - 2u_{i,t+\Delta t} + u_{i+1,t+\Delta t} \,]\} \qquad (43)$$

Where Φ is the time weighing parameter

The finite difference method consist of substituting finite ranges for the differential in, factoring the resulting equation into a form suitable for analysis, stabling rules to ensure that the method of solution is stable and achieve a solution

The solution has 2 steps:

1. The excess pore water pressure is calculated at a series of points, (nodes), which are distributed vertically throughout the deposit, at a series of times.
2. The effective stresses, average degree of consolidation, and settlement are calculated from the known total stresses and pore-water pressure.

In this method the solution is evaluated at a number of points at different times as indicated on the figure 8 below.

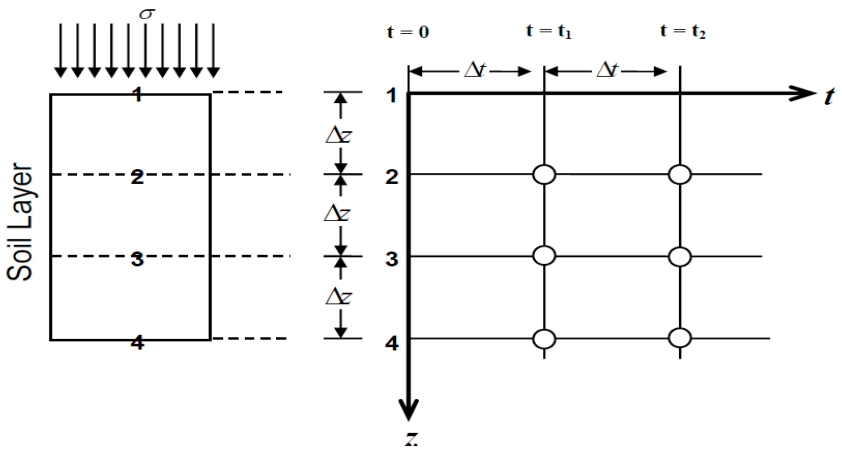

Figure 3.5: Discretization of space and time

(Courtesy: GeoEdmonton'08/GéoEdmonton2008)

The explicit solution uses a value of $\Phi = 0$ and calculates the pressure at time $t+\Delta t$ for each node sequentially. Initial excess pore pressures at time t are calculated for all nodes based on the applied stress. The pore pressure at time $t+\Delta t$ for node i is then calculated by setting f = 0 in equation (3.33) and rearranging to give:

$$U_{i,t+\Delta t} = u_{i,t} + \frac{c_v.\Delta t}{(\Delta h)^2}(u_{i-1,t} - 2u_{i,t} + u_{i+1,t}) \quad (44)$$

A constraint of the explicit solution is that the time-step, Δt, must be small for stability of solution:

$$\Delta t < \beta \frac{\Delta h^2}{c_v}$$

where β is a dimensionless factor which is less than 0.5.

For implicit solution

$$u_{i,t+\Delta t} = \frac{u_{i,t} + \frac{c_v}{(\Delta h)^2}\Delta t(u_{i-1,t+\Delta t} + u_{i+1,t+\Delta t})}{1+2c_v\Delta t/(\Delta h)^2} \quad (45)$$

The Implict solution is unconditionally stable for any time step. Implicit analysis is performed for large strain problems. It gives oscillatory results for small strain problems.The solution for pressure for a given position at time $t+\Delta t$ depends on the pressures at adjacent locations at $t+\Delta t$. Therefore the the equation must be solved either by iterating solution or by simultaneously solving for all pressures at Δt using matrix inversion. If the solution is obtained by iterative method the accuracy of result also depends on the number of iteration. For better result the large number of iteration are taken.

Chapter 4—Materials and Methodology

4.1 Material

The specimen soil was bentonite and sand. Bentonite specimen was purchase from N.K Enterprise, Industrial estate, Okhla Phase- III. Sand was taken from DTU passing 600µm and retaining on 300µm. Laboratory tests to determine various index and engineering properties of bentonite and sand were conducted according to Indian Standard methods of testing.

4.2 List of experiment done

The experimental work consists of the following steps:

1. Specific gravity of bentonite and sand mix.
2. Hydrometer test.
3. Determination of Atterberg Limits

i) Liquid limit by Casagrande's apparatus

ii) Plastic limit

4. Determination of consolidation properties of bentonite.

4.2.1 Specific gravity [IS:2720 (Part III)]

The specific gravity of soil is the ratio between the weight of the soil solids and weight of equal volume of water. It is measured by the help of a volumetric flask in a very simple experimental setup where the volume of the soil is found out and its weight is divided by the weight of equal volume of water.

$$G = \frac{W2 - W1}{[(W2 - W1) - (W3 - W4)]}$$

W1 = Weight of bottle in grams

W2 = Weight of bottle + Dry soil in grams

W3 = Weight of bottle + Soil + Water

W4 = Weight of bottle + Water

Specific gravity of all 5 samples is determined separately, i.e specific gravity of sample with 10%, 15%, 20%, 25%, and 100% bentonite content is determined. Oven dry bentonite and sand are taken as per their percentage in mix and then mix thoroughly. After that the sample is taken for test purpose.

4.2.2 Hydrometer test [IS:2720 (Part IV)]

The hydrometer method is based on the measurement of velocity of soil particles in a sedimentation solution and the dry mass of soil in the solution in different intervals of time. The velocity of falling particles and dry mass of soil at a specific depth are measured by a hydrometer. The results are combined with Stokes' law, which gives the relation between velocity of a spherical particle and its diameter while settling within its solution. The tests are carried out according to procedure mentioned inn IS 2720 Part 4 1985.

Figure 4.1: Grain size analysis through hydrometer

4.2.3 Liquid limit and plastic limit determination

4.2.3 (i) Liquid limit determination [IS: 2720 (Part V)]

Theoretical background

Liquid limit is the minimum water content at which the soil is still in liquid state but has a small shearing strength against flowing. In other words it is the water content at which soil suspension gains an infinitesimal strength from zero strength. In the standard liquid limit apparatus from practical purposes, it is the minimum water content at which part of soil cut by groove of standard dimensions, will flow together for as a distance of 12 mm (1/2 inch) under an impact of 25 blows**.** Plot

the flow curve on semi log graph water content as the ordinate and no. of blows as abscissa. The water content corresponding to 25 blows is taken as the liquid limit of the soil.

Figure 4.2:- Liquid Limit Apparatus

4.2.3 (ii) Plastic limit determination [IS:2720 (Part V)] Plastic limit is the minimum water content at which a soil just deigns to crumble when rolled into a thread of 3 mm in diameter. This water content in is between the plastic and semi-soil states of soil.

4.2.4 Consolidation by odeometer [IS 2720(part 15)]

The process of compression resulting from long term steady load and gradual reduction of pore space by escaping of pore water is termed as consolidation. The permeability of an undisturbed sample of clay is determined directly at several different void ratios while running a consolidation test.

Figure 4.3:- Consolidation Ring

Figure 4.4:- Consolidometer Test Apparatus at loading

The sample is prepared by mixing the bentonite and sand percentage by weight and they are mixed thoroughly in dry condition then water is added in mix. Then test is performed as IS 2720(part 15). The usual loading intensity which has been adopted are as follows: 10, 20, 40, 80, 160, 320 and 640 kN/m^2 . The load increment ration is taken as one. At this increment load ratio of load secondary consolidation starts after 90% degree of consolidation.

Chapter 5—Experimental and Numerical Result and Comparison

5.1 Specific gravity result

Table 5.1:- Specific gravity value at different percent of bentonite in mix.

Sl. No.	Sample (sand bentonite mixture) with different bentonite percent	Specific gravity
1	10% bentonite content	2.635
2	15% bentonite content	2.615
3	20% bentonite content	2.596
4	25% bentonite content	2.577
5	100% bentonite content	2.318

.

5.2 Liquid limit and plastic limit of bentonite

5.2.1 Liquid Limit

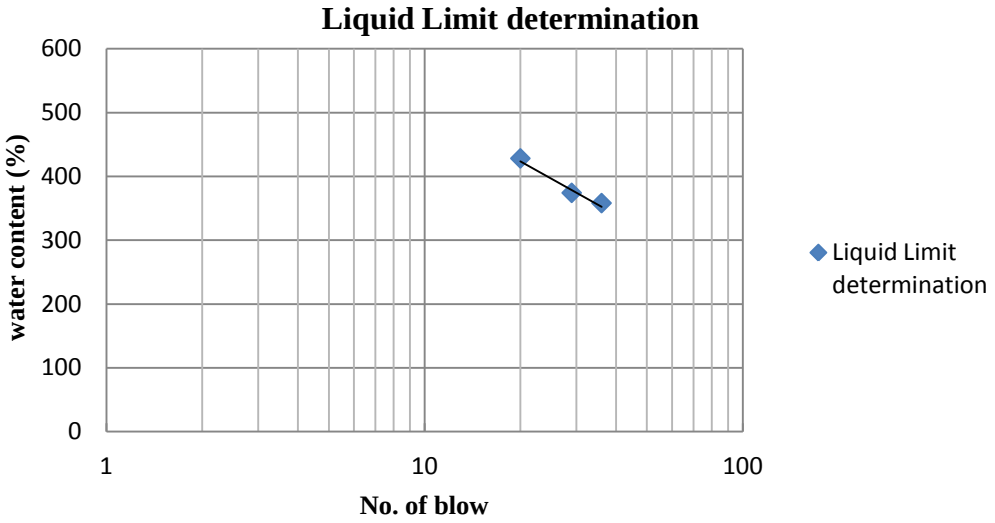

Graph 5.1:- Liquid limit determination of bentonite

Liquid Limit = 386%

5.2.2 Plastic Limit:-

Plastic Limit of bentonite sample = **111.48%**

5.3 Grain size distribution of bentonite

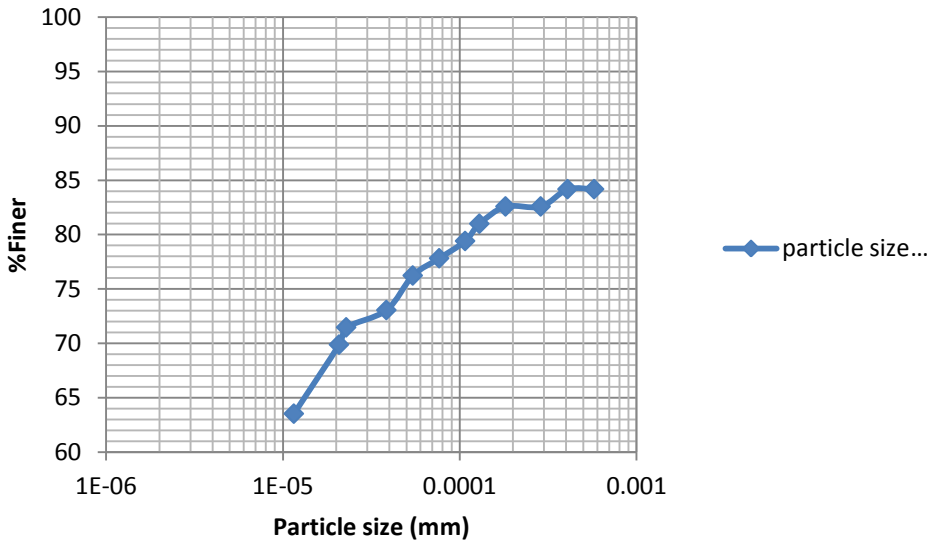

Graph 5.2:- Grain size distribution of bentonite

5.4 Comparison of parameter at different conditions

5.4.1 Dial gauge reading Vs time plot for different stress increment at 10% bentonite content:-

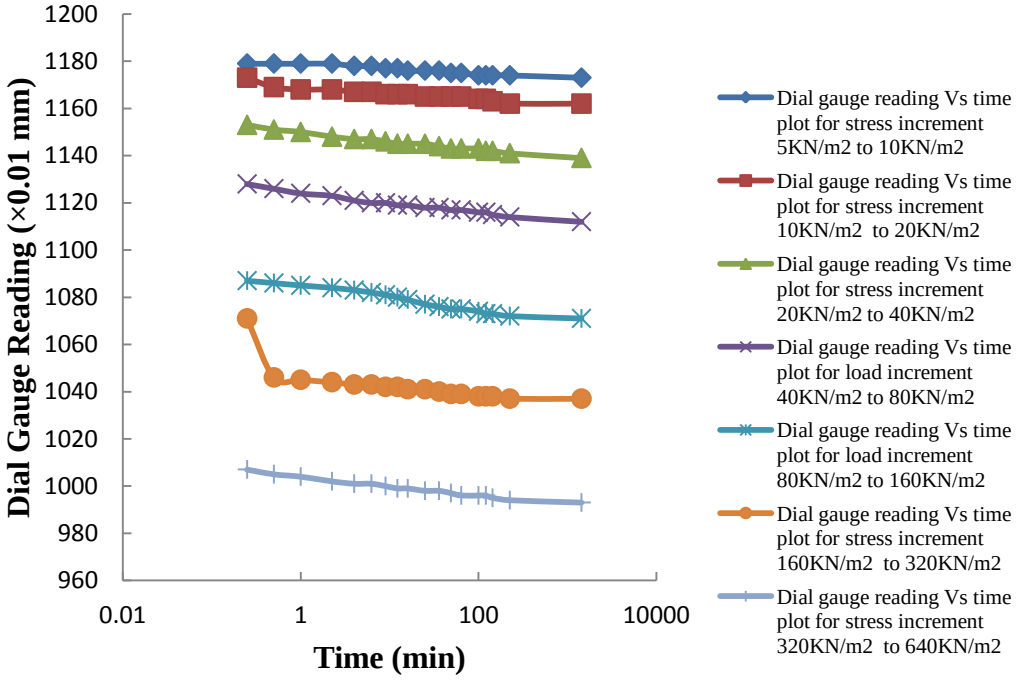

Graph 5.3:- Dial gauge reading Vs time plot for different stress increment at 10% bentonite content.

5.4.2 Dial gauge reading Vs time plot for different stress increment at 15% bentonite content:-

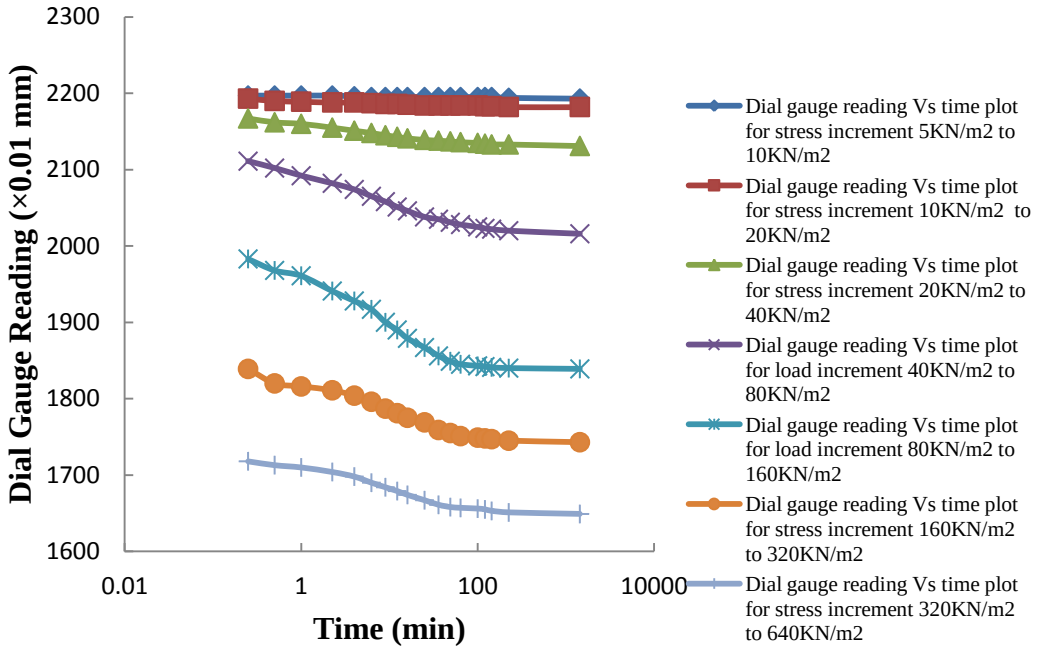

Graph 5.4:- Dial gauge reading Vs time plot for different stress increment at 15% bentonite content.

5.4.3 Dial gauge reading Vs time plot for different stress increment at 20% bentonite content:-

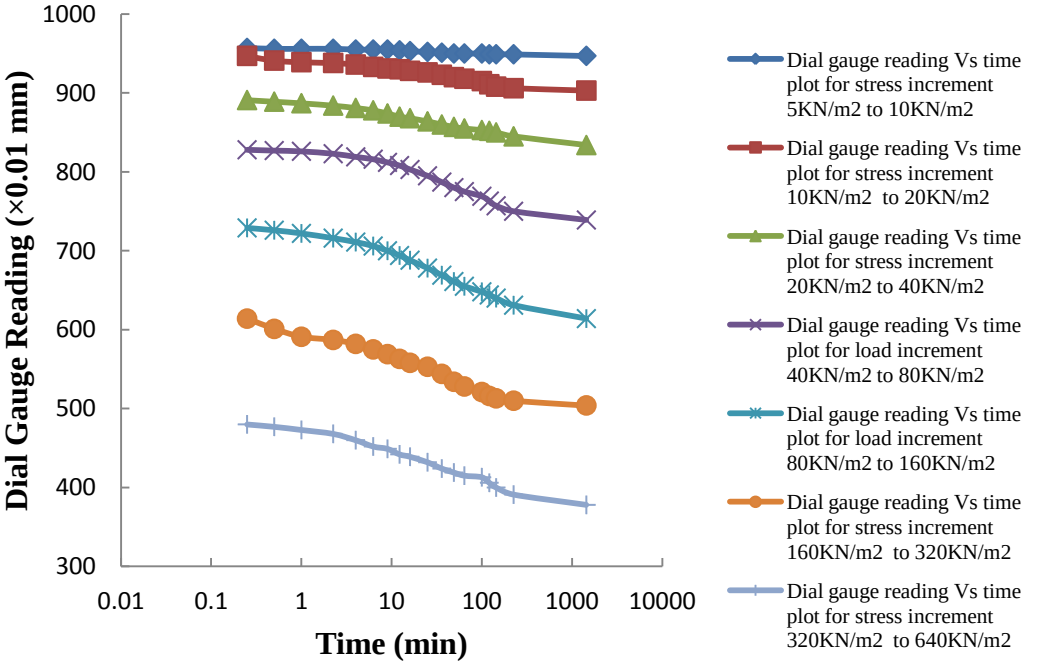

Graph 5.5:- Dial gauge reading Vs time plot for different stress increment at 20% bentonite content.

5.4.4 Dial gauge reading Vs time plot for different stress increment at 25% bentonite content:-

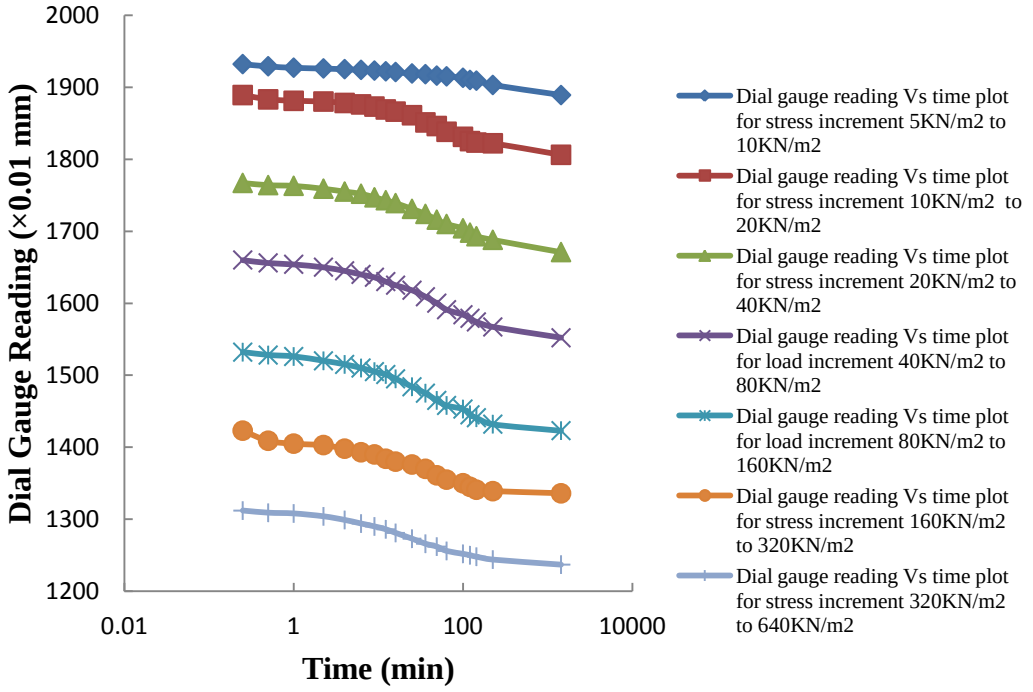

Graph 5.6:- Dial gauge reading Vs time plot for different stress increment at 25% bentonite content.

5.4.5 Dial gauge reading Vs time plot for different stress increment at 100% bentonite content:-

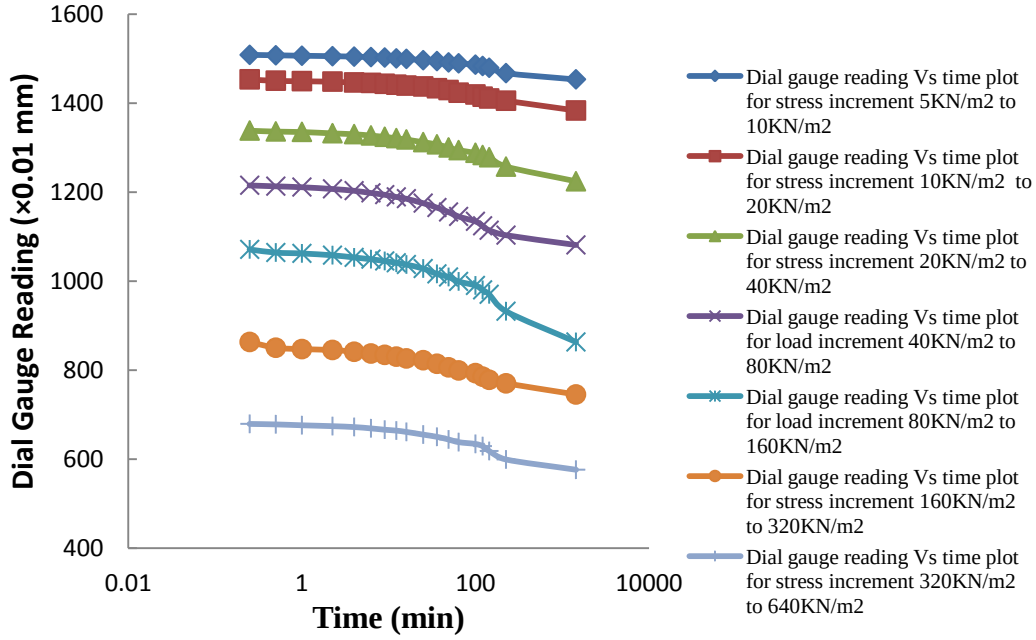

Graph 5.7:- Dial gauge reading Vs time plot for different stress increment at 100% bentonite content.

5.4.6 Comparison of Void ratio (e) Vs log σ plot for different mix:-

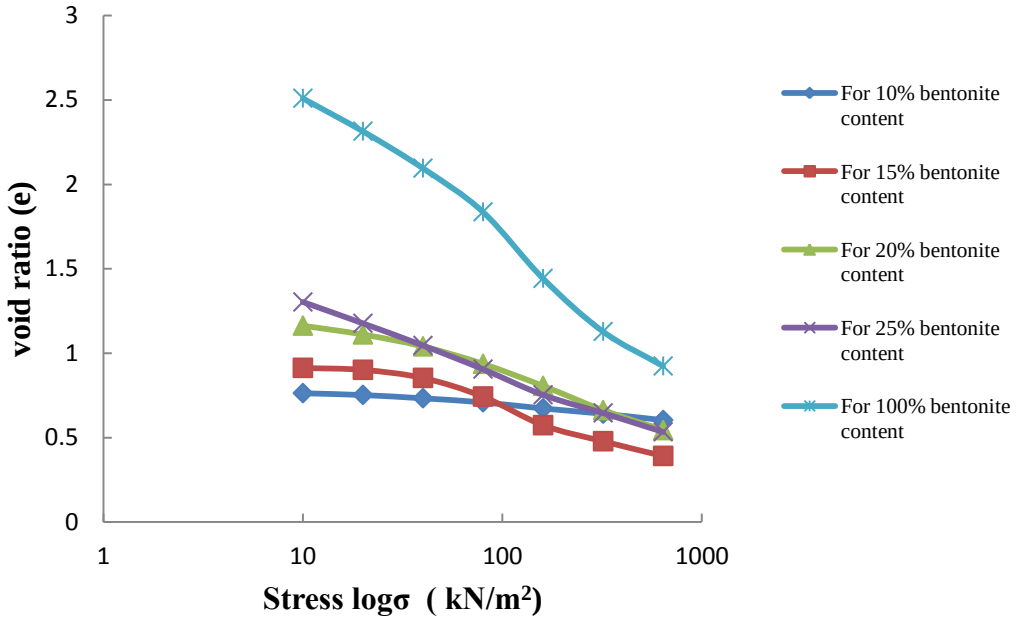

Graph 5.8:- Void ratio (e) Vs log σ plot for different bentonite content.

5.4.7 Stress Settlement curve for different mix (sample thickness=20mm):-

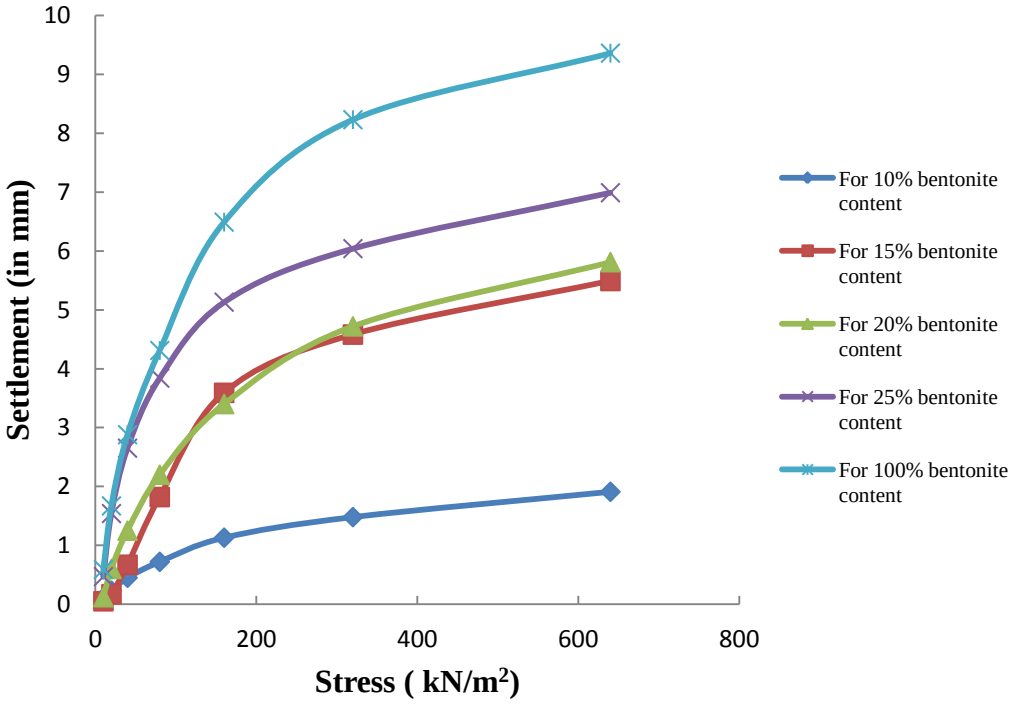

Graph 5.9:- Stress Settlement curve for different bentonite content.

5.4.8 Effective stress (Δσ) Vs coefficient. of volume change (m_v) plot for different mix:-

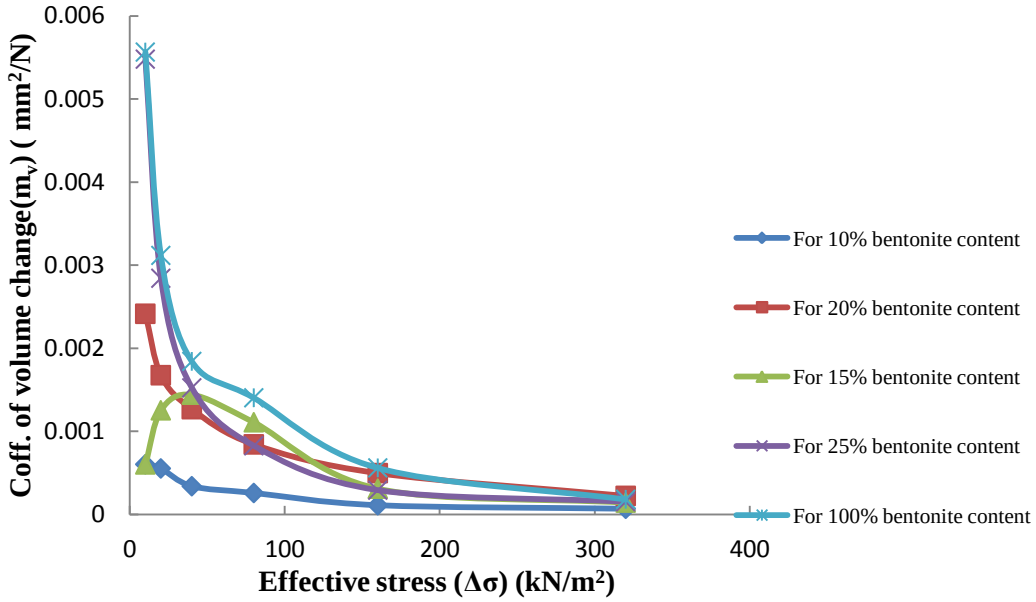

Graph 5.10:- Effective stress(Δσ)Vs coefficient. of volume change(m_v) for different bentonite content.

5.4.9 Log Δσ Vs coefficient. of permeability (K) plot for different mix:-

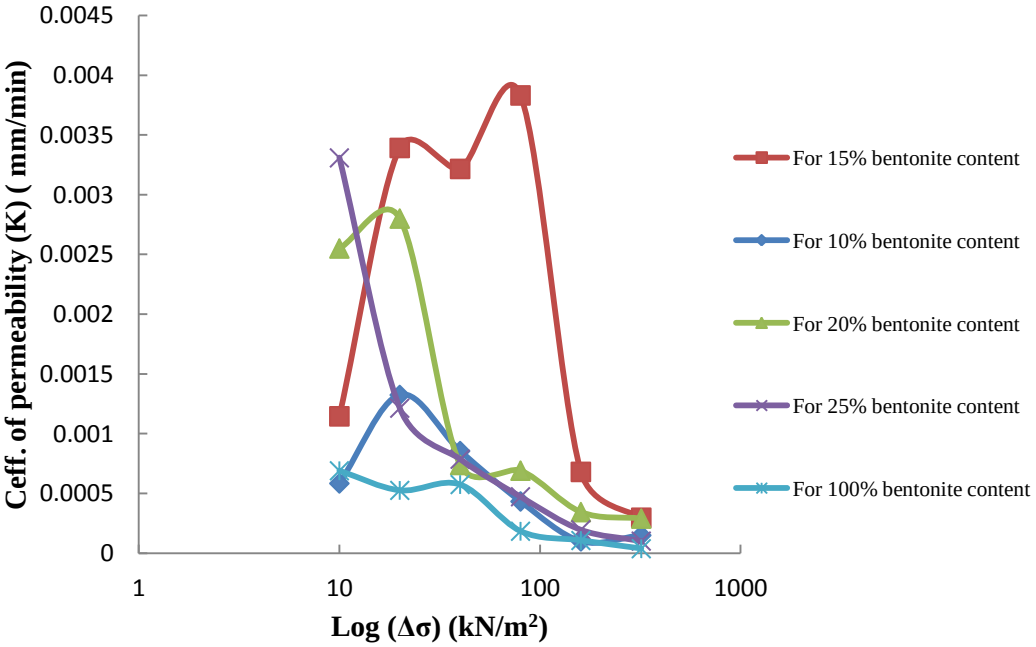

Graph 5.11:- Log Δσ Vs coefficient. of permeability (K) for different bentonite content.

5.4.10 Log Δσ Vs coefficient. of consolidation (C_v) plot for different mix:-

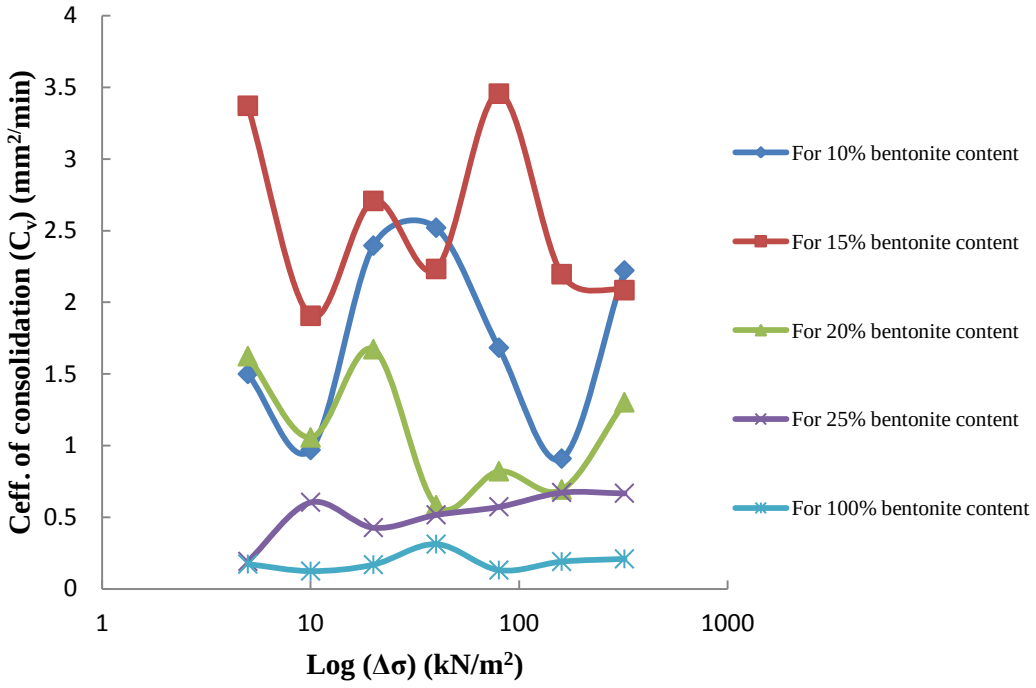

Graph 5.12:- Log Δσ Vs coefficient. of consolidation (C_v) for different bentonite content.

5.5 Average value of coefficient. of permeability (k) & coff. of consolidation (c_v) for different mix

Table 5.2:-Average value of coefficient. of permeability (K) and coefficient. of consolidation (C_v) at different bentonite content in mix.

Sl.No	Percent bentonite content in sample	Coefficient of permeability (K) (mm/min)	Coefficient of consolidation (C_v) (mm^2/min)
1	10	0.000574655	1.7423513
2	15	0.002094155	2.5643071
3	20	0.001236211	1.1072835
4	25	0.001013445	0.5217687
5	100	0.000353346	0.1868969

5.6 Comparison of experimental fourier solution and finite difference solution for different condition

5.6.1 Tv-U% Curve loading 10(kN/m^2) at 10% bentonite:-

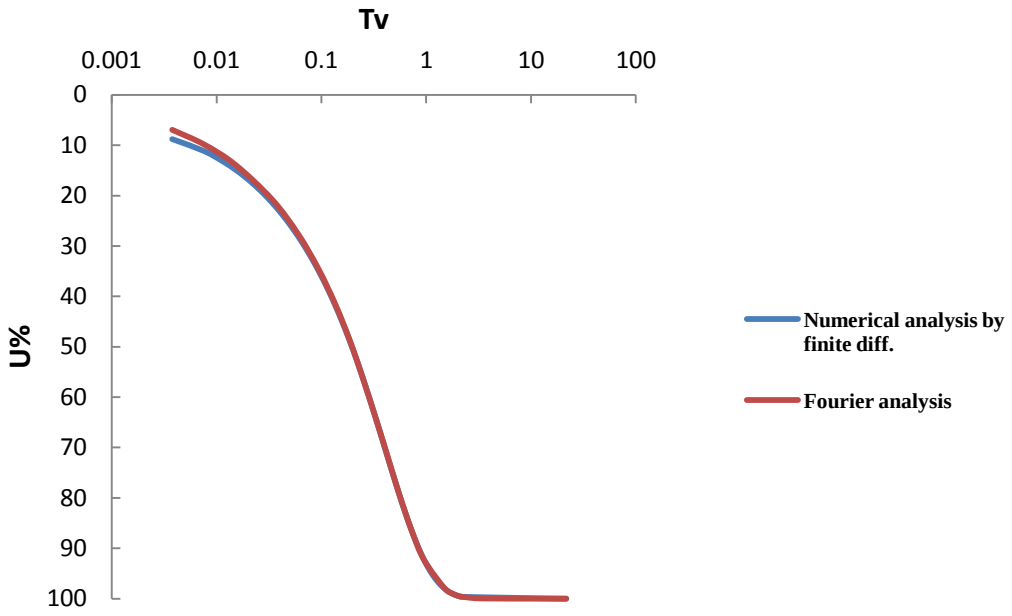

Graph 5.13:- Comparison of experimental and numerical solution for loading 10(kN/m^2) at 10% bentonite.

5.6.2 Tv-U% Curve loading 20(kN/m^2) at 10% bentonite:-

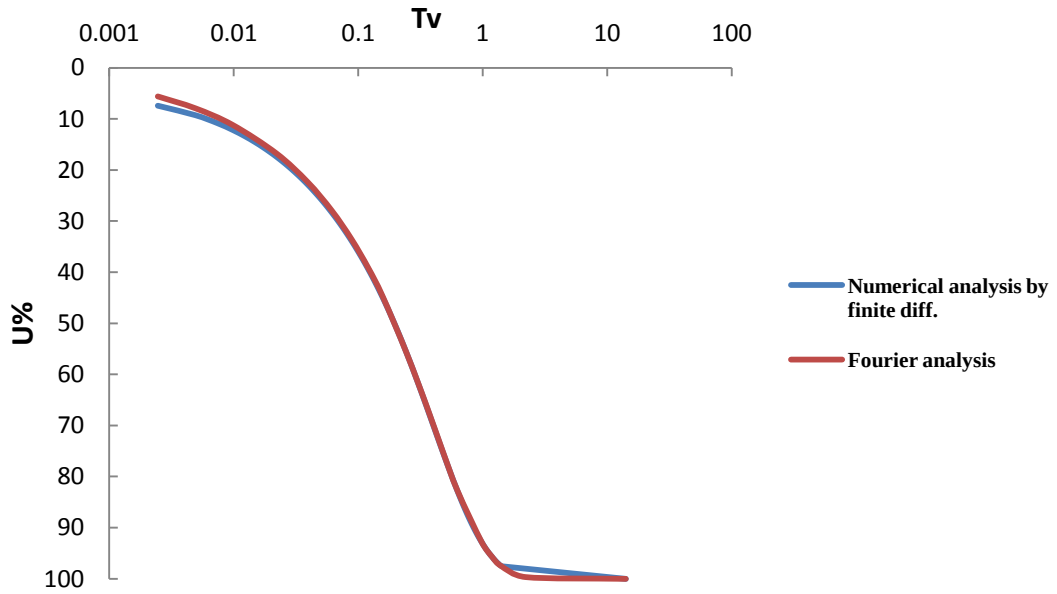

Graph 5.14:- Comparison of experimental and numerical solution for loading 20(kN/m^2) at 10% bentonite.

5.6.3 Tv-U% Curve loading 40 (kN/m^2) at 10% bentonite:-

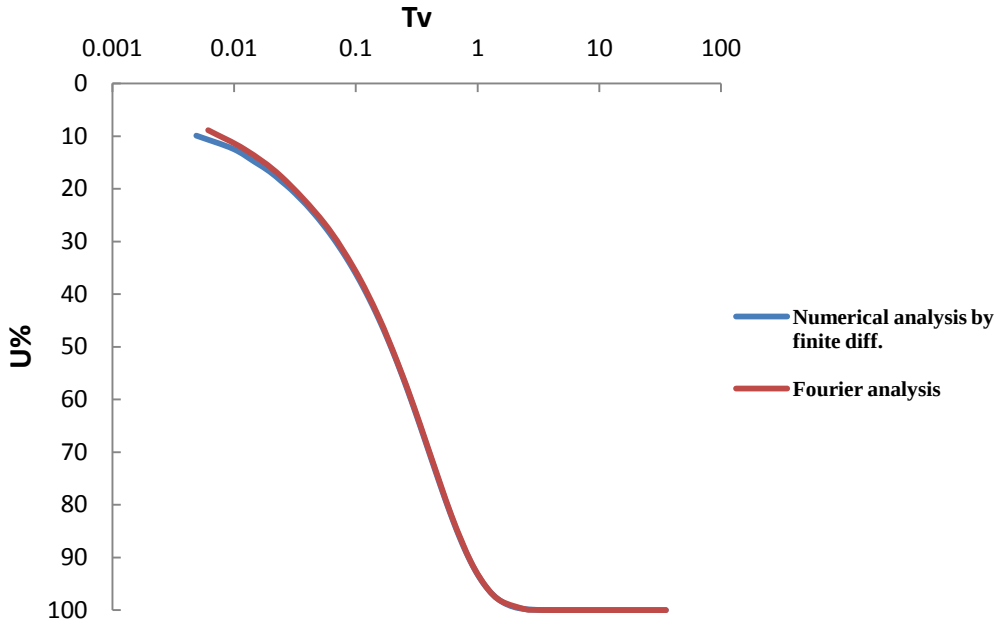

Graph 5.15:- Comparison of experimental and numerical solution for loading 40 (kN/m^2) at 10% bentonite.

5.6.4 Tv-U% Curve loading 80 (kN/m^2) at 10% bentonite:-

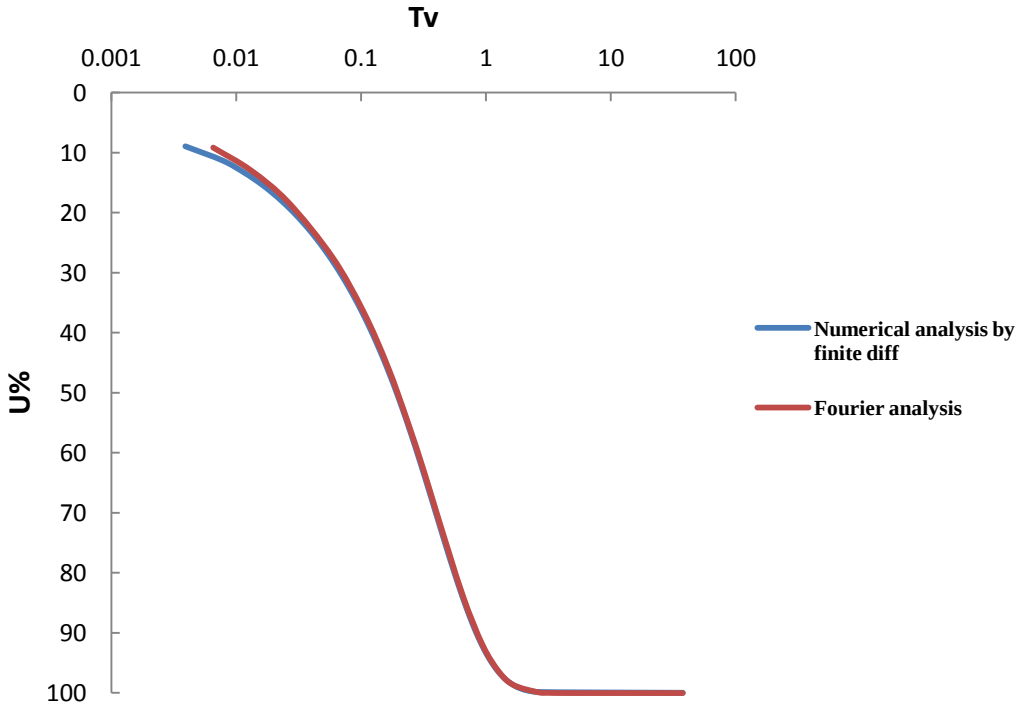

Graph 5.16:- Comparison of experimental and numerical solution for loading 80(kN/m^2) at 10% bentonite.

5.6.5 Tv-U% Curve loading 160 (kN/m^2) at 10% bentonite:-

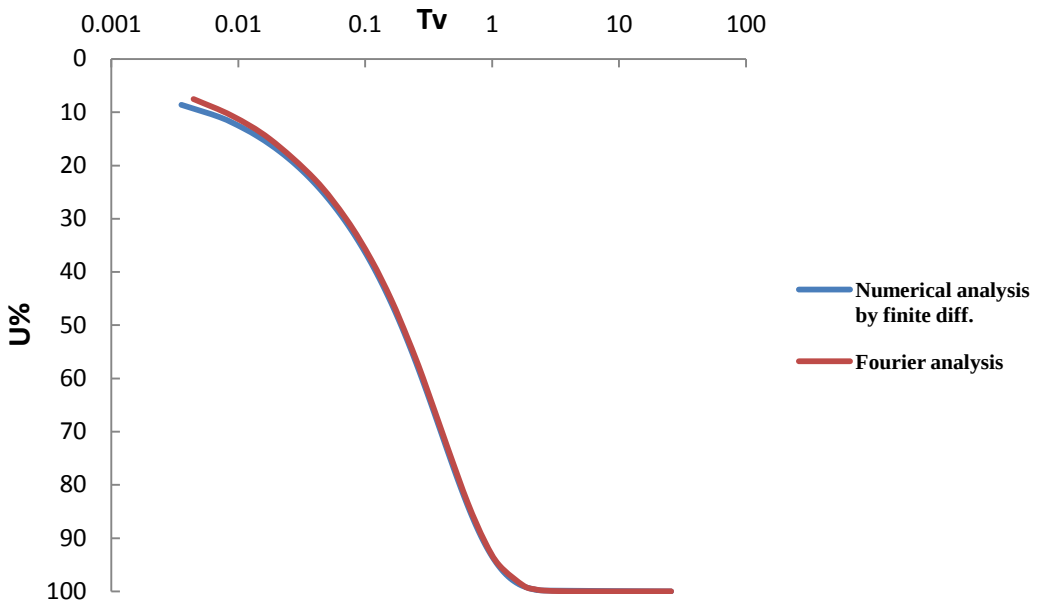

Graph 5.17:- Comparison of experimental and numerical solution for loading 160(kN/m^2) at 10% bentonite.

5.6.6 Tv-U% Curve loading 320 (kN/m^2) at 10% bentonite:-

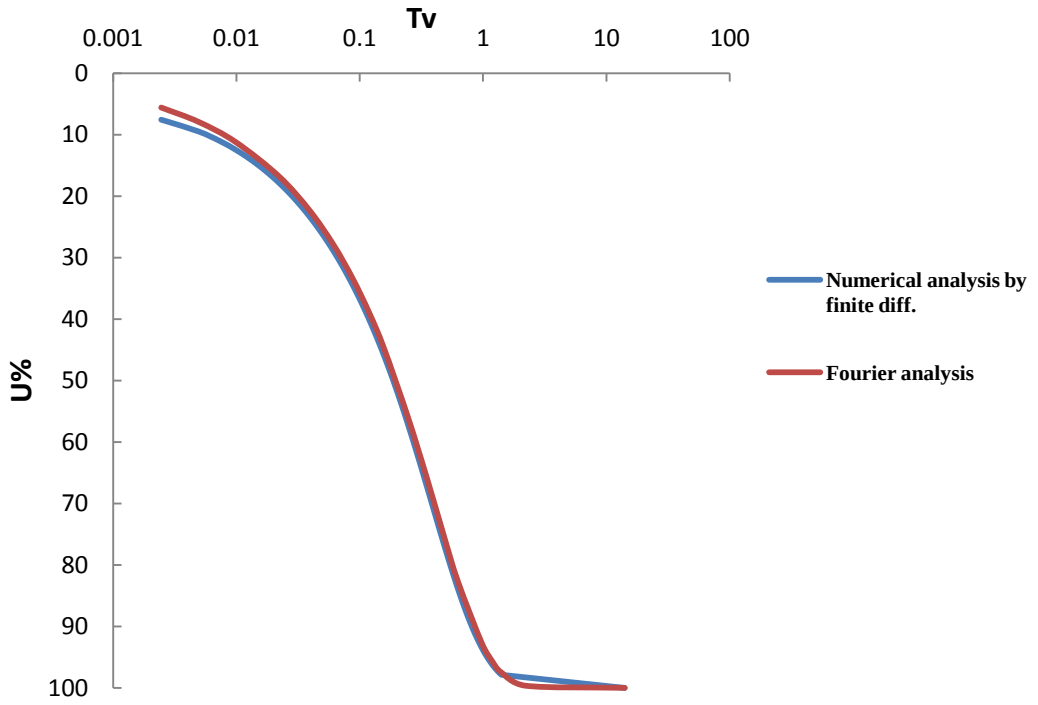

Graph 5.18:- Comparison of experimental and numerical solution for loading 320(kN/m^2) at 10% bentonite.

5.6.7 Tv-U% Curve loading 640 (kN/m^2) at 10% bentonite:-

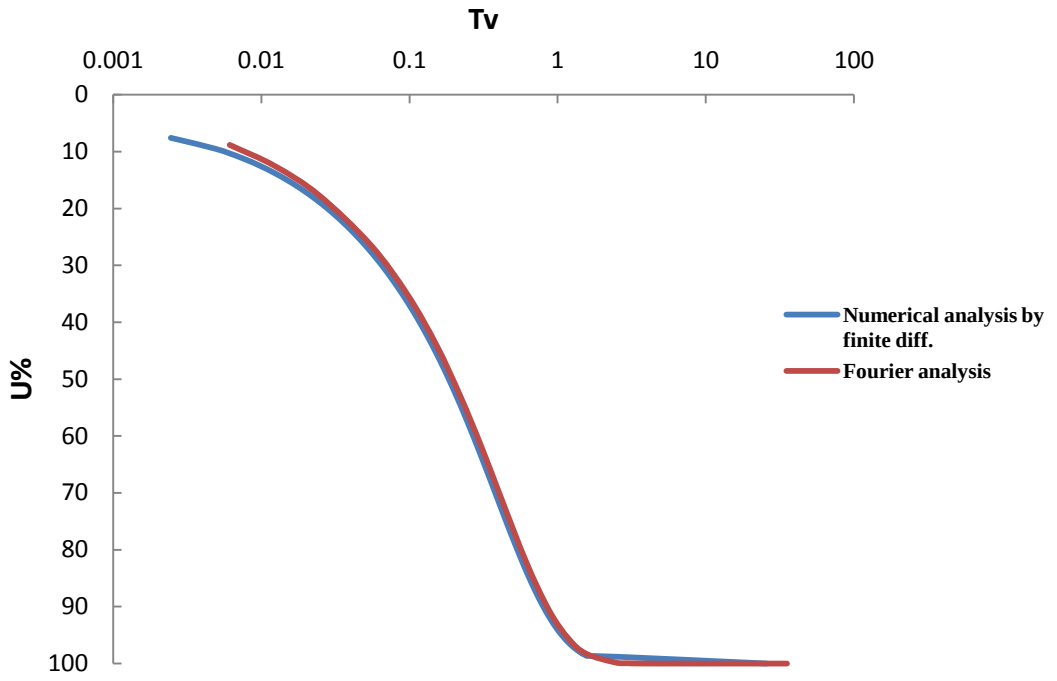

Graph 5.19:- Comparison of experimental and numerical solution for loading 640(kN/m^2) at 10% bentonite.

5.6.8 Tv-U% Curve loading 10 (kN/m^2) at 15% bentonite:-

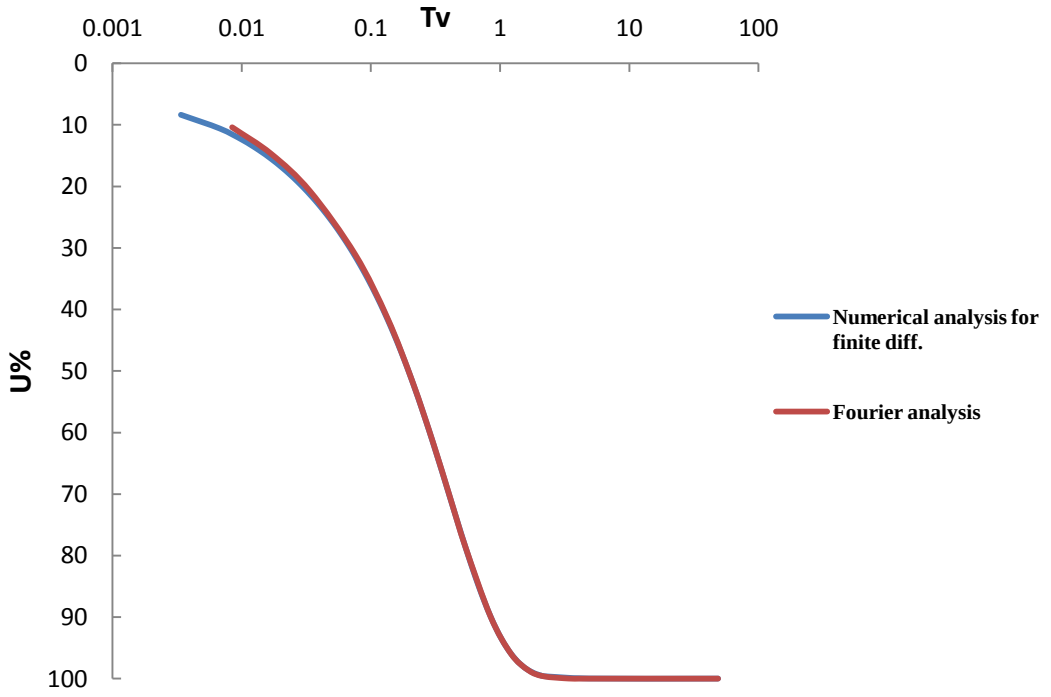

Graph 5.20:- Comparison of experimental and numerical solution for loading 10(kN/m^2) at 15% bentonite.

5.6.9 Tv-U% Curve loading 20 (kN/m^2) at 15% bentonite:-

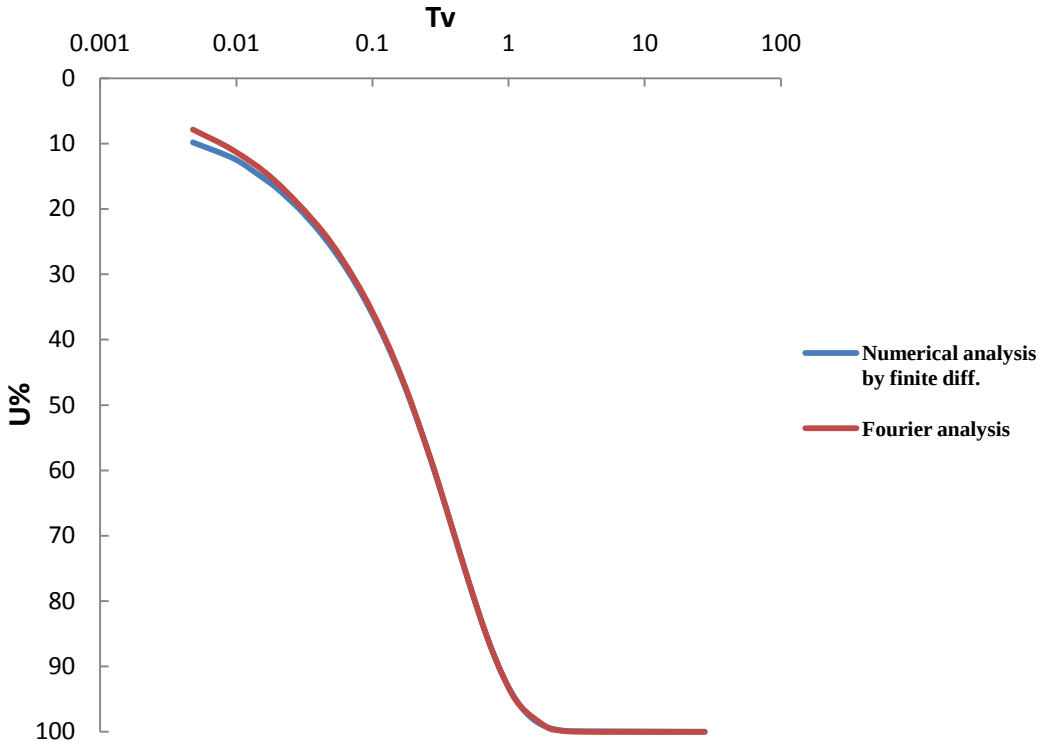

Graph 5.21:- Comparison of experimental and numerical solution for loading 20(kN/m^2) at 15% bentonite.

5.6.10 Tv-U% Curve loading 40 (kN/m^2) at 15% bentonite:-

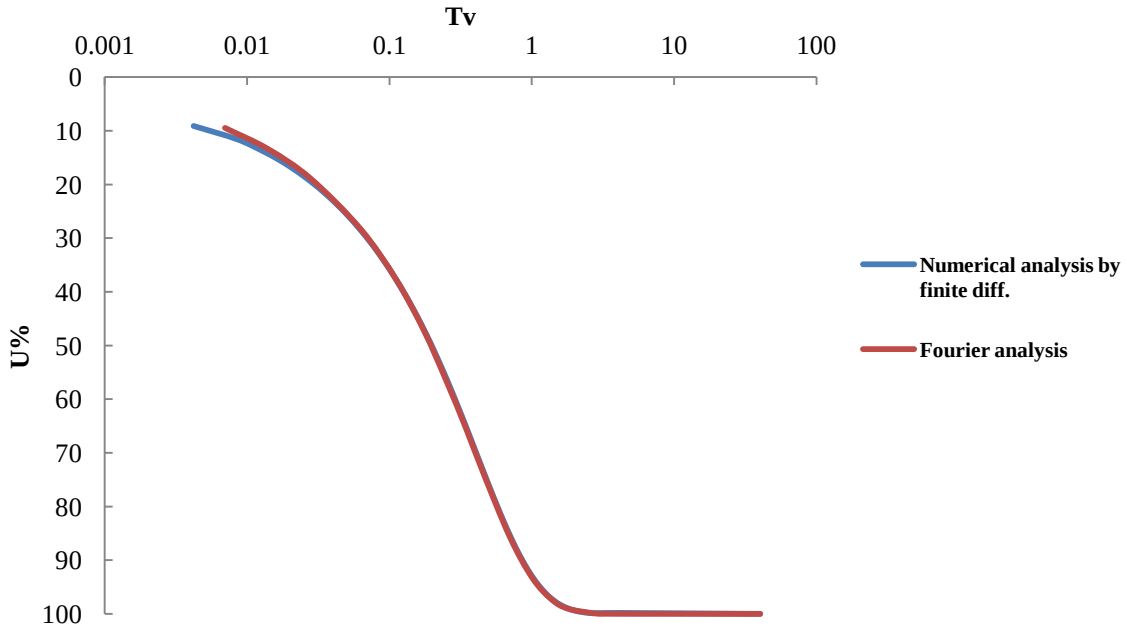

Graph 5.22:- Comparison of experimental and numerical solution for loading 40(kN/m^2) at 15% bentonite.

5.6.11 Tv-U% Curve loading 80 (kN/m^2) at 15% bentonite:-

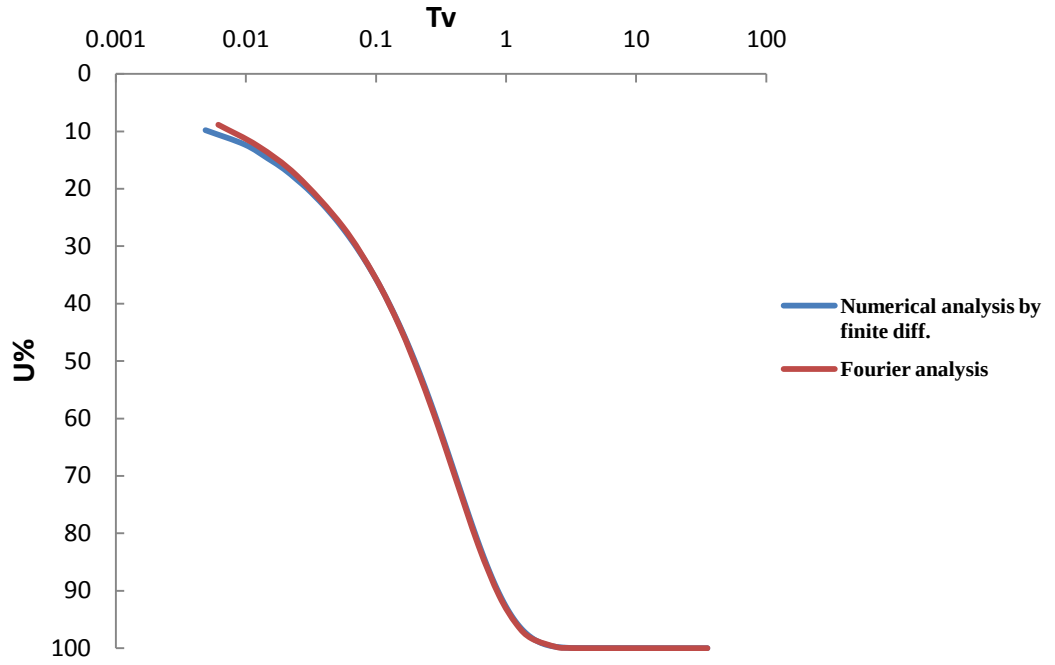

Graph 5.23:- Comparison of experimental and numerical solution for loading 80(kN/m^2) at 15% bentonite.

5.6.12 Tv-U% Curve loading 160 (kN/m^2) at 15% bentonite:-

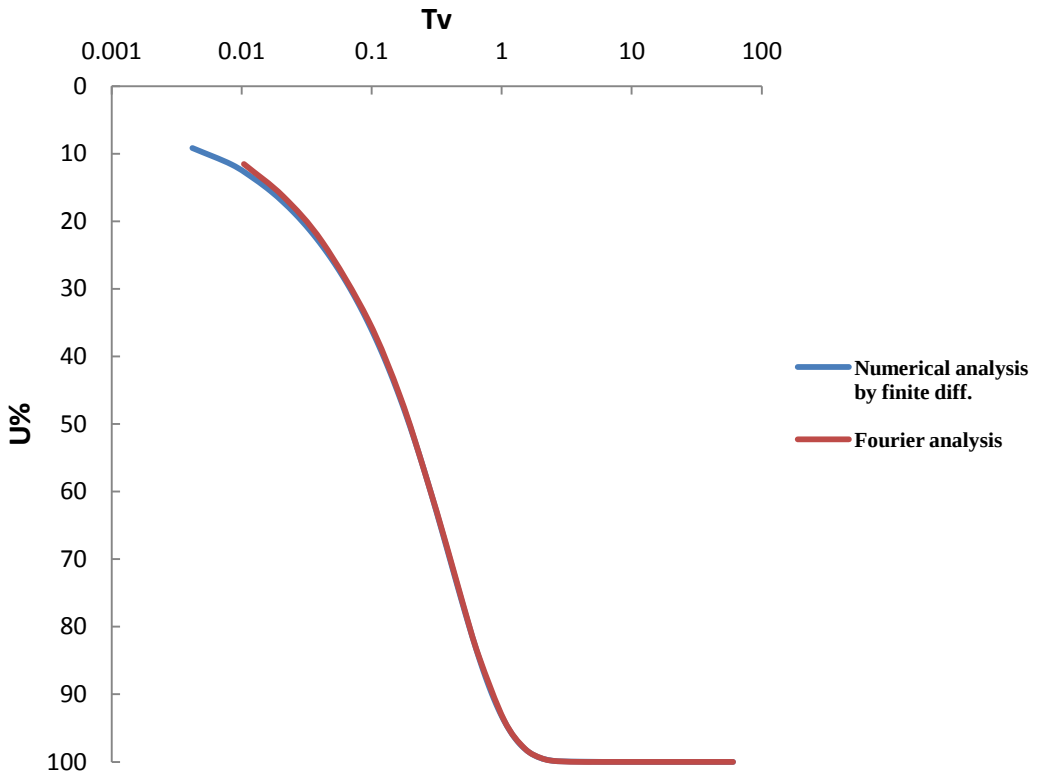

Graph 5.24:- Comparison of experimental and numerical solution for loading 160(kN/m^2) at 15% bentonite.

5.6.13 Tv-U% Curve loading 320 (kN/m^2) at 15% bentonite:-

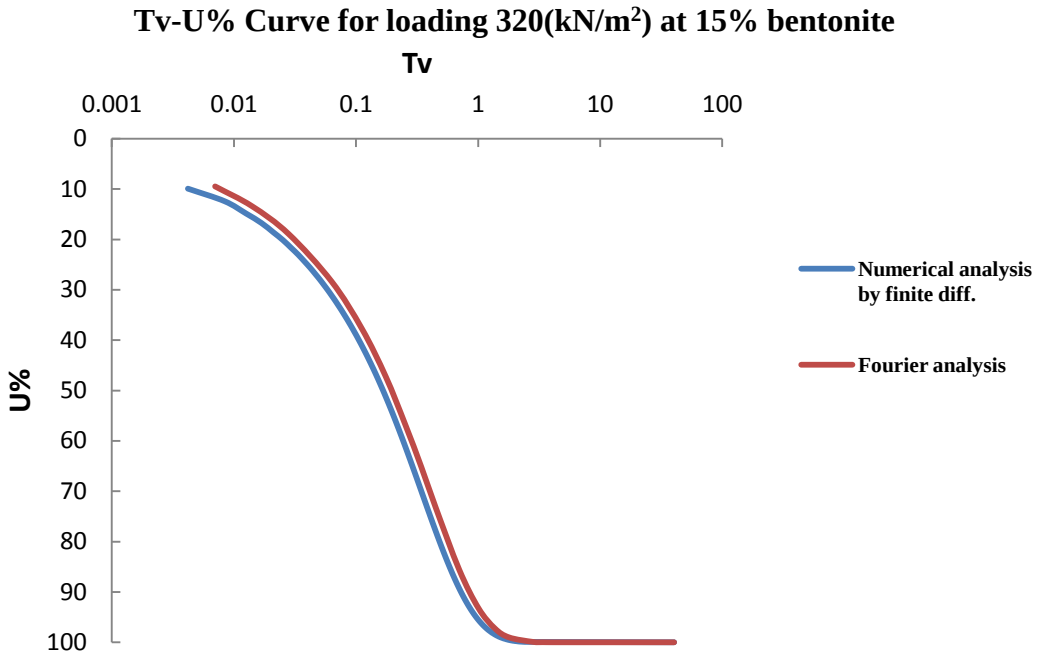

Graph 5.25:- Comparison of experimental and numerical solution for loading 320(kN/m^2) at 15% bentonite.

5.6.14 Tv-U% Curve loading 640 (kN/m^2) at 15% bentonite:-

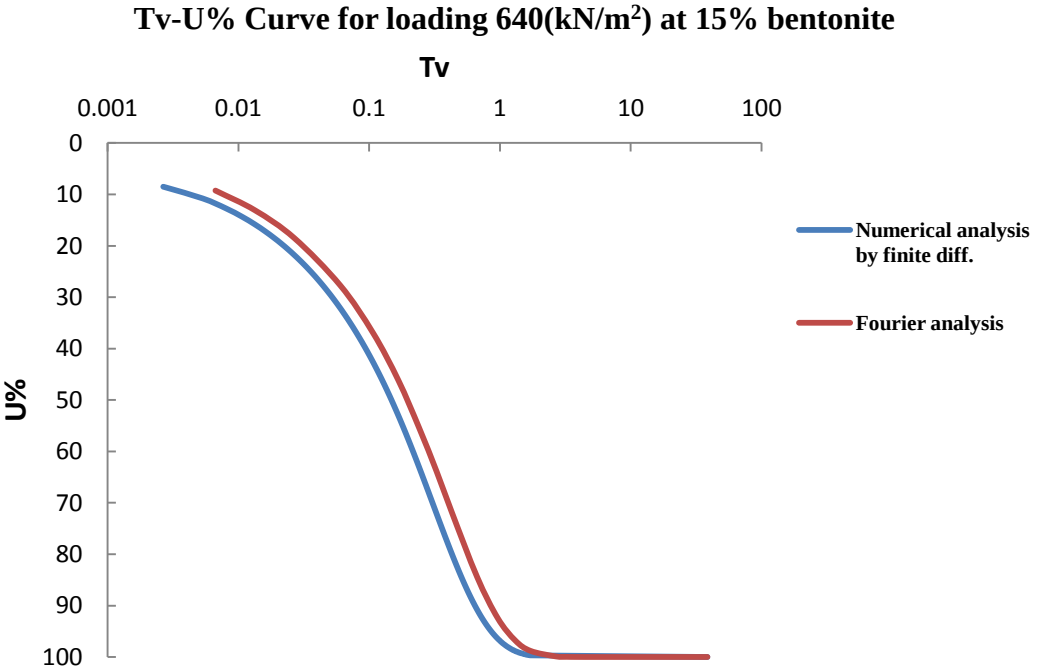

Graph 5.26:- Comparison of experimental and numerical solution for loading 640(kN/m^2) at 15% bentonite.

5.6.15 Tv-U% Curve loading 10 (kN/m^2) at 20% bentonite:-

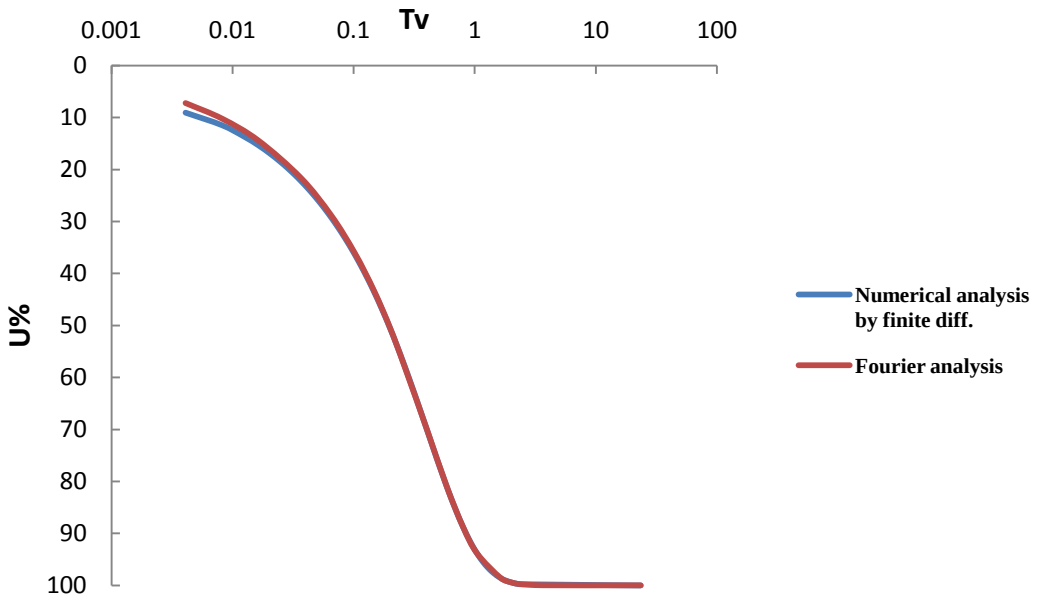

Graph 5.27:- Comparison of experimental and numerical solution for loading 10(kN/m^2) at 20% bentonite.

5.6.16 Tv-U% Curve loading 20 (kN/m^2) at 20% bentonite:-

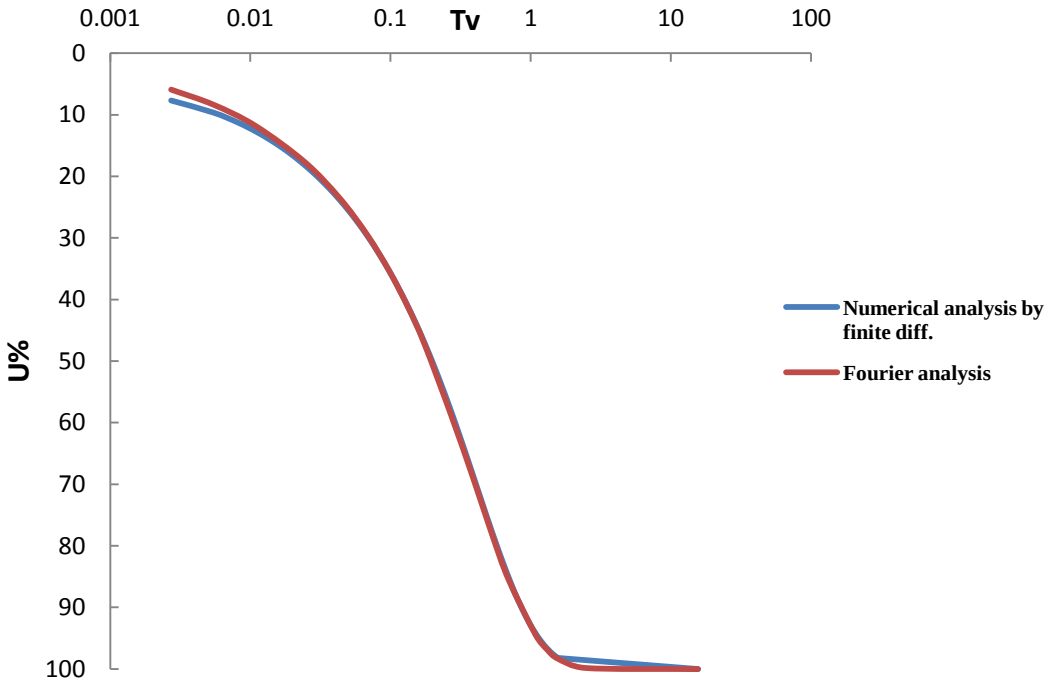

Graph 5.28:- Comparison of experimental and numerical solution for loading 20(kN/m^2) at 20% bentonite.

5.6.17 Tv-U% Curve loading 40 (kN/m^2) at 20% bentonite:-

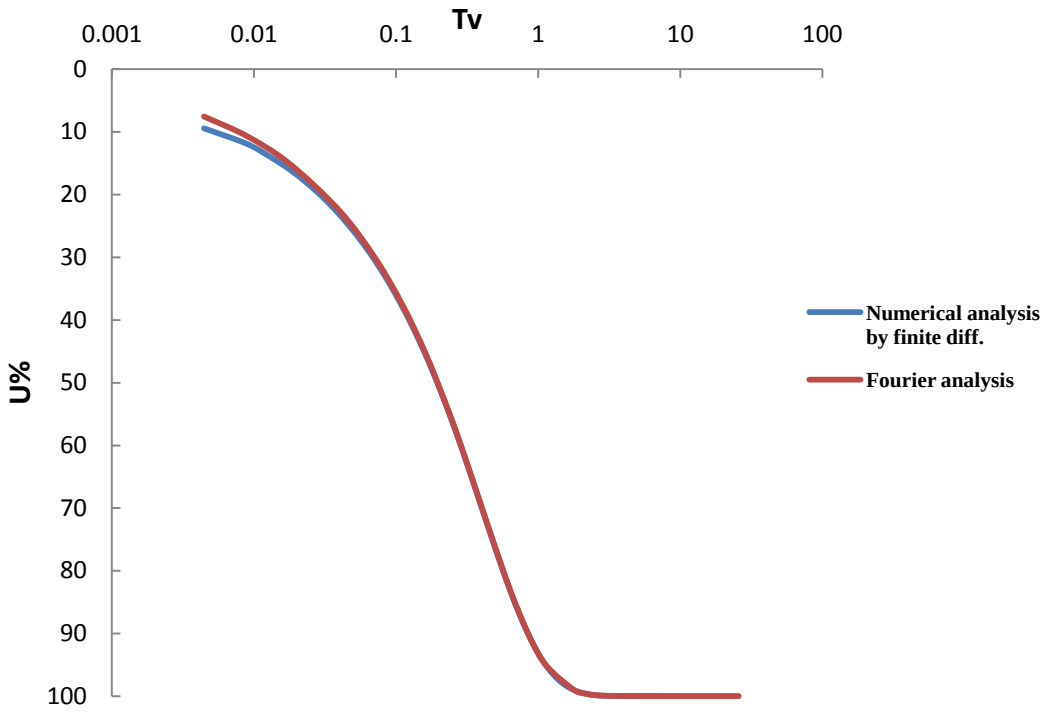

Graph 5.29:- Comparison of experimental and numerical solution for loading 40(kN/m^2) at 20% bentonite.

5.6.18 Tv-U% Curve loading 80 (kN/m^2) at 20% bentonite:-

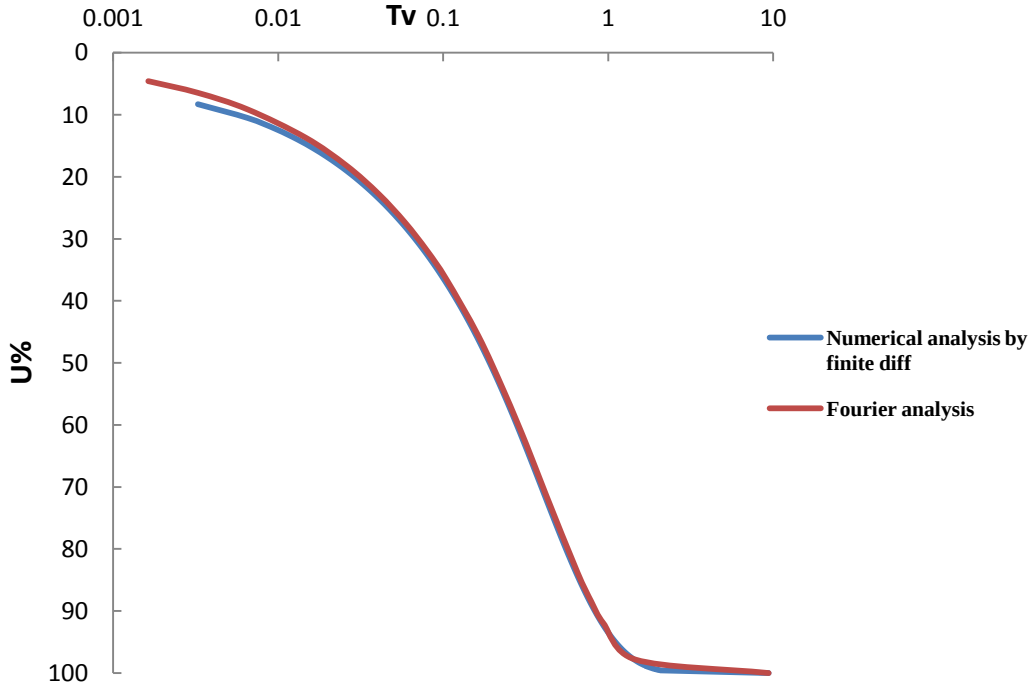

Graph 5.30:- Comparison of experimental and numerical solution for loading 80(kN/m^2) at 20% bentonite.

5.6.19 Tv-U% Curve loading 160 (kN/m^2) at 20% bentonite:-

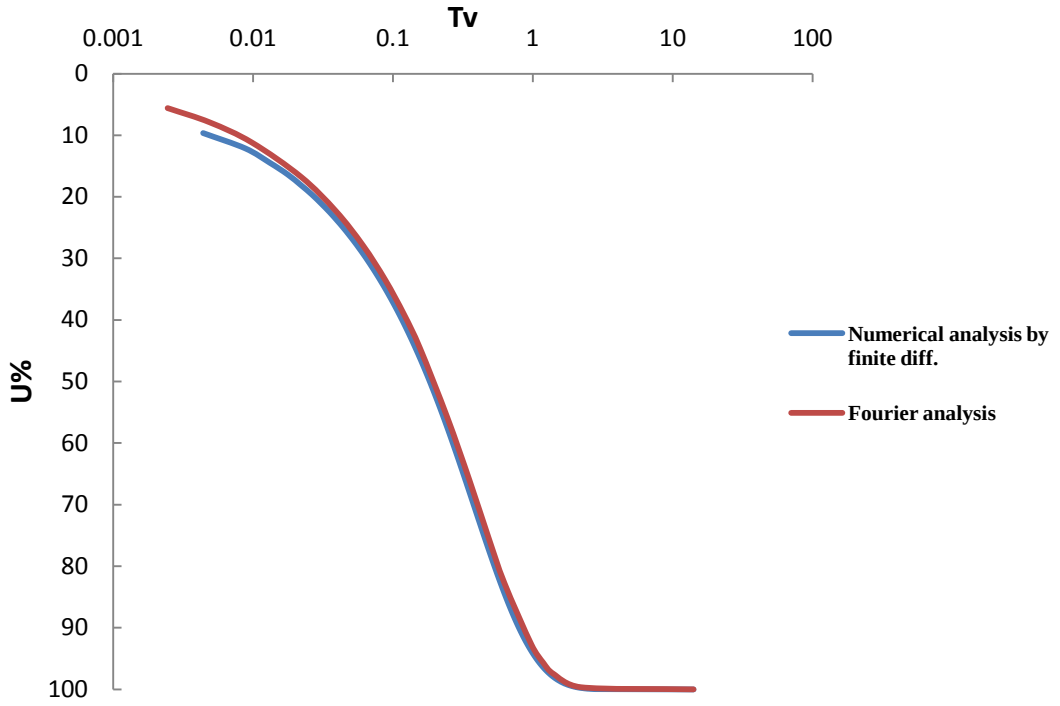

Graph 5.31:- Comparison of experimental and numerical solution for loading 160(kN/m^2) at 20% bentonite.

5.6.20 Tv-U% Curve loading 320 (kN/m^2) at 20% bentonite:-

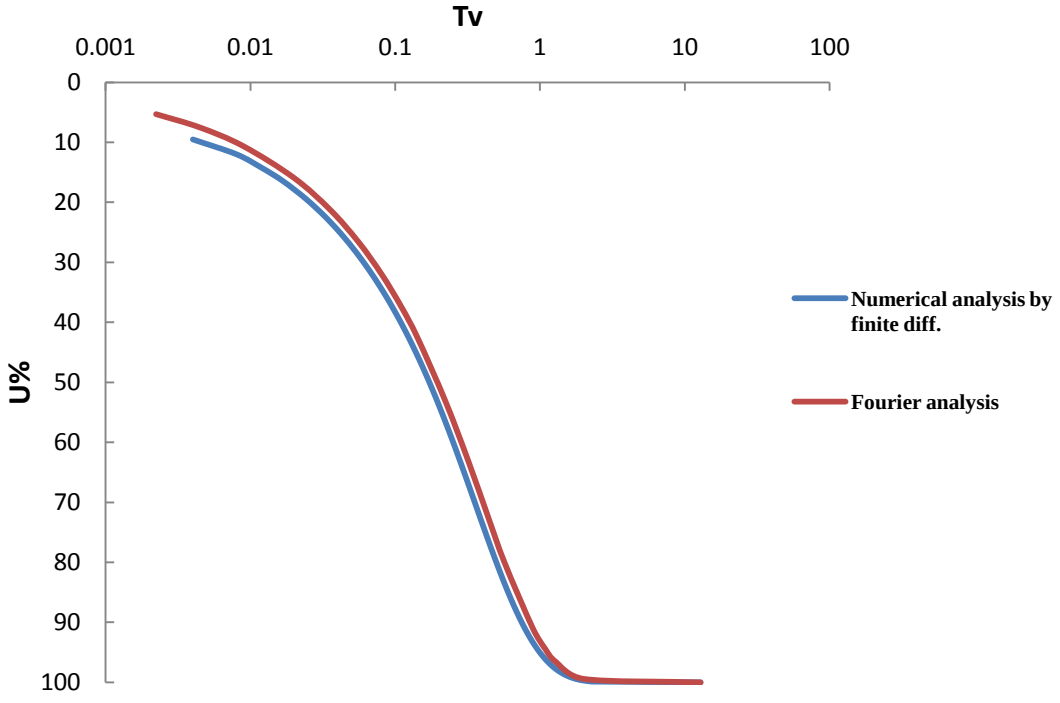

Graph 5.32:- Comparison of experimental and numerical solution for loading 320(kN/m^2) at 20% bentonite.

5.6.21 Tv-U% Curve loading 640 (kN/m^2) at 20% bentonite:-

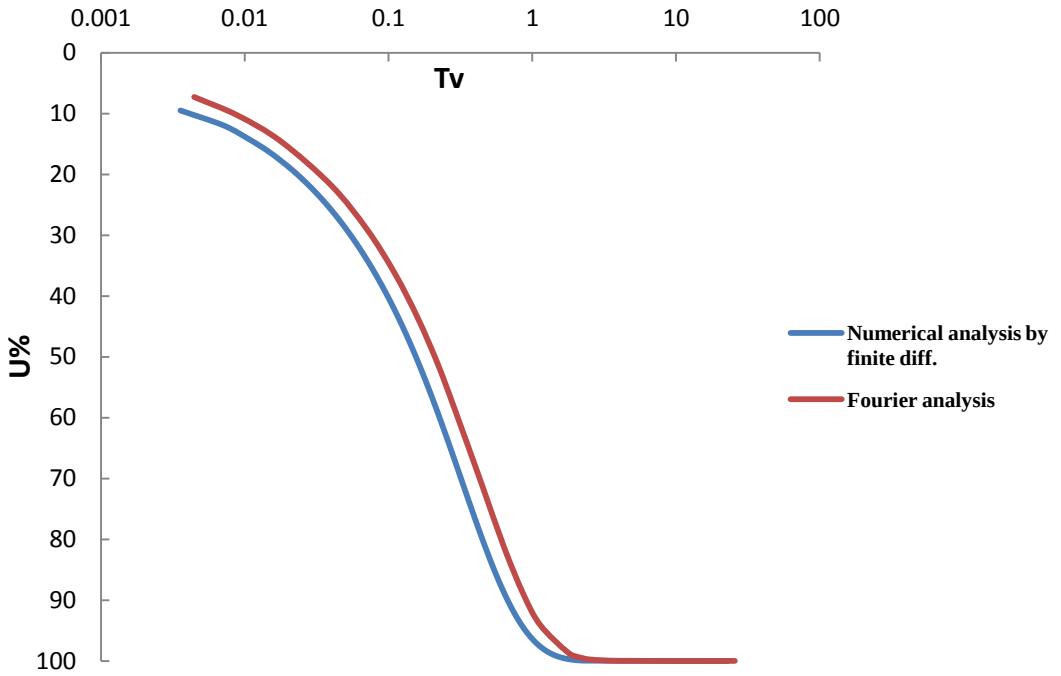

Graph 5.33:- Comparison of experimental and numerical solution for loading 640(kN/m^2) at 20% bentonite.

5.6.22 Tv-U% Curve loading 10 (kN/m^2) at 25% bentonite:-

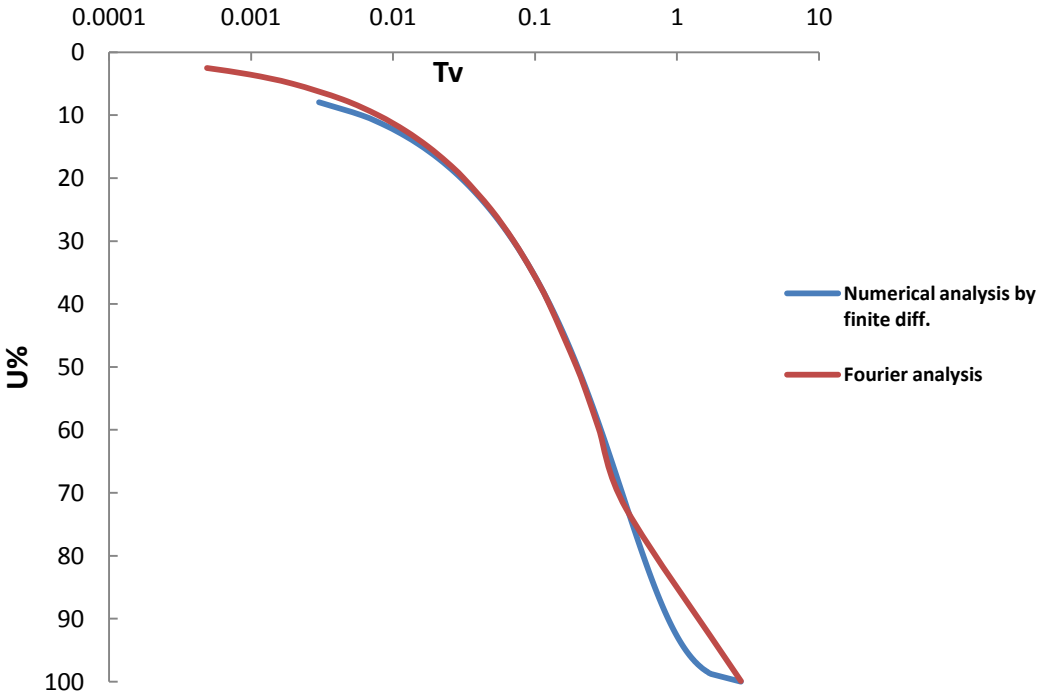

Graph 5.34:- Comparison of experimental and numerical solution for loading 10(kN/m^2) at 25% bentonite.

5.6.23 Tv-U% Curve loading 20 (kN/m^2) at 25% bentonite:-

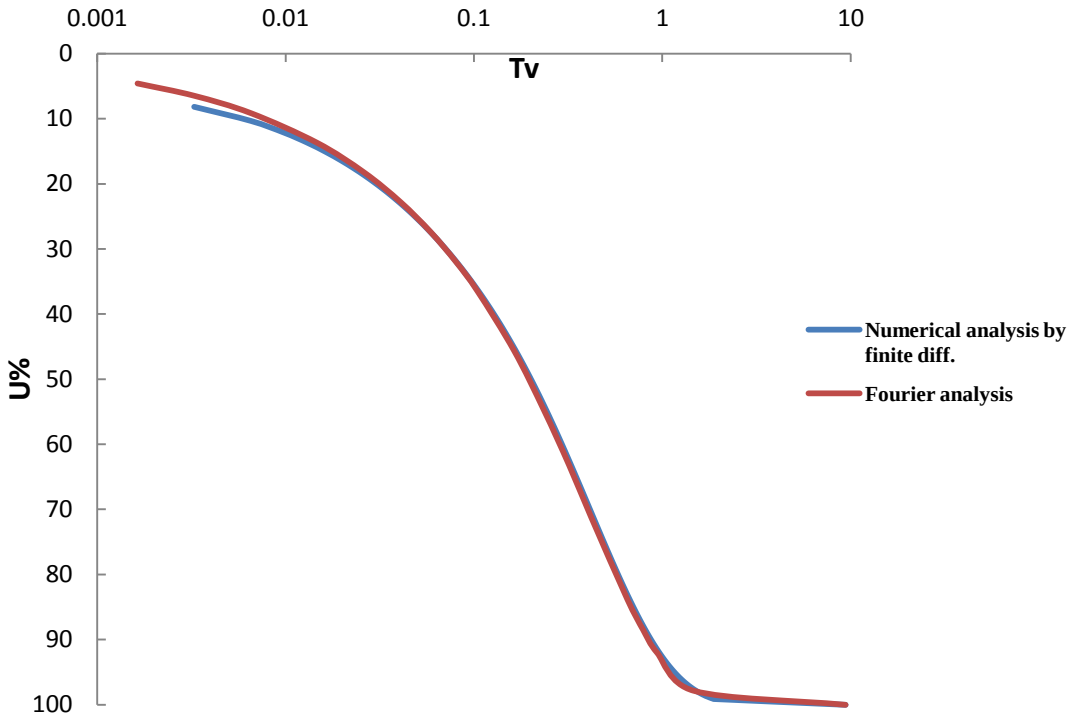

Graph 5.35:- Comparison of experimental and numerical solution for loading 20(kN/m^2) at 25% bentonite.

5.6.24 Tv-U% Curve loading 40 (kN/m^2) at 25% bentonite:-

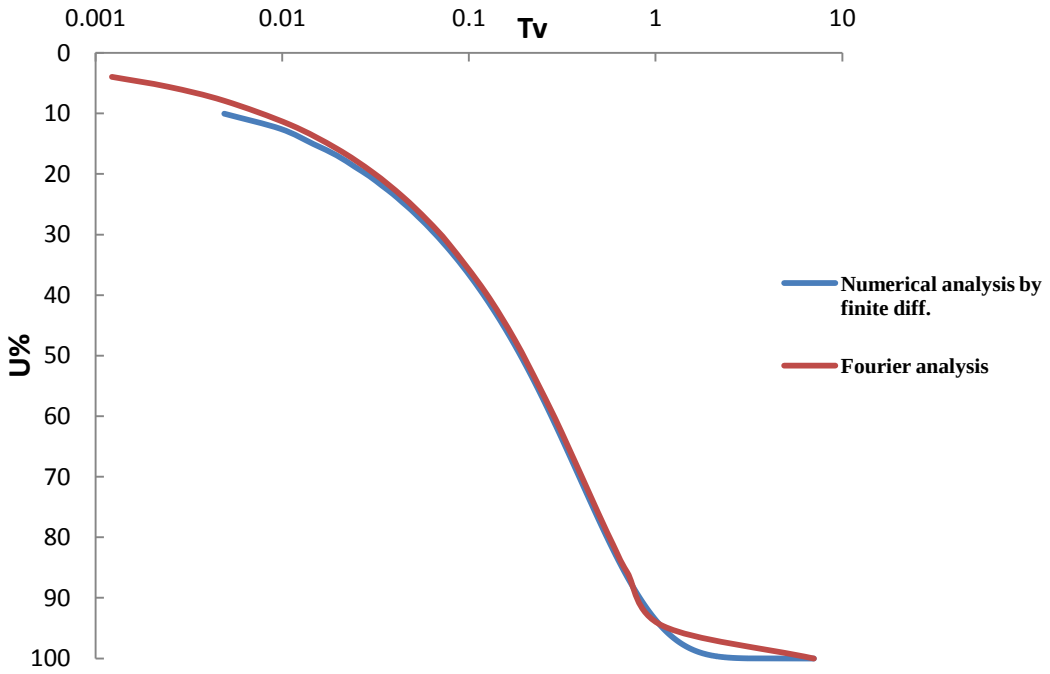

Graph 5.36:- Comparison of experimental and numerical solution for loading 40(kN/m^2) at 25% bentonite.

5.6.25 Tv-U% Curve loading 80 (kN/m^2) at 25% bentonite:-

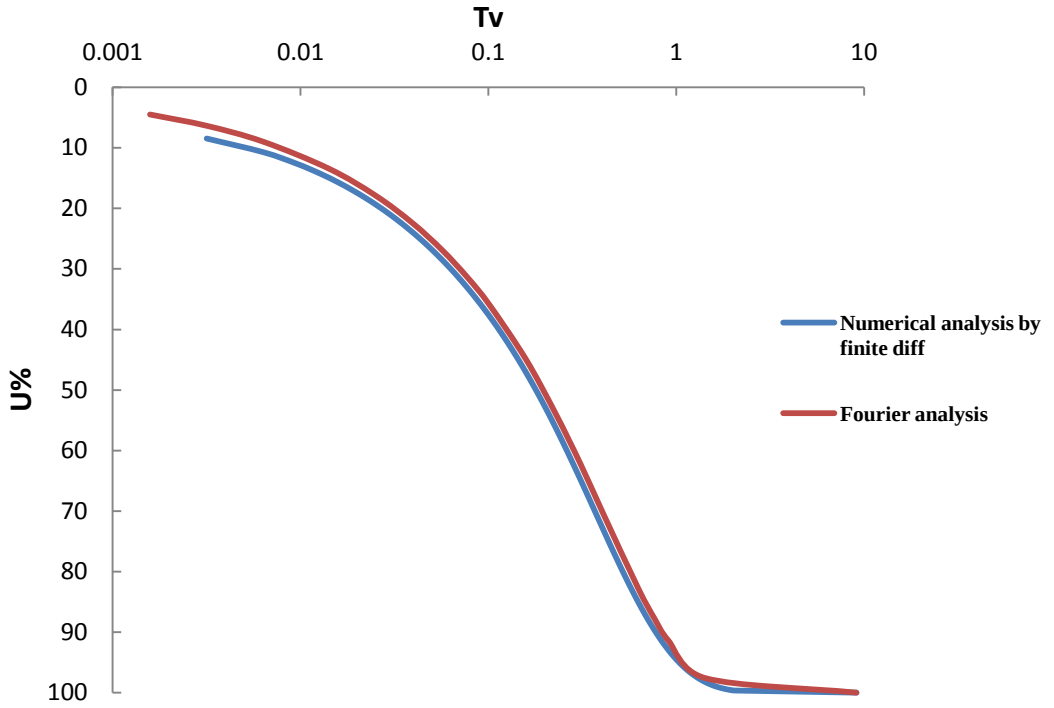

Graph 5.37:- Comparison of experimental and numerical solution for loading 80(kN/m^2) at 25% bentonite.

5.6.26 Tv-U% Curve loading 160 (kN/m^2) at 25% bentonite:-

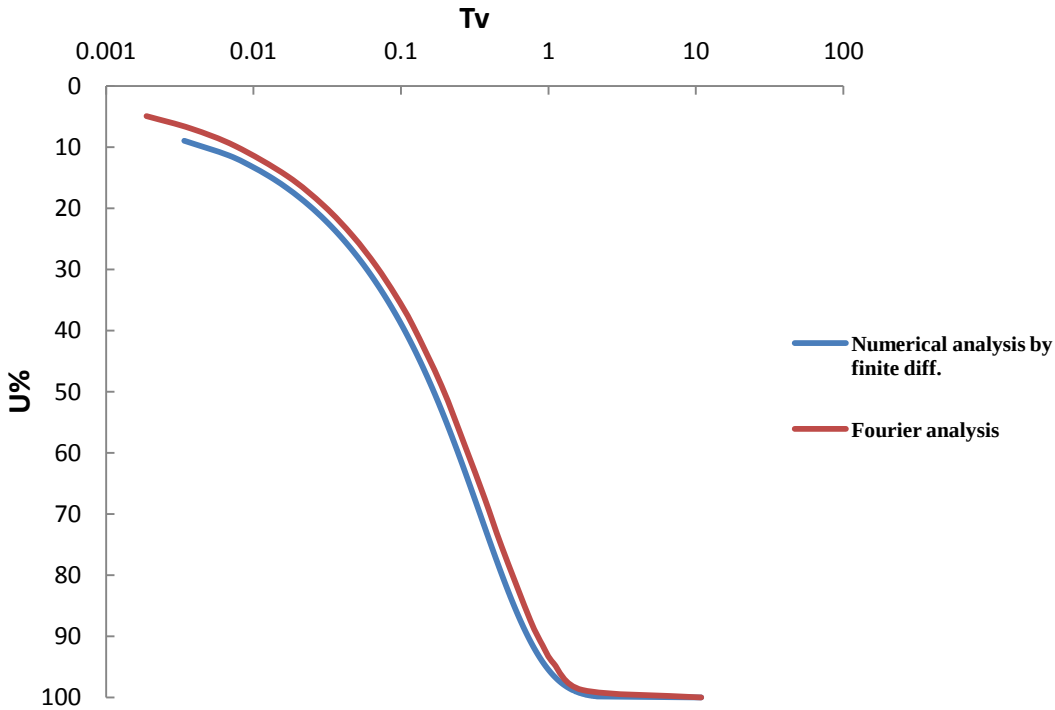

Graph 5.38:- Comparison of experimental and numerical solution for loading 160(kN/m^2) at 25% bentonite.

5.6.27 Tv-U% Curve loading 320 (kN/m^2) at 25% bentonite:-

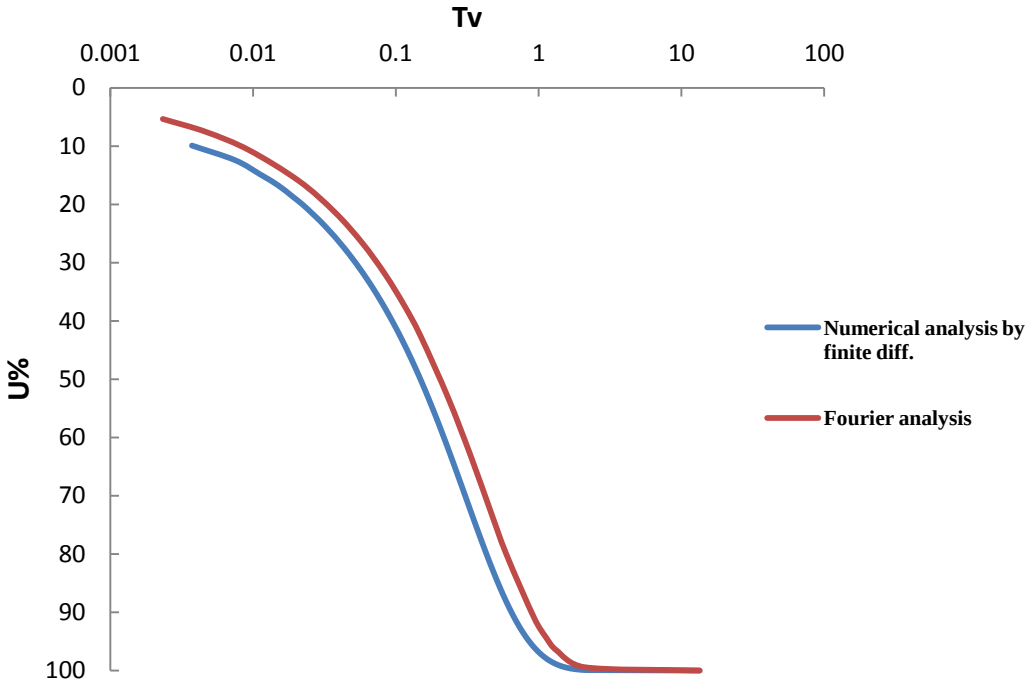

Graph 5.39:- Comparison of experimental and numerical solution for loading 320(kN/m^2) at 25% bentonite.

5.6.28 Tv-U% Curve loading 640 (kN/m^2) at 25% bentonite:-

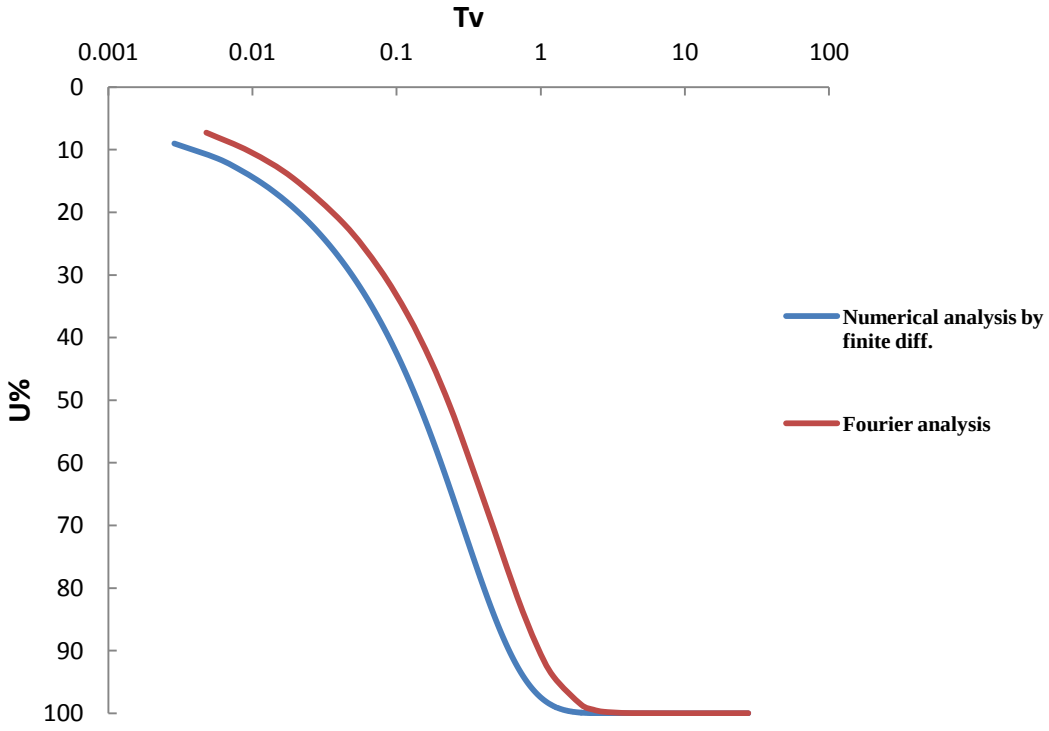

Graph 5.40:- Comparison of experimental and numerical solution for loading 640(kN/m^2) at 25% bentonite.

5.6.29 Tv-U% Curve loading 10 (kN/m^2) at 100% bentonite:-

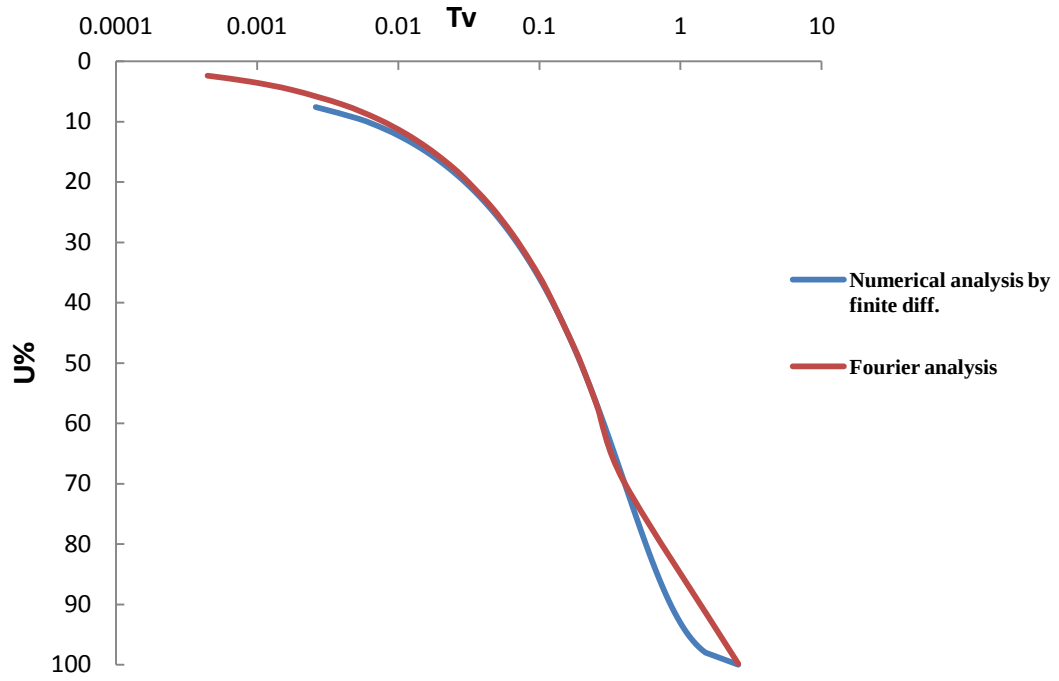

Graph 5.41:- Comparison of experimental and numerical solution for loading 10(kN/m^2) at 100% bentonite.

5.6.30 Tv-U% Curve loading 20 (kN/m^2) at 100% bentonite:-

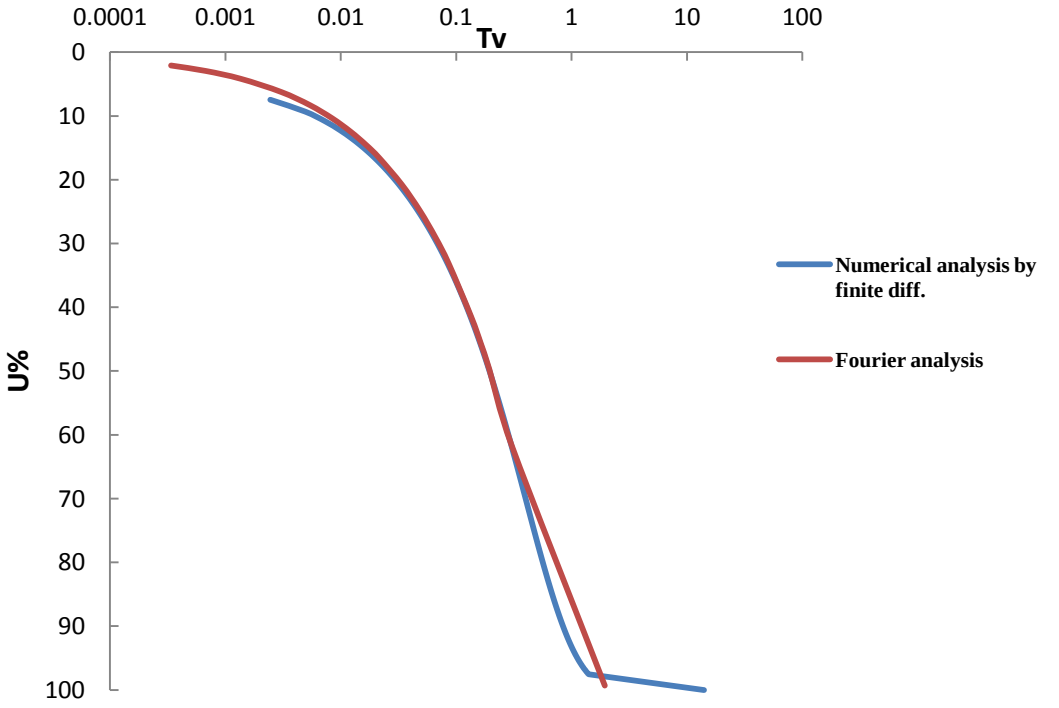

Graph 5.42:- Comparison of experimental and numerical solution for loading 20(kN/m^2) at 100% bentonite.

5.6.31 Tv-U% Curve loading 40 (kN/m^2) at 100% bentonite:-

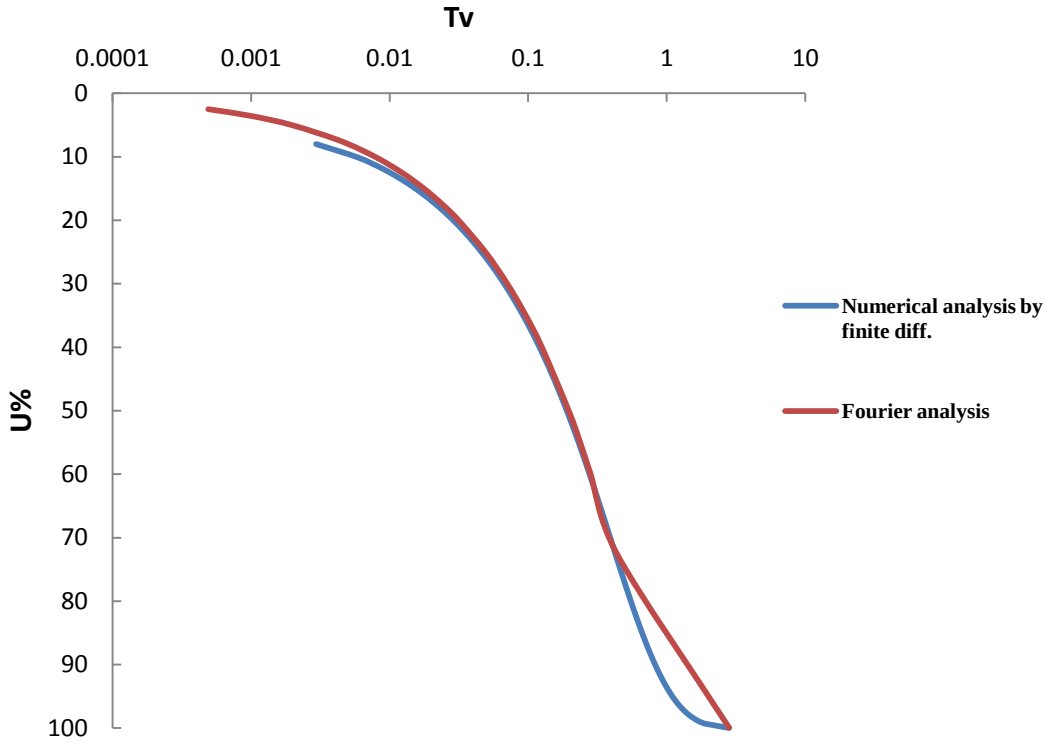

Graph 5.43:- Comparison of experimental and numerical solution for loading 40(kN/m^2) at 100% bentonite.

5.6.32 Tv-U% Curve loading 80 (kN/m^2) at 100% bentonite:-

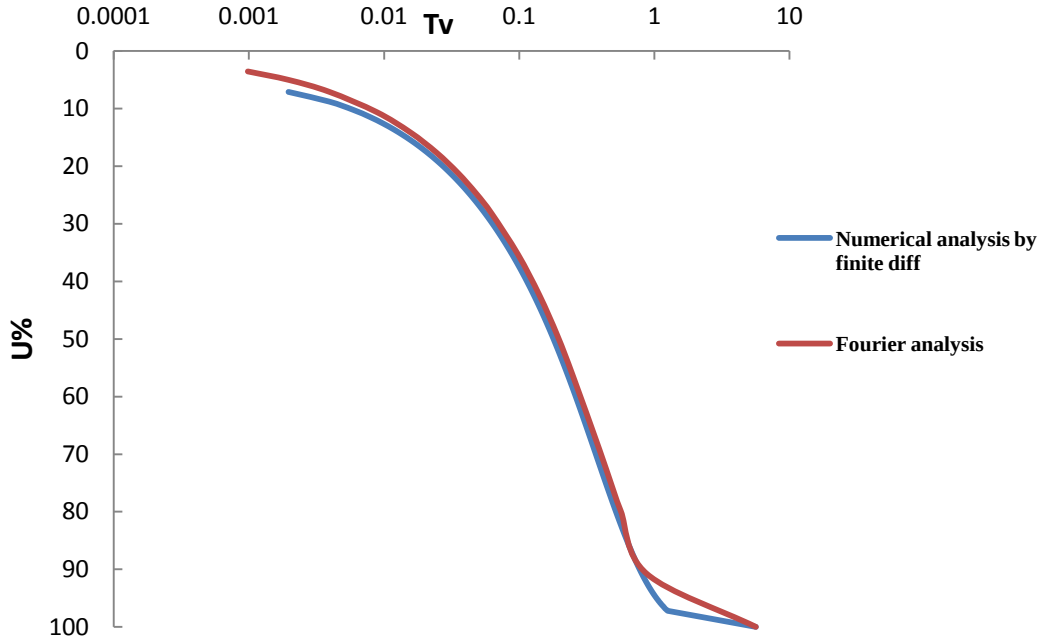

Graph 5.44:- Comparison of Experimental and Numerical solution for loading 80(kN/m^2) at 100% bentonite.

5.6.33 Tv-U% Curve loading 160 (kN/m^2) at 100% bentonite:-

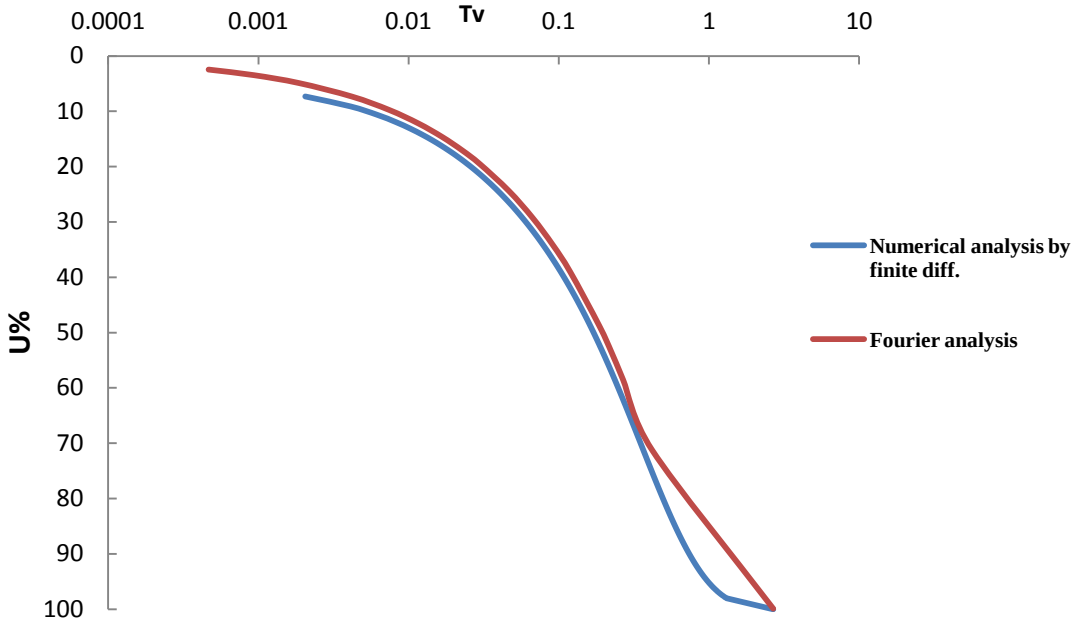

Graph 5.45:- Comparison of experimental and numerical solution for loading 160(kN/m^2) at 100% bentonite.

5.6.34 Tv-U% Curve loading 320 (kN/m^2) at 100% bentonite:-

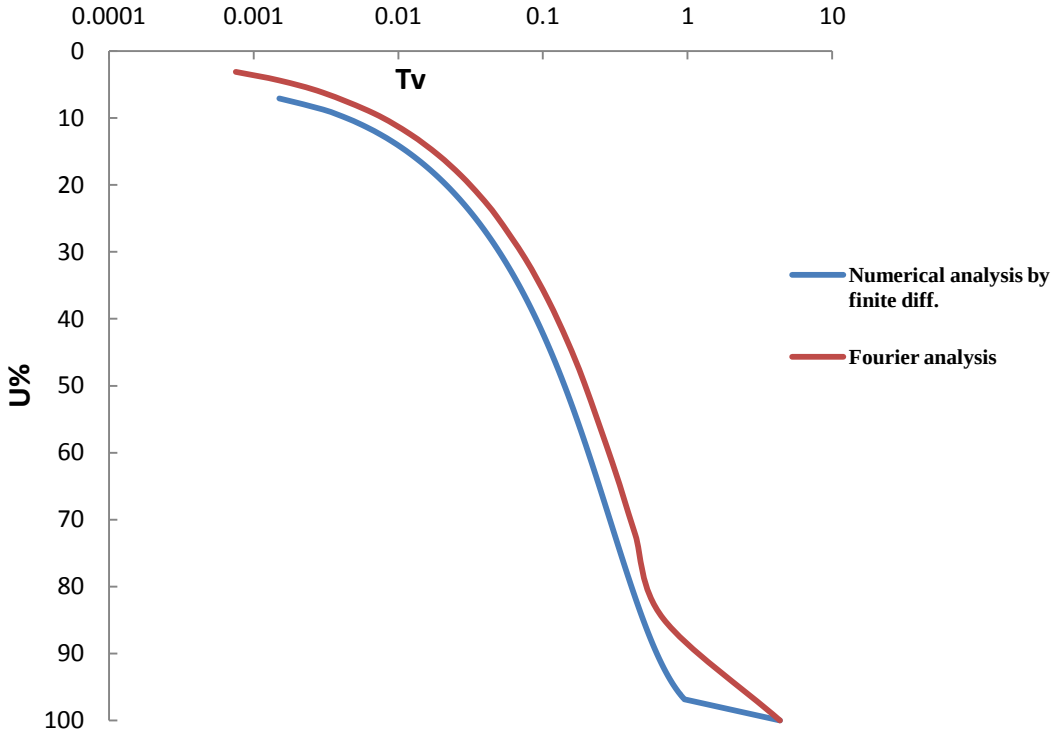

Graph 5.46:- Comparison of experimental and numerical solution for loading 320(kN/m^2) at 100% bentonite.

5.6.35 Tv-U% Curve loading 640 (kN/m^2) at 100% bentonite:-

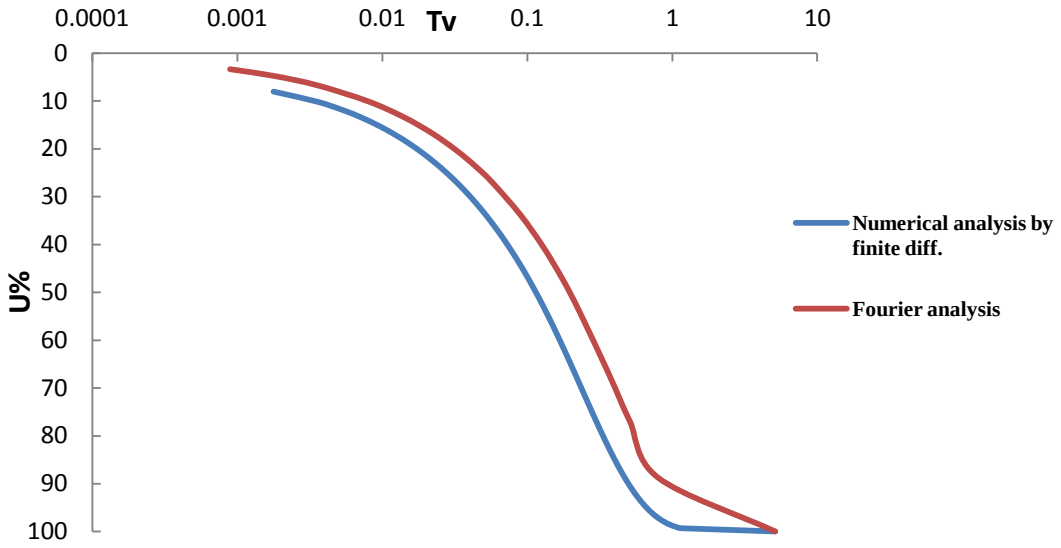

Graph 5.47:- Comparison of experimental and numerical solution for loading 640(kN/m^2) at 100% bentonite.

5.7 Variation in % difference in u% in numerical finite difference and fourier solution for different condition at Tv= 0.005

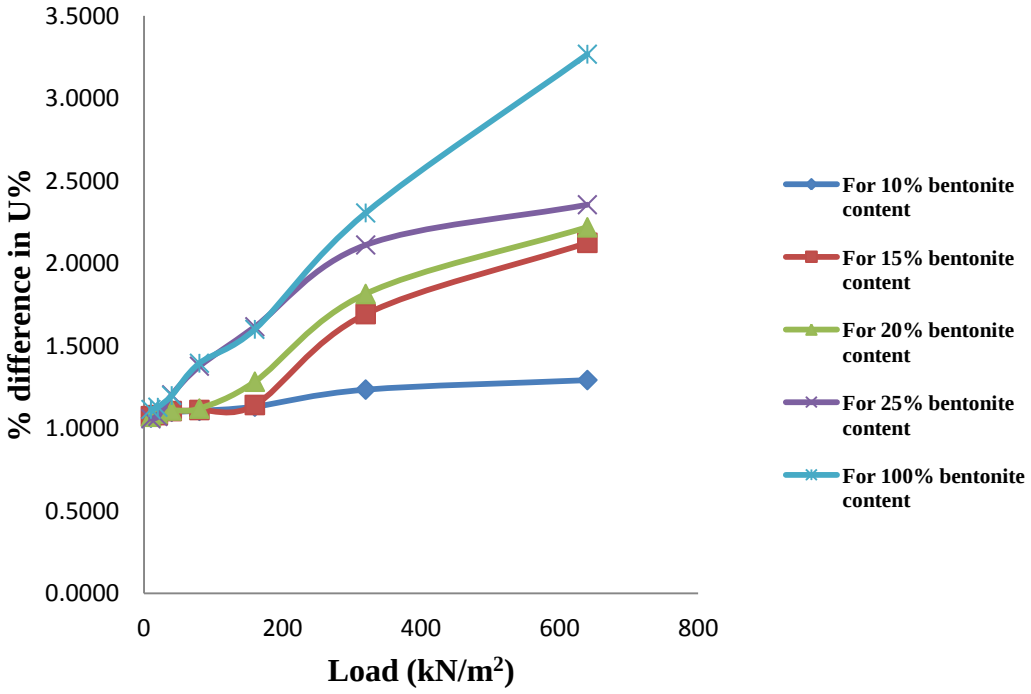

Graph 5.48:- Variation in % difference in u% in numerical finite difference and fourier solution for different condition at Tv=0.005

5.8 Implicit solution of consolidation analysis and comparison for different time step

5.8.1 Comparison graph for different time step by implicit method for loading 10(kN/m^2) at 10% bentonite:-

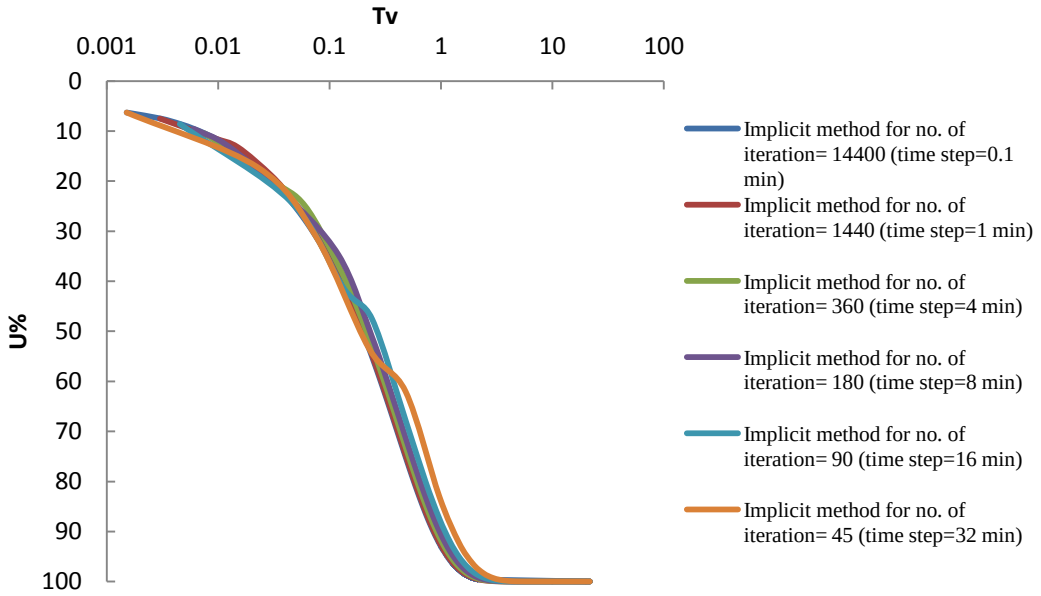

Graph 5.49:- Comparison graph for different no of iteration (by implicit method) for loading 10(kN/m^2) at 10% bentonite.

5.8.2 Comparison graph for different time step by implicit method for loading 20(kN/m^2) at 10% bentonite:-

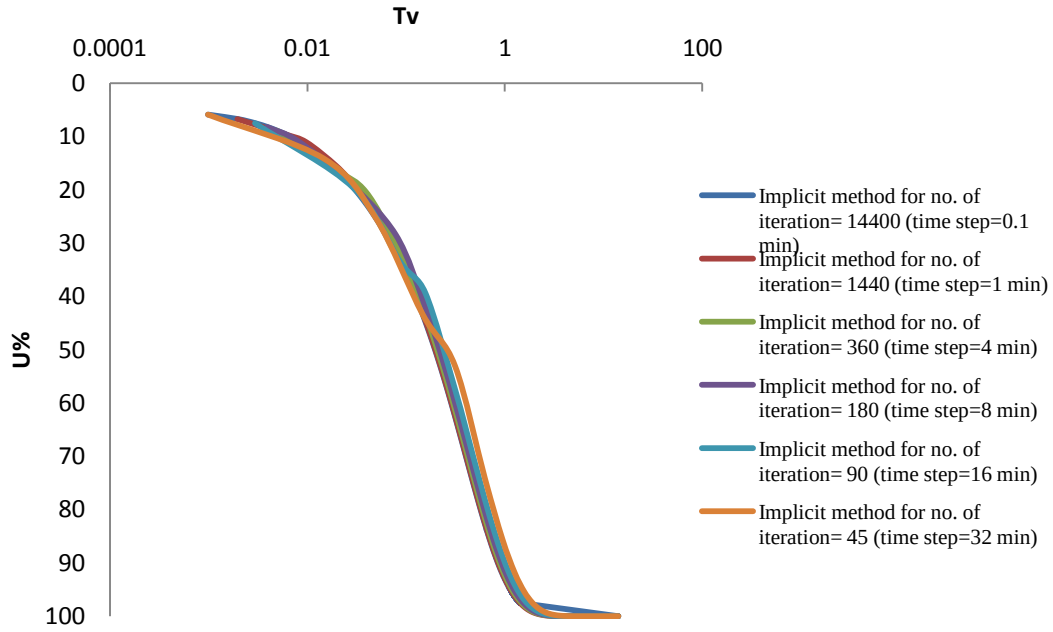

Graph 5.50:- Comparison graph for different no of iteration (by implicit method) for loading 20(kN/m^2) at 10% bentonite.

5.8.3 Comparison graph for different time step by implicit method for loading 40(kN/m^2) at 10% bentonite:-

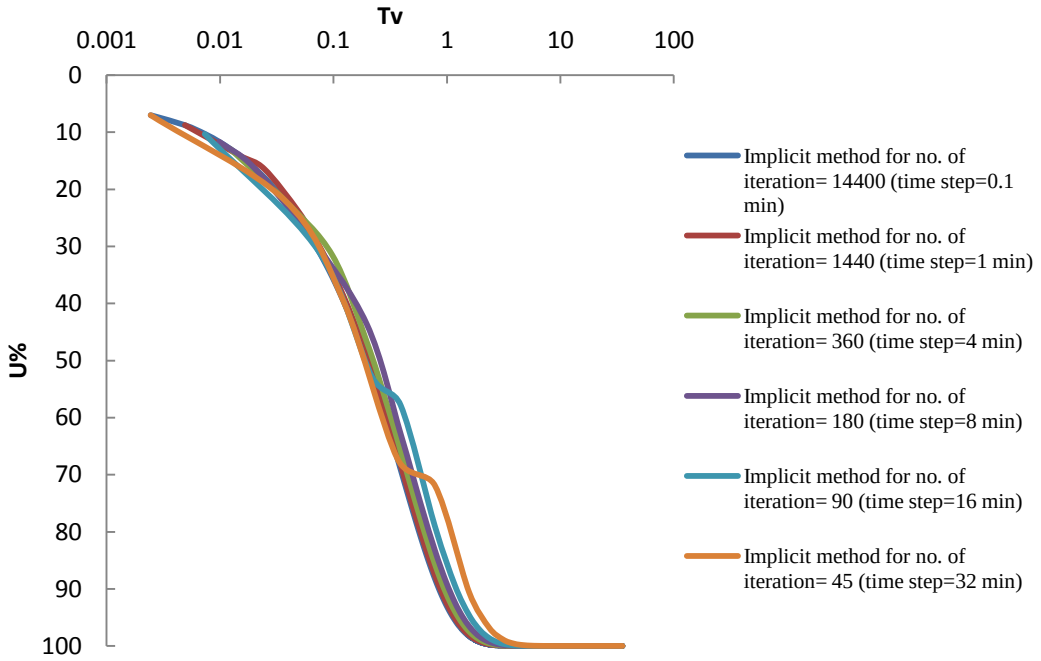

Graph 5.51:- Comparison graph for different no of iteration (by implicit method) for loading 40(kN/m^2) at 10% bentonite.

5.8.4 Comparison graph for different time step by implicit method for loading 80(kN/m^2) at 10% bentonite:-

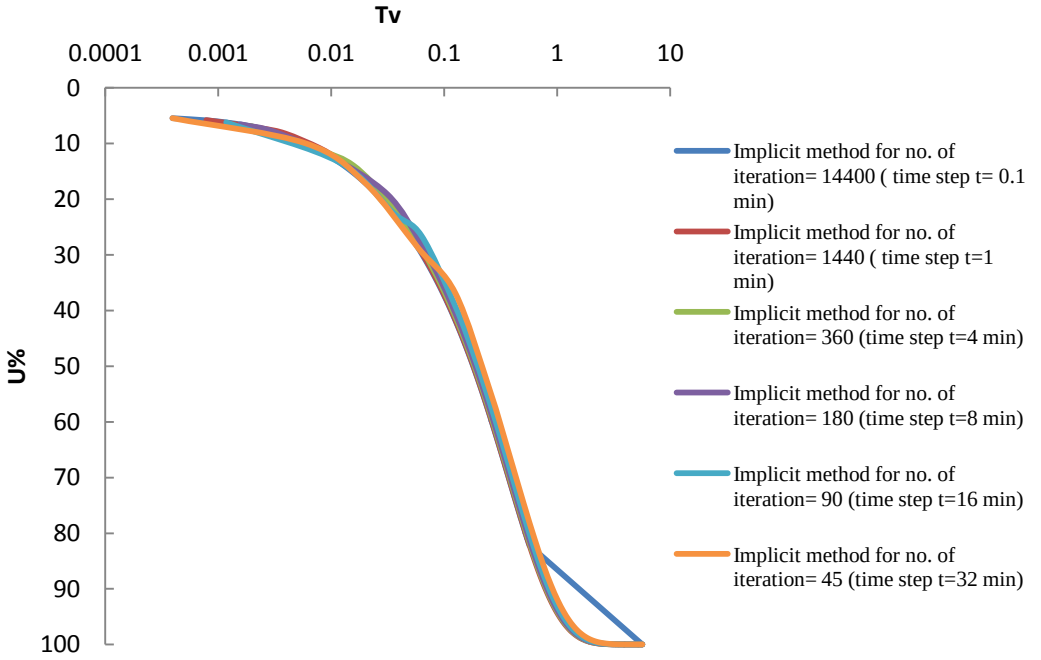

Graph 5.52:- Comparison graph for different no of iteration (by implicit method) for loading 80(kN/m^2) at 10% bentonite.

5.8.5 Comparison graph for different time step by implicit method for loading 160(kN/m^2) at 10% bentonite:-

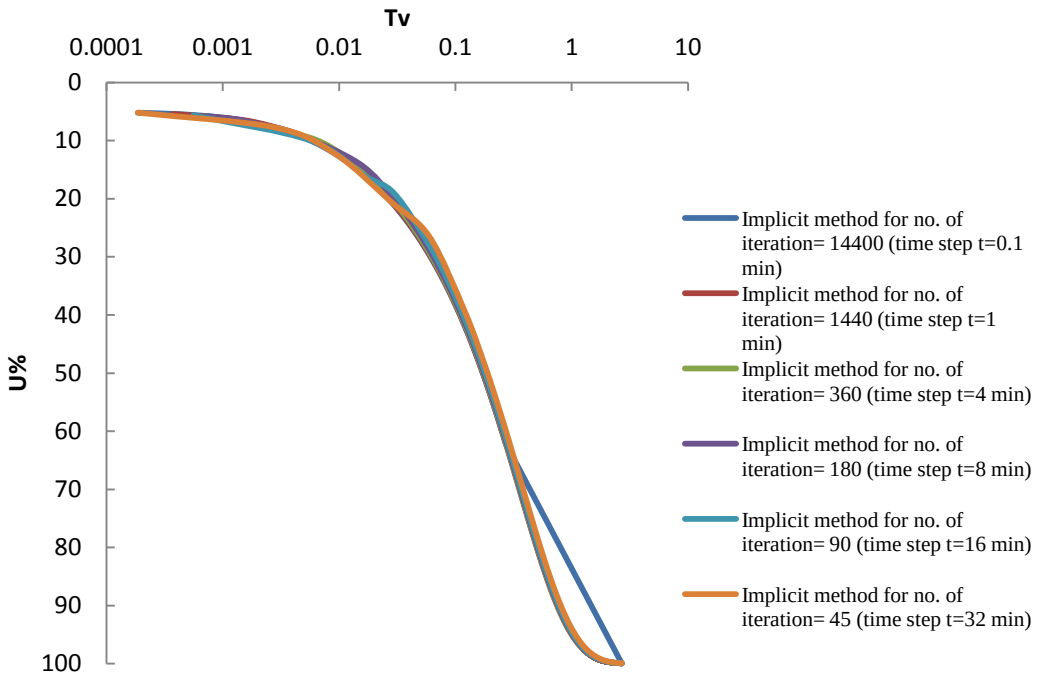

Graph 5.53:- Comparison graph for different no of iteration (by implicit method) for loading 160(kN/m^2) at 10% bentonite.

5.8.6 Comparison graph for different time step by implicit method for loading 320(kN/m^2) at 10% bentonite:-

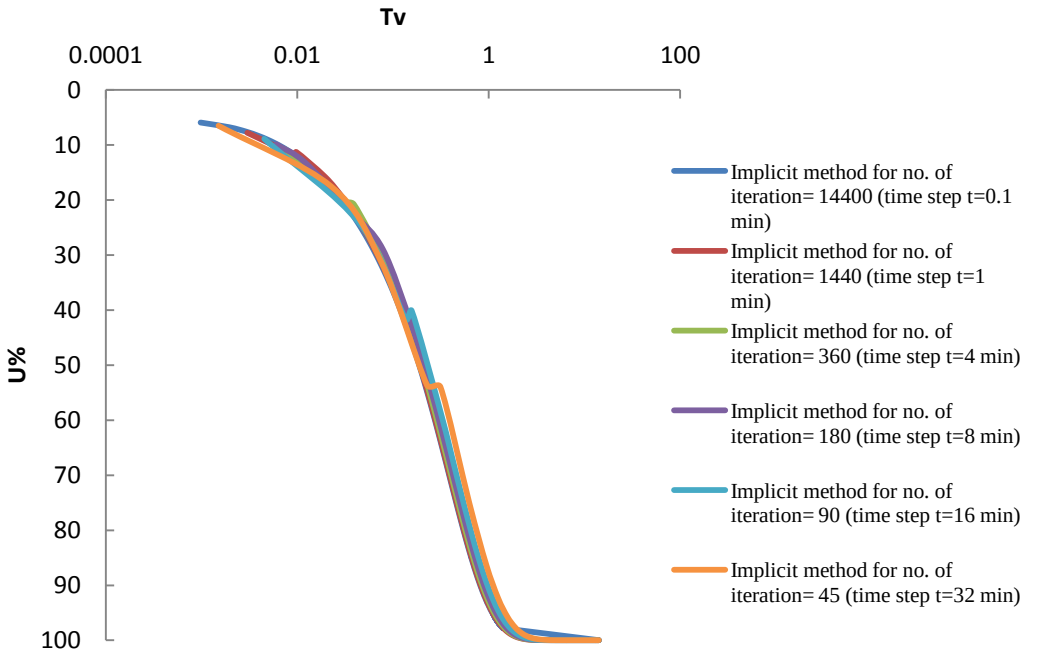

Graph 5.54:- Comparison graph for different no of iteration (by implicit method) for loading 320(kN/m^2) at 10% bentonite.

5.8.7 Comparison graph for different time step by implicit method for loading 640(kN/m^2) at 10% bentonite:-

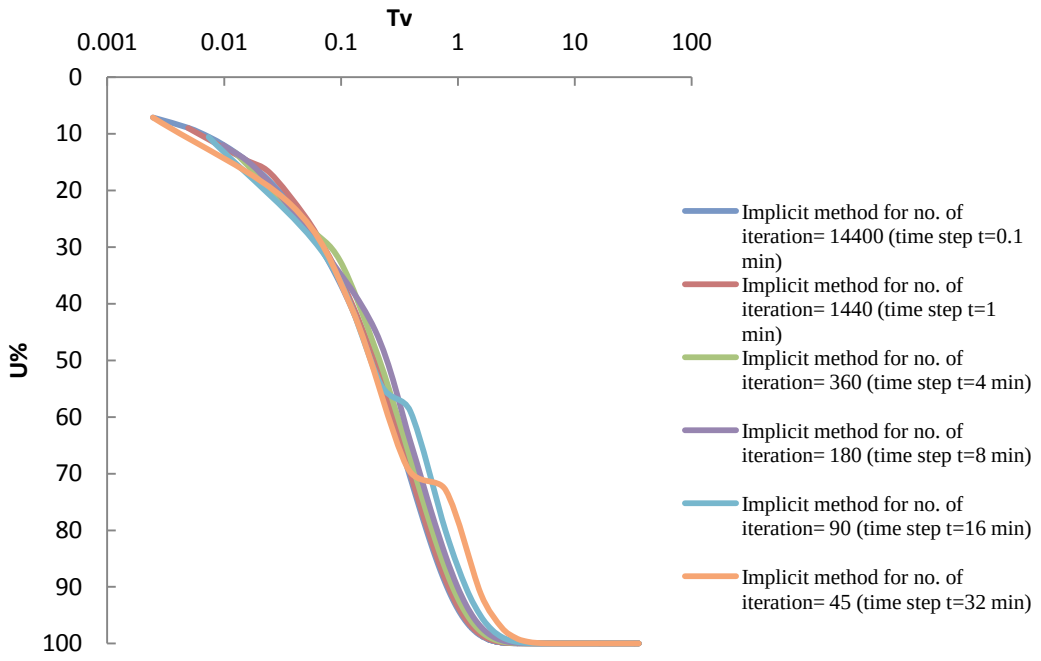

Graph 5.55:- Comparison graph for different no of iteration (by implicit method) for loading 640(kg/cm^2) at 10% bentonite.

5.8.8 Comparison graph for different time step by implicit method for loading 10(kN/m^2) at 15% bentonite:-

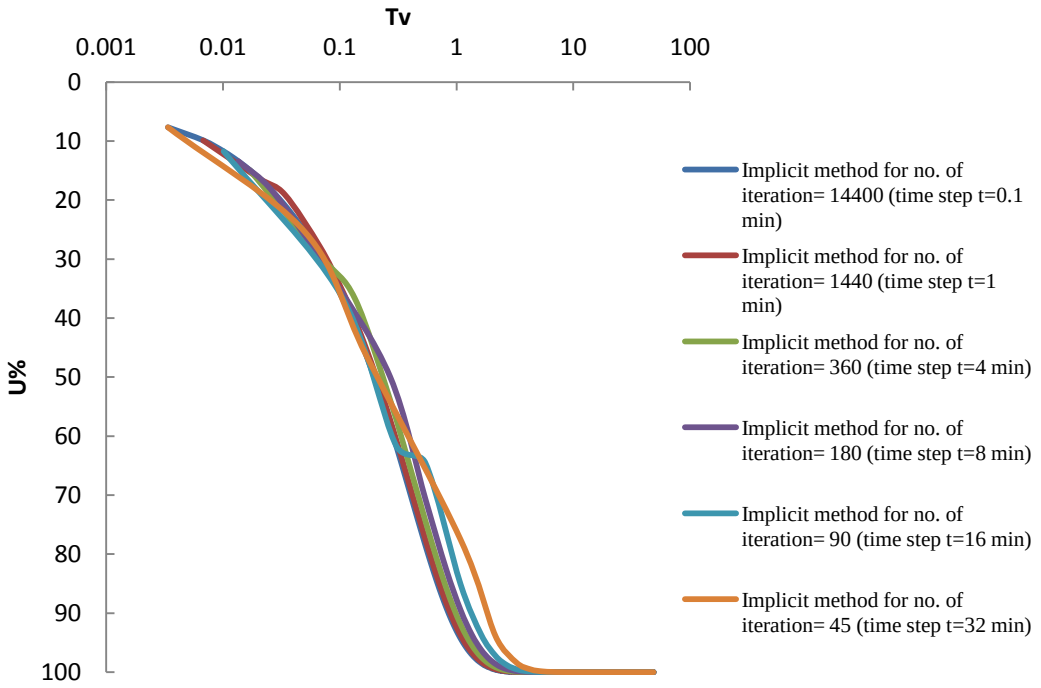

Graph 5.56:- Comparison graph for different no of iteration (by implicit method) for loading 10(kN/m^2) at 15% bentonite.

5.8.9 Comparison graph for different time step by implicit method for loading 20(kN/m^2) at 15% bentonite:-

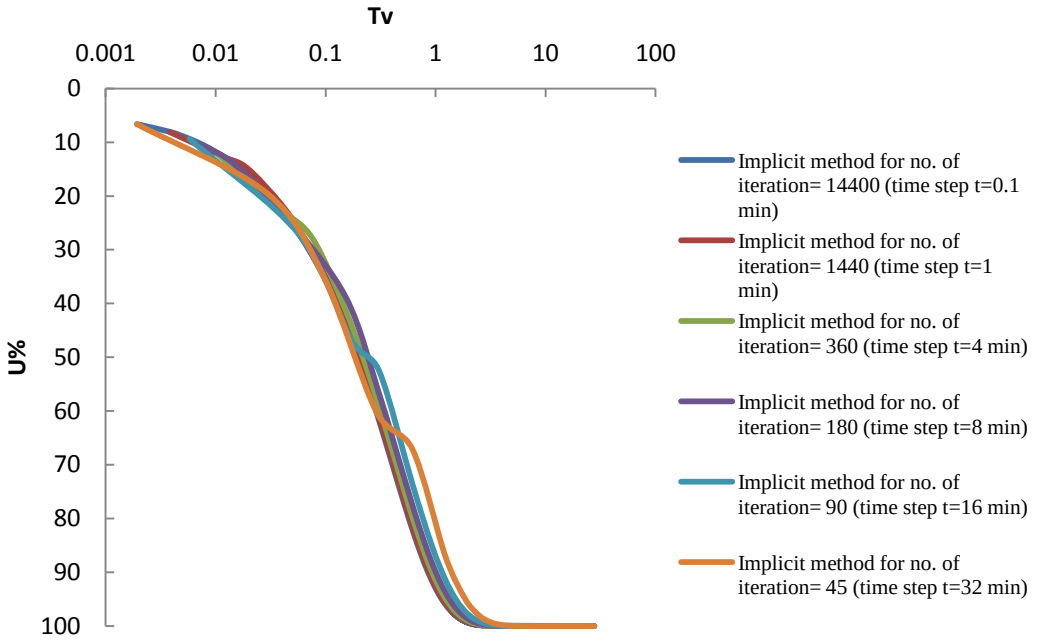

Graph 5.57:- Comparison graph for different no of iteration (by implicit method) for loading 20(kN/m^2) at 15% bentonite.

5.8.10 Comparison graph for different time step by implicit method for loading 40(kN/m^2) at 15% bentonite:-

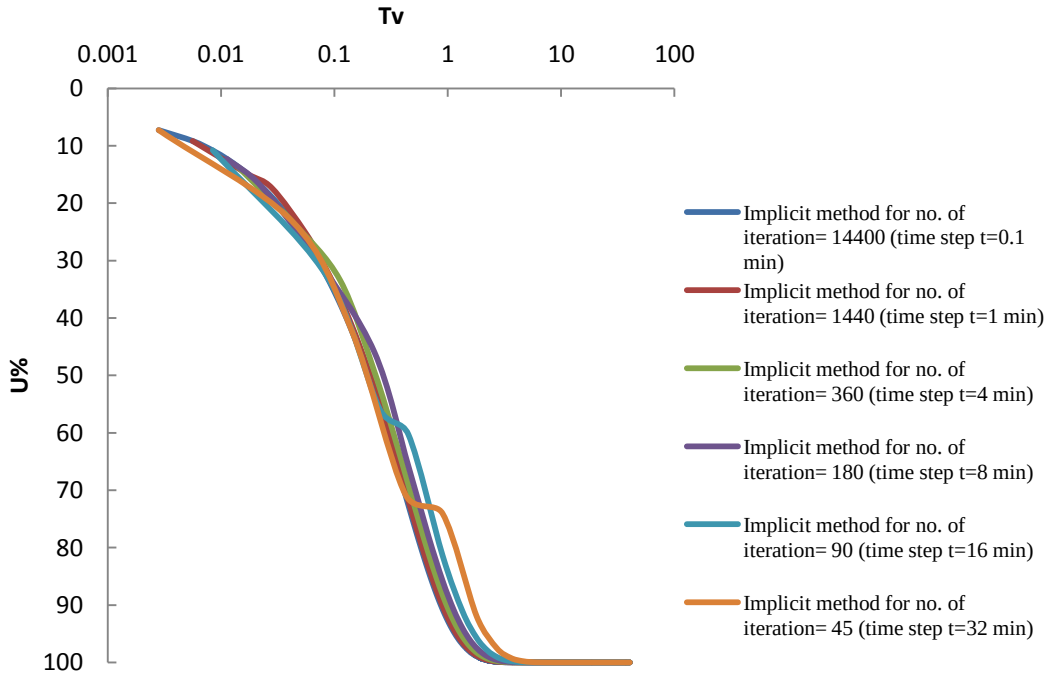

Graph 5.58:- Comparison graph for different no of iteration (by implicit method) for loading 40(kN/m^2) at 15% bentonite.

5.8.11 Comparison graph for different time step by implicit method for loading 80(kN/m^2) at 15% bentonite:-

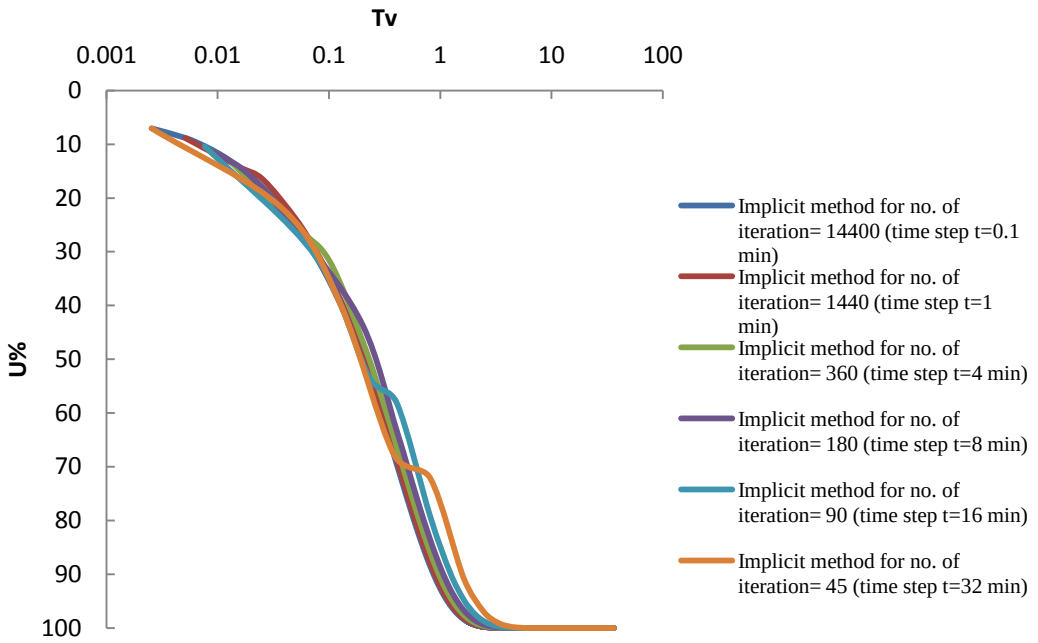

Graph 5.59:- Comparison graph for different no of iteration (by implicit method) for loading 80(kN/m^2) at 15% bentonite.

5.8.12 Comparison graph for different time step by implicit method for loading 160(kN/m^2) at 15% bentonite:-

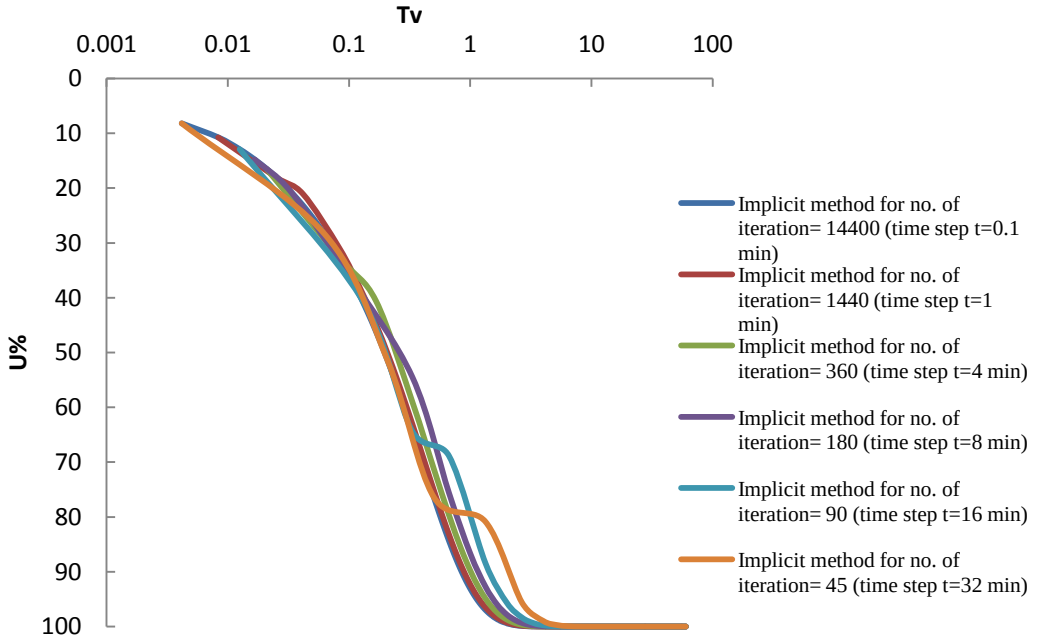

Graph 5.60:- Comparison graph for different no of iteration (by implicit method) for loading 160(kN/m^2) at 15% bentonite.

5.8.13 Comparison graph for different time step by implicit method for loading 320(kN/m^2) at 15% bentonite:-

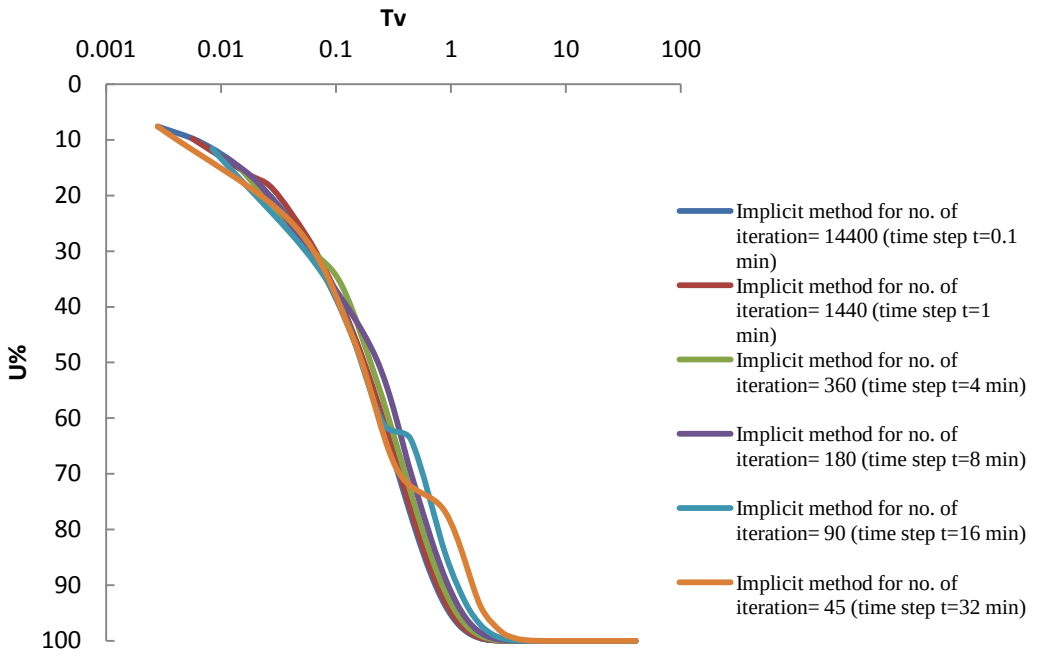

Graph 5.61:- Comparison graph for different no of iteration (by implicit method) for loading 320(kN/m^2) at 15% bentonite.

5.8.14 Comparison graph for different time step by implicit method for loading 640(kN/m^2) at 15% bentonite:-

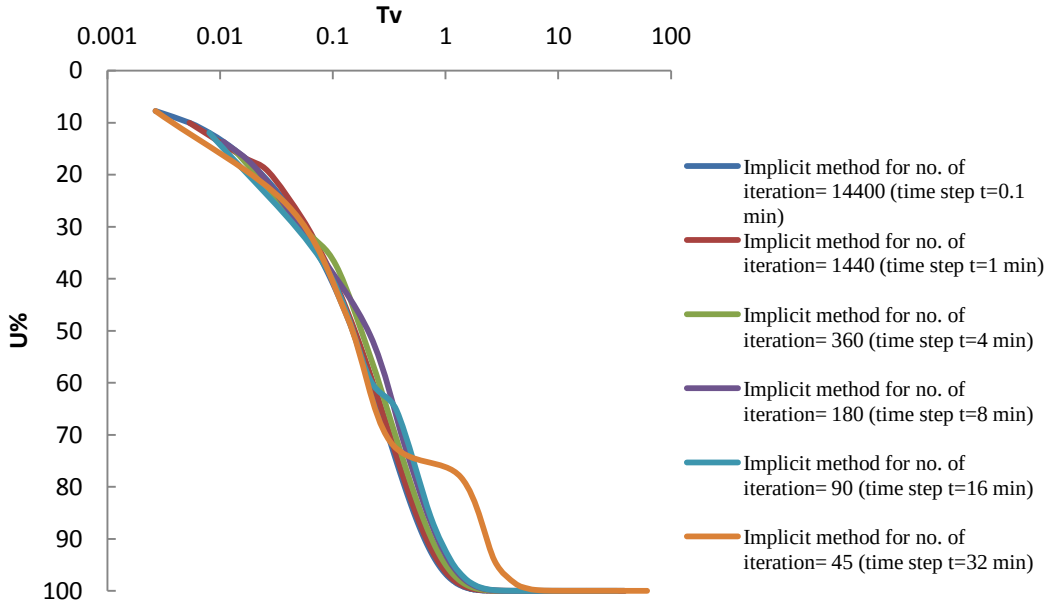

Graph 5.62:- Comparison graph for different no of iteration (by implicit method) for loading 604(kN/m^2) at 15% bentonite.

5.8.15 Comparison graph for different time step by implicit method for loading 10(kN/m^2) at 20% bentonite:-

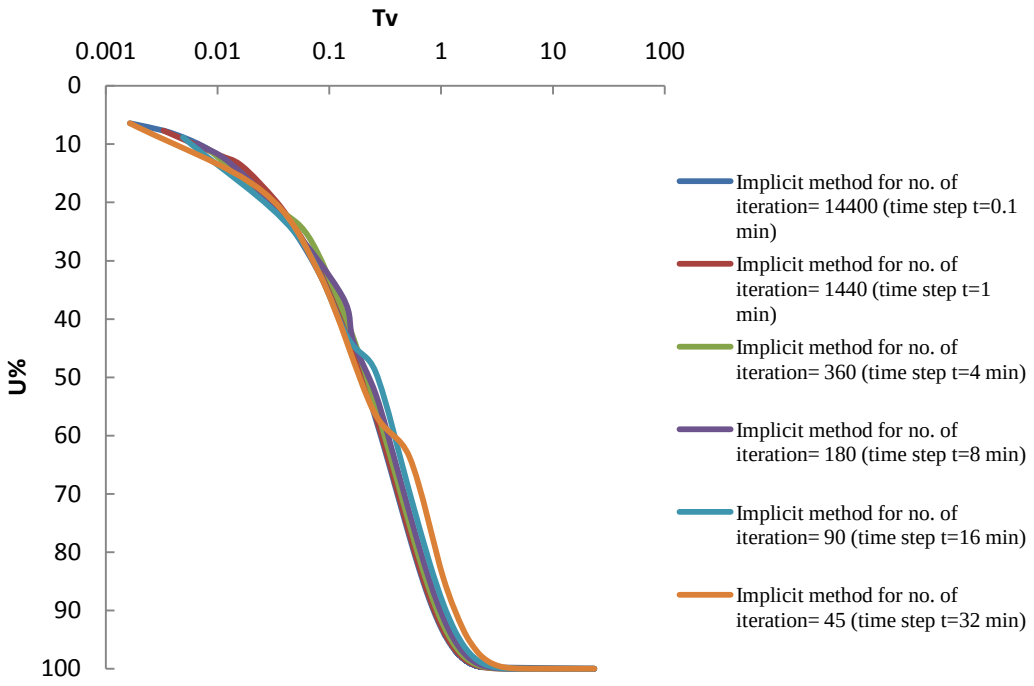

Graph 5.63:- Comparison graph for different no of iteration (by implicit method) for loading 10(kN/m^2) at 20% bentonite.

5.8.16 Comparison graph for different time step by implicit method for loading 20(kN/m^2) at 20% bentonite:-

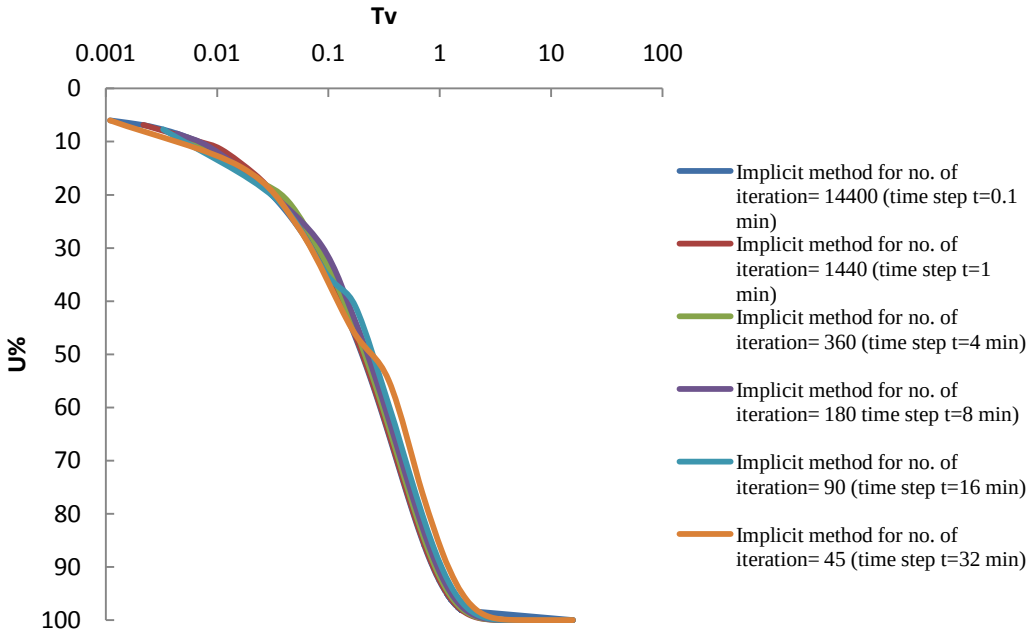

Graph 5.64:- Comparison graph for different no of iteration (by implicit method) for loading 20(kN/m^2) at 20% bentonite.

5.8.17 Comparison graph for different time step by implicit method for loading 40(kN/m^2) at 20% bentonite:-

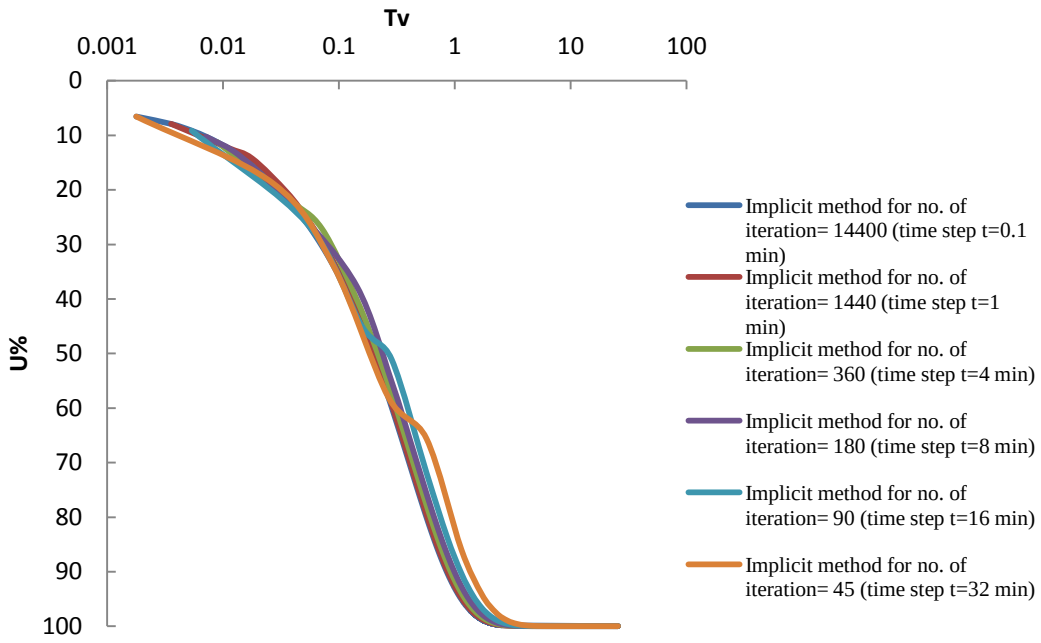

Graph 5.65:- Comparison graph for different no of iteration (by implicit method) for loading 40(kN/m^2) at 20% bentonite.

5.8.18 Comparison graph for different time step by implicit method for loading 80(kN/m^2) at 20% bentonite:-

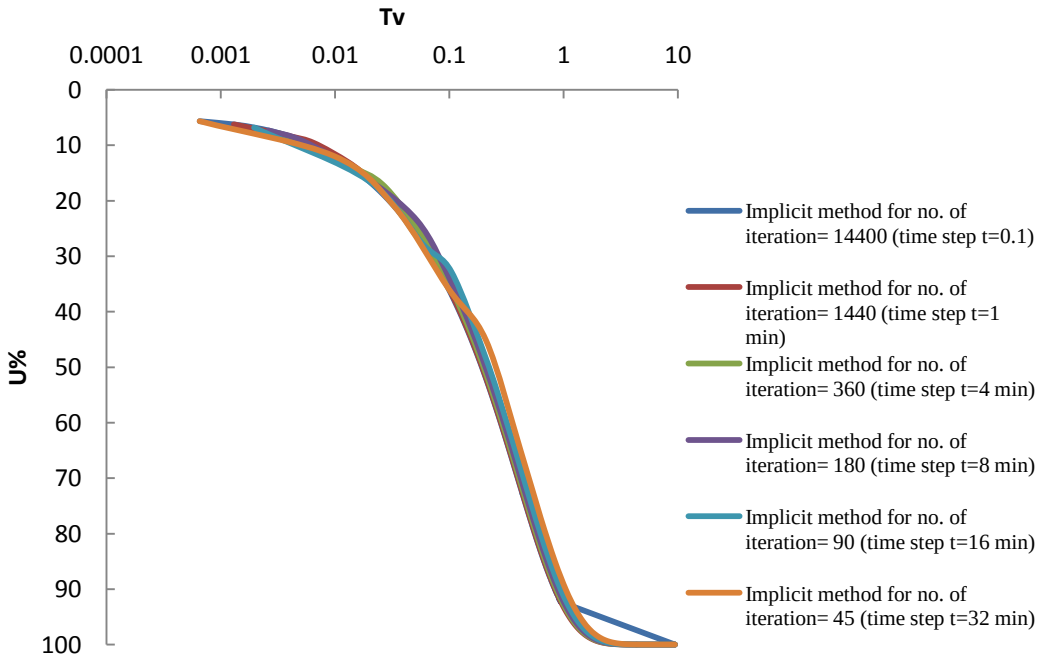

Graph 5.66:- Comparison graph for different no of iteration (by implicit method) for loading 80(kN/m^2) at 20% bentonite.

5.8.19 Comparison graph for different time step by implicit method for loading 160(kN/m^2) at 20% bentonite:-

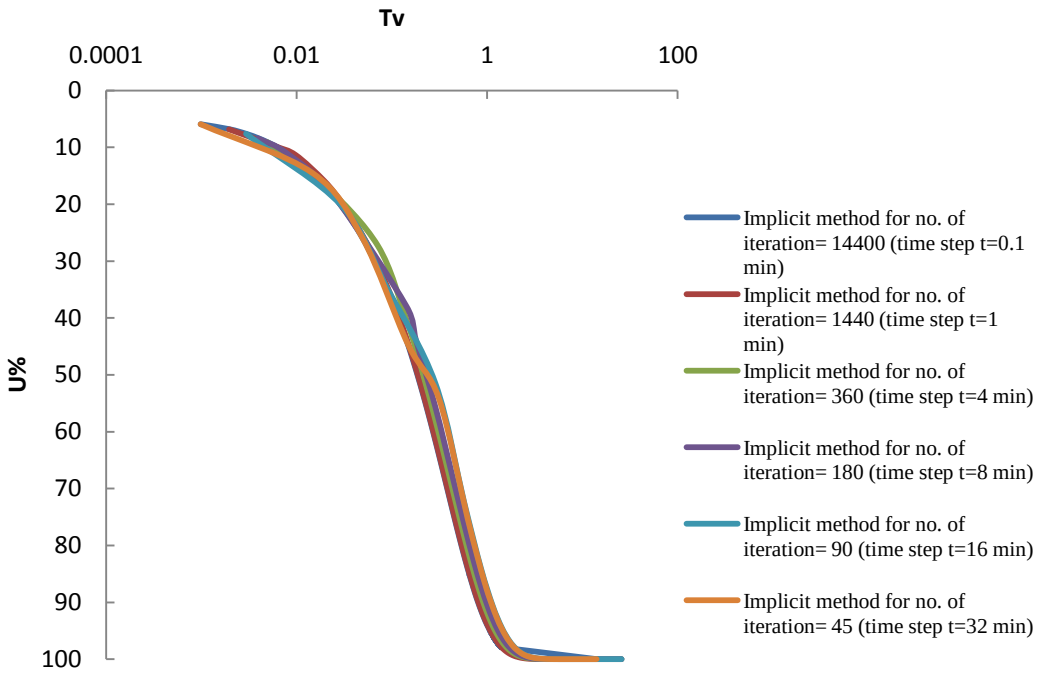

Graph 5.67:- Comparison graph for different no of iteration (by implicit method) for loading 160(kN/m^2) at 20% bentonite.

5.8.20 Comparison graph for different time step by implicit method for loading 320(kN/m^2) at 20% bentonite:-

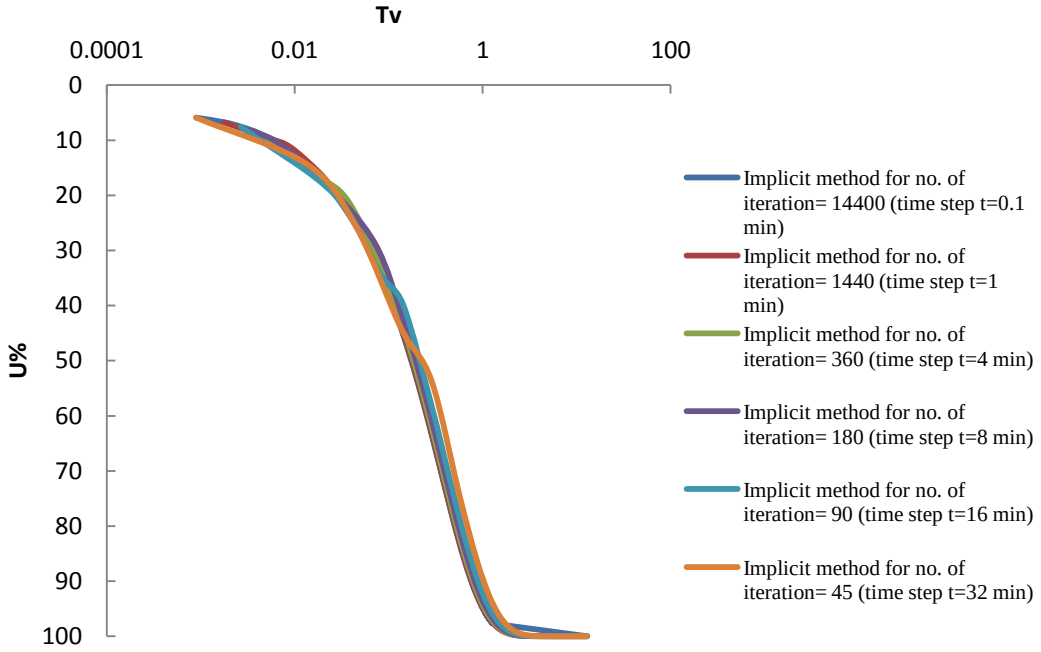

Graph 5.68:- Comparison graph for different no of iteration (by implicit method) for loading 320(kN/m^2) at 20% bentonite.

5.8.21 Comparison graph for different time step by implicit method for loading 640(kN/m^2) at 20% bentonite:-

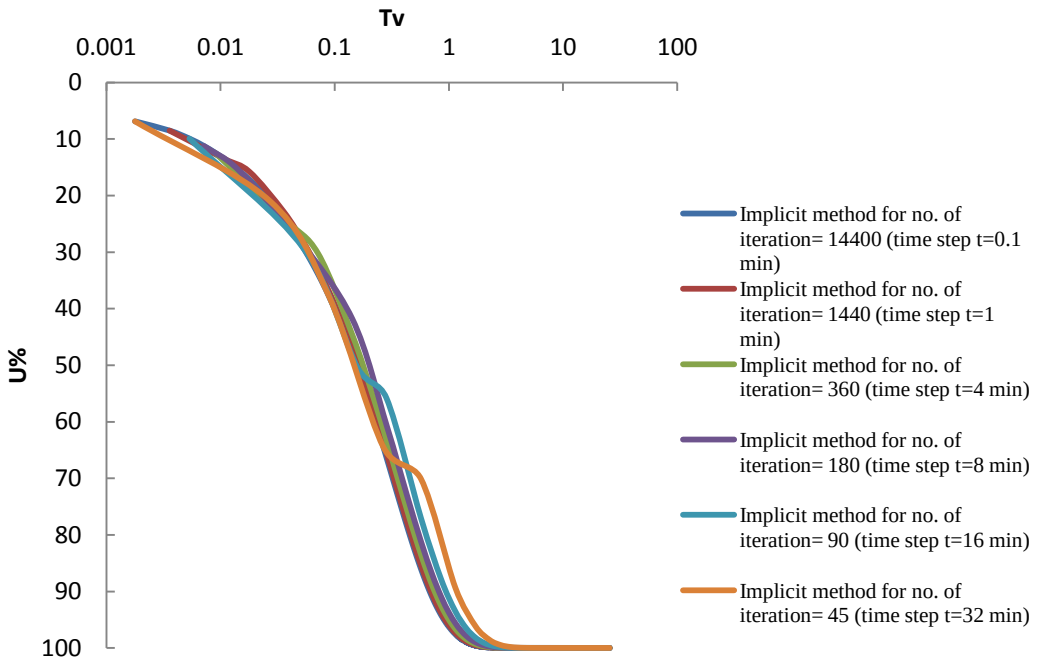

Graph 5.69:- Comparison graph for different no of iteration (by implicit method) for loading 640(kN/m^2) at 20% bentonite.

5..22 Comparison graph for different time step by implicit method for loading 10(kN/m^2) at 25% bentonite:-

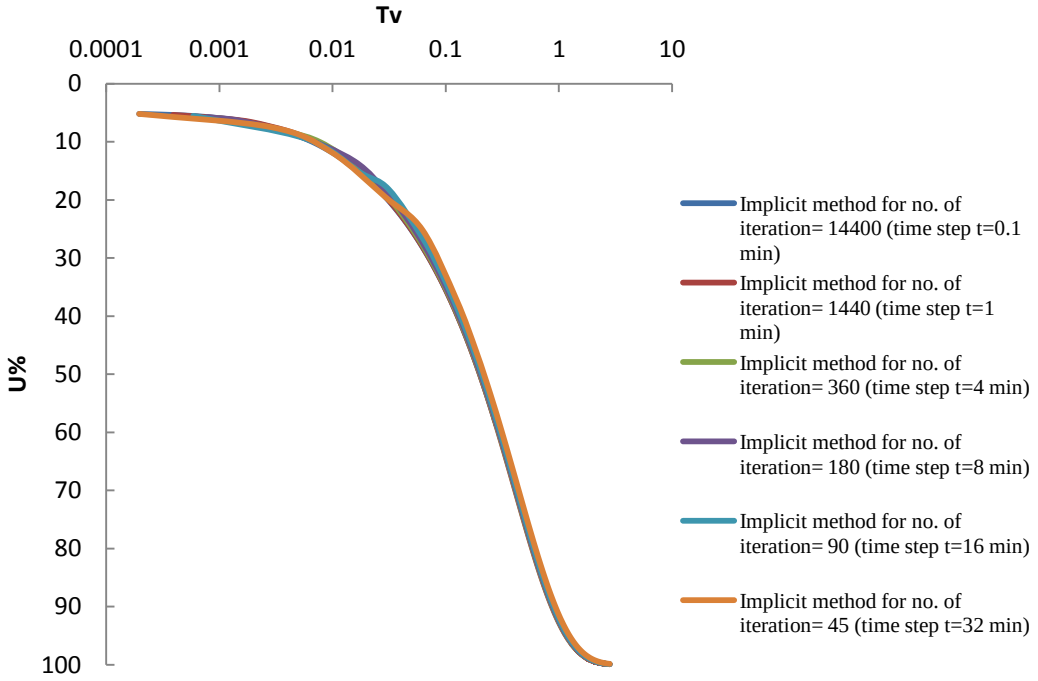

Graph 5.70:- Comparison graph for different no of iteration (by implicit method) for loading 10(kN/m^2) at 25% bentonite.

5.8.23 Comparison graph for different time step by implicit method for loading 20(kN/m^2) at 25% bentonite:-

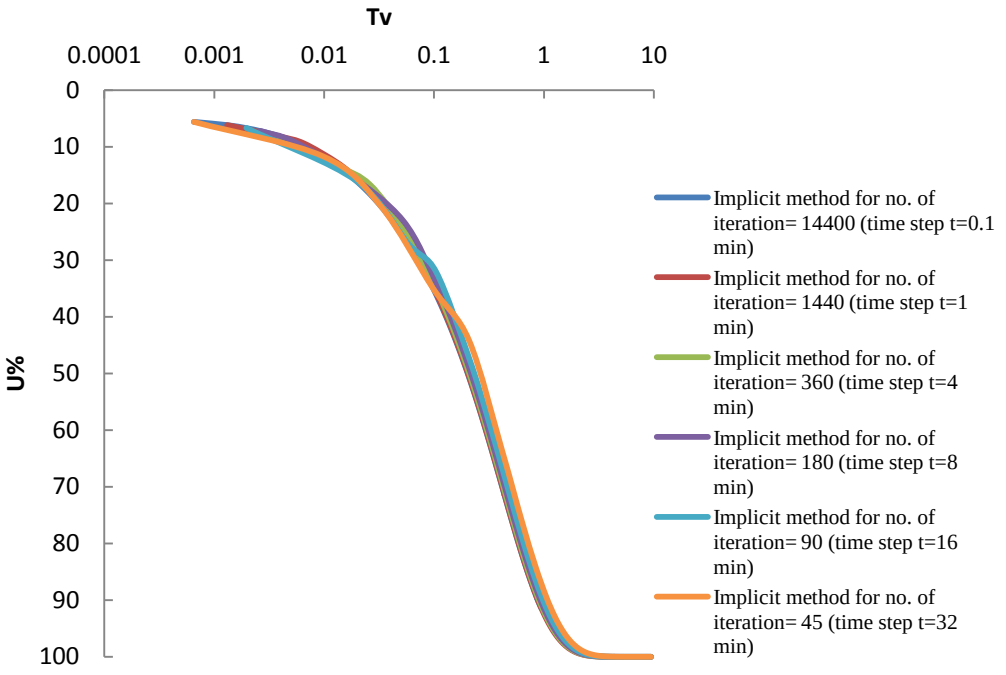

Graph 5.71:- Comparison graph for different no of iteration (by implicit method) for loading 20(kN/m^2) at 25% bentonite.

5.8.24 Comparison graph for different time step by implicit method for loading 40(kN/m^2) at 25% bentonite:-

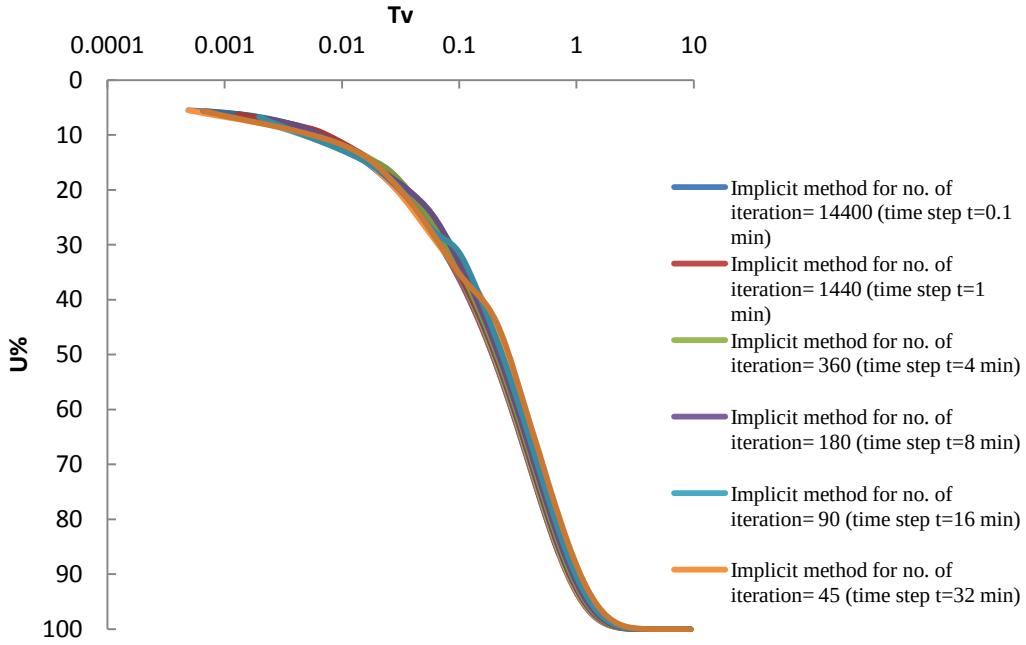

Graph 5.72:- Comparison graph for different no of iteration (by implicit method) for loading 40(kN/m^2) at 25% bentonite.

5.8.25 Comparison graph for different time step by implicit method for loading 80(kN/m^2) at 25% bentonite:-

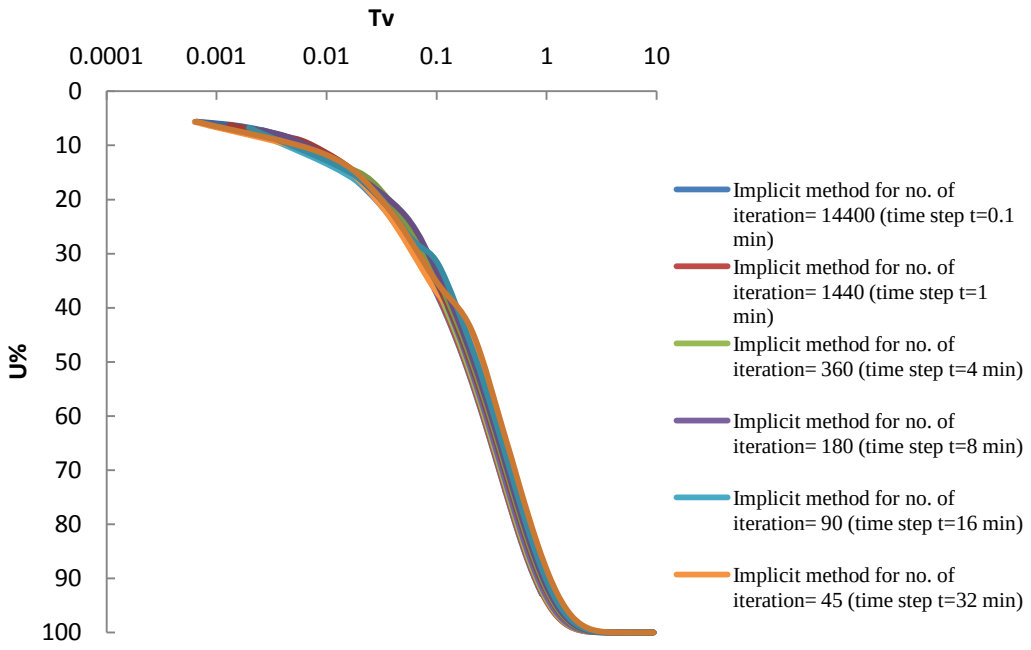

Graph 5.73:- Comparison graph for different no of iteration for (by implicit method) loading 80(kN/m^2) at 25% bentonite.

5.8.26 Comparison graph for different time step by implicit method for loading 160(kN/m^2) at 25% bentonite:-

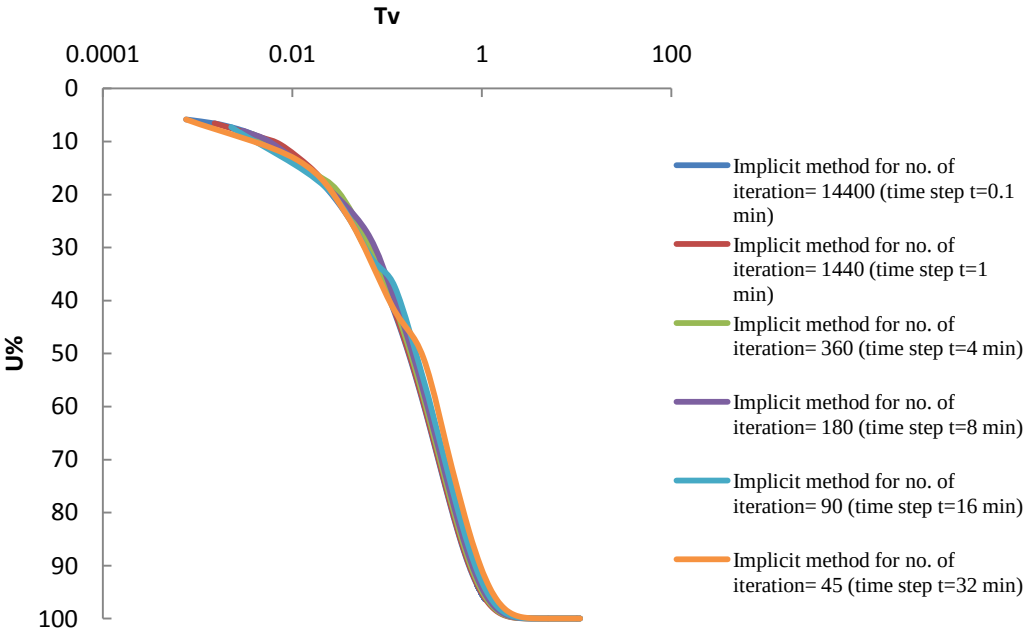

Graph 5.74:- Comparison graph for different no of iteration for loading 160(kN/m^2) at 25% bentonite.

5.8.27 Comparison graph for different time step by implicit method for loading 320(kN/m^2) at 25% bentonite:-

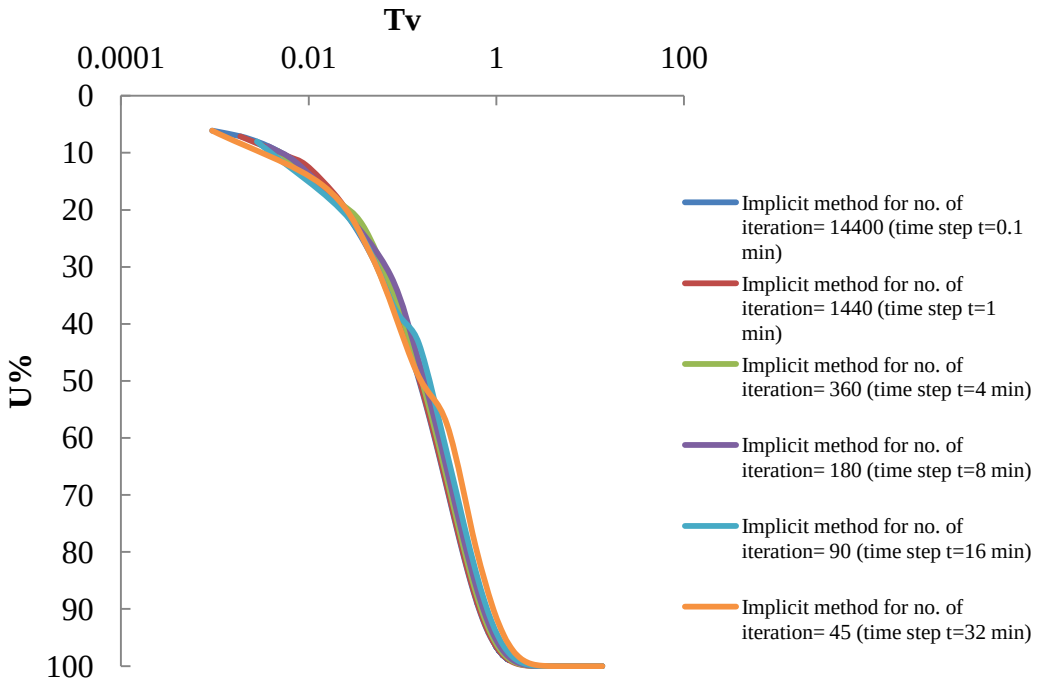

Graph 5.75:- Comparison graph for different no of iteration for loading 320(kN/m^2) at 25% bentonite.

5.8.28 Comparison Graph for different time step by implicit method for loading 640(kN/m^2) at 25% bentonite:-

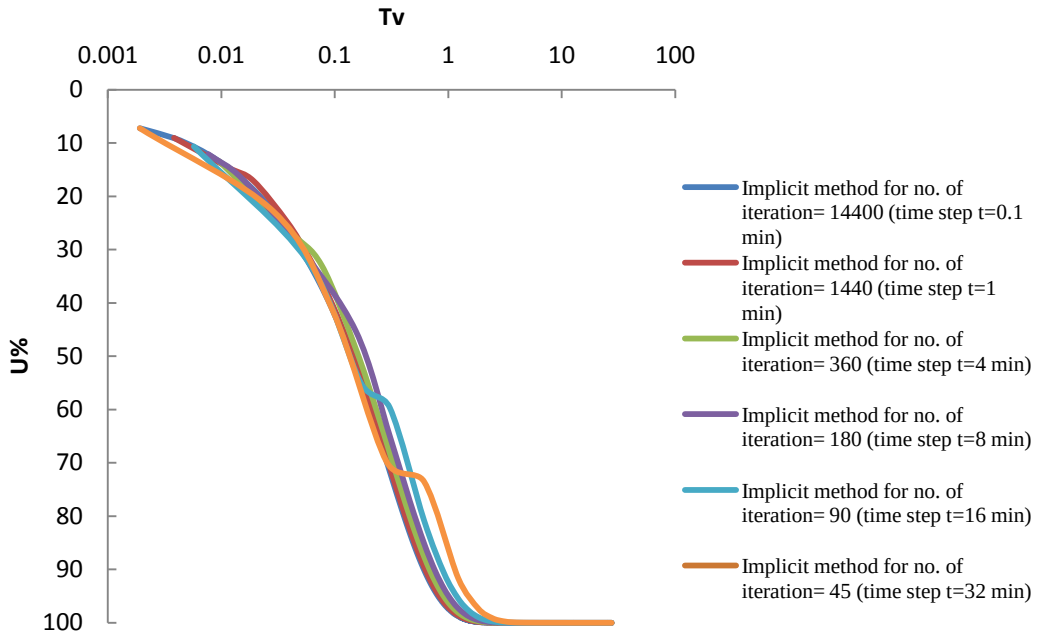

Graph 5.76:- Comparison graph for different no of iteration for loading 640(kN/m^2) at 25% bentonite.

5.8.29 Comparison graph for different time step by implicit method for loading 10(kN/m^2) at 100% bentonite:-

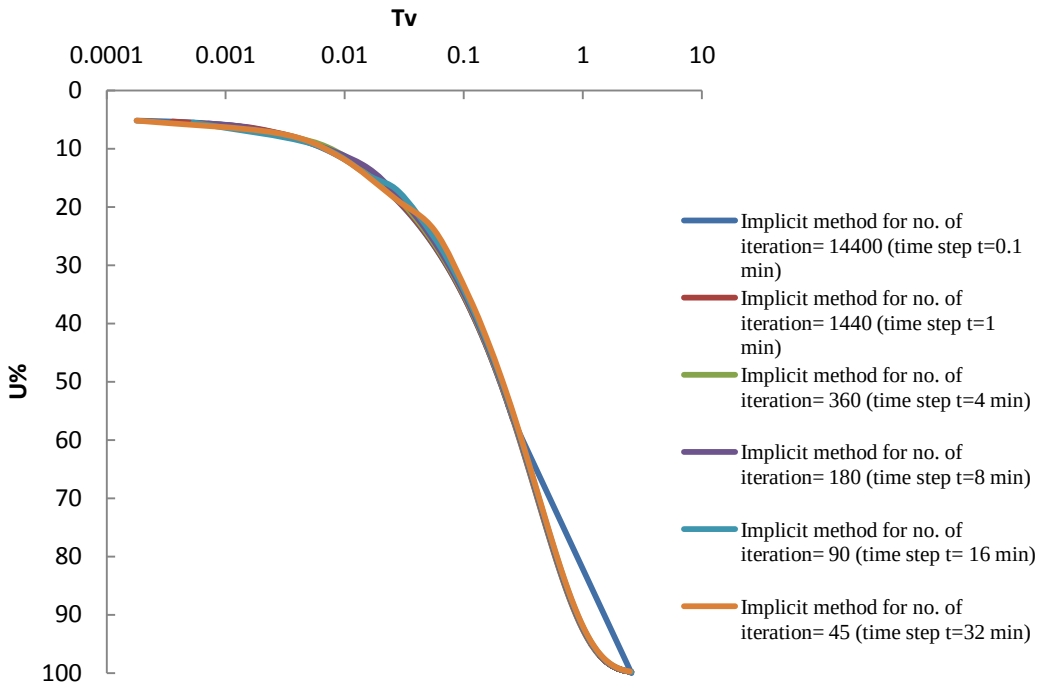

Graph 5.77:- Comparison graph for different no of iteration for loading 10(kN/m^2) at 100% bentonite.

5.8.30 Comparison graph for different time step by implicit method for loading 20(kN/m^2) at 100% bentonite:-

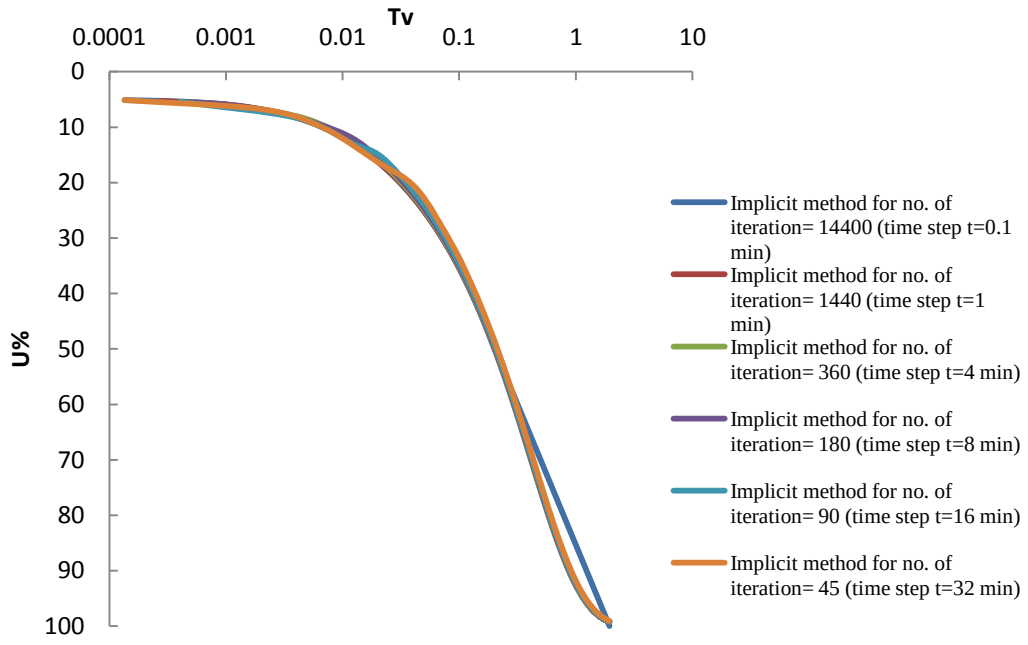

Graph 5.78:- Comparison graph for different no of iteration for loading 20(kN/m^2) at 100% bentonite.

5.8.31 Comparison graph for different time step by implicit method for loading 40(kN/m^2) at 100% bentonite:-

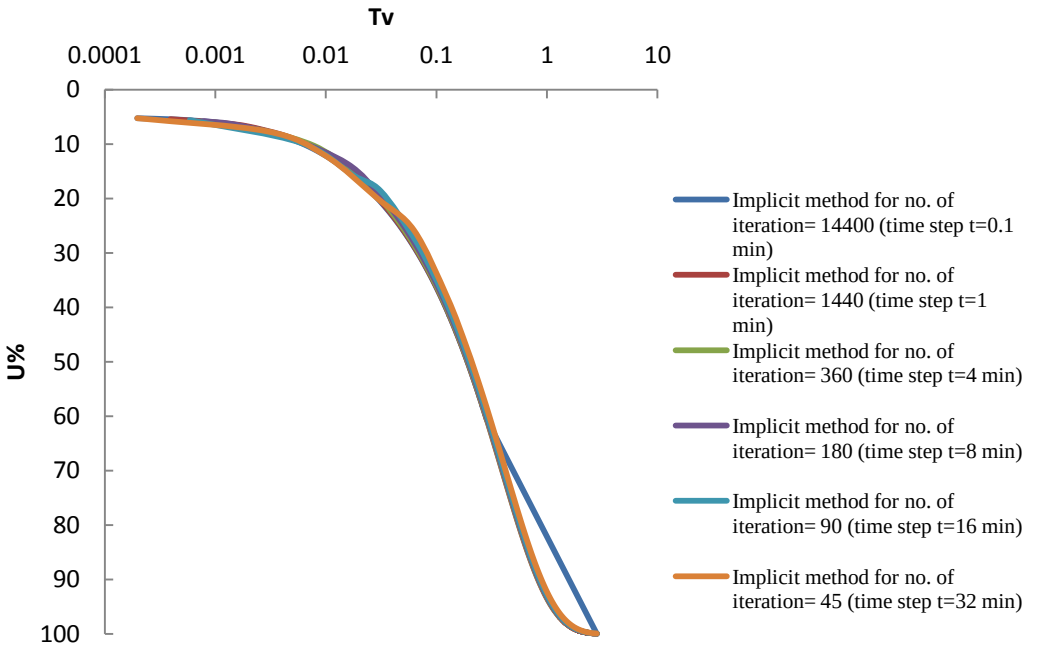

Graph 5.79:- Comparison graph for different no of iteration for loading 40(kN/m^2) at 100% bentonite.

5.8.32 Comparison graph for different time step by implicit method for loading 80(kN/m^2) at 100% bentonite:-

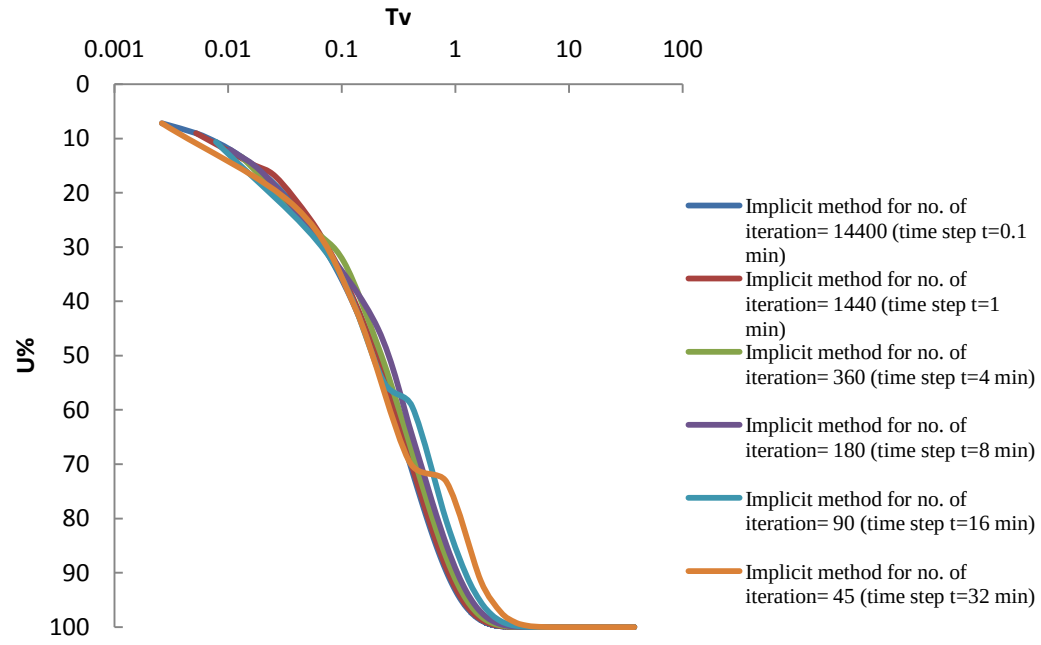

Graph 5.80:- Comparison graph for different no of iteration for loading 80(kN/m^2) at 100% bentonite.

5.8.33 Comparison graph for different time step by implicit method for loading 160(kN/m^2) at 100% bentonite:-

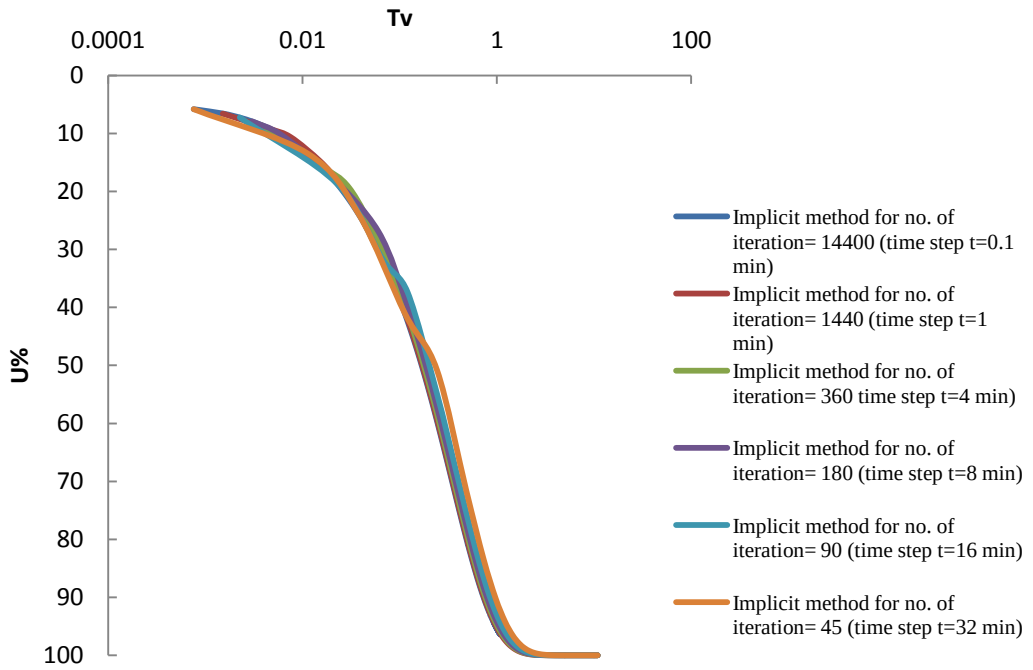

Graph 5.81:- Comparison graph for different no of iteration for loading 160(kN/m^2) at 100% bentonite.

5.8.34 Comparison graph for different time step by implicit method for loading 320(kN/m^2) at 100% bentonite:-

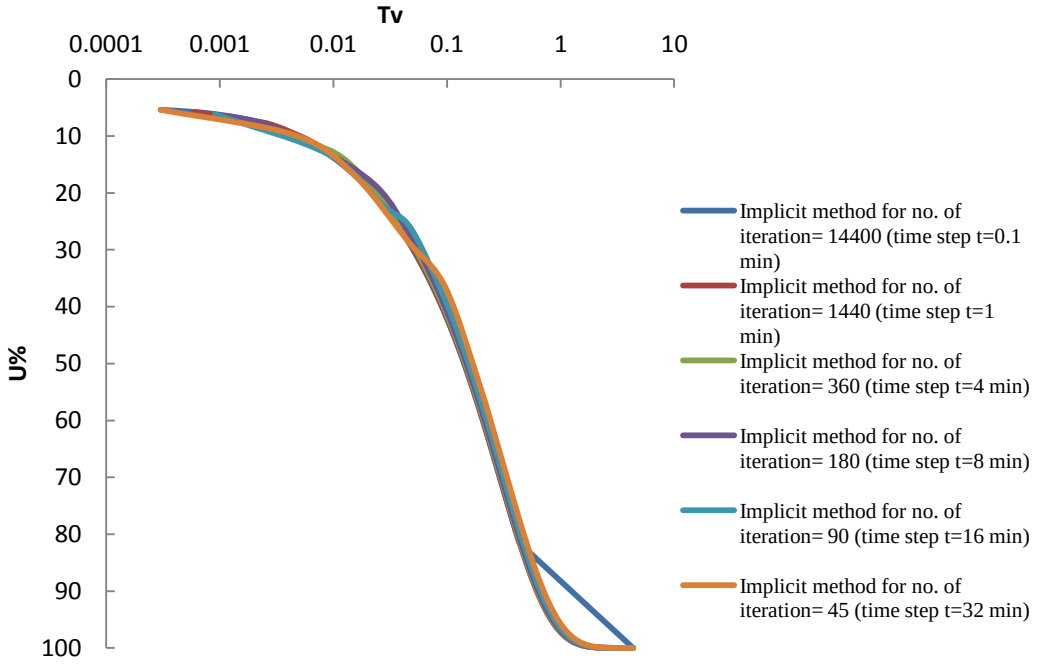

Graph 5.82:- Comparison graph for different no of iteration (by implicit method) for loading 320(kN/m^2) at 100% bentonite.

5.8.35 Comparison graph for different time step by implicit method for loading 640(kN/m^2) at 100% bentonite:-

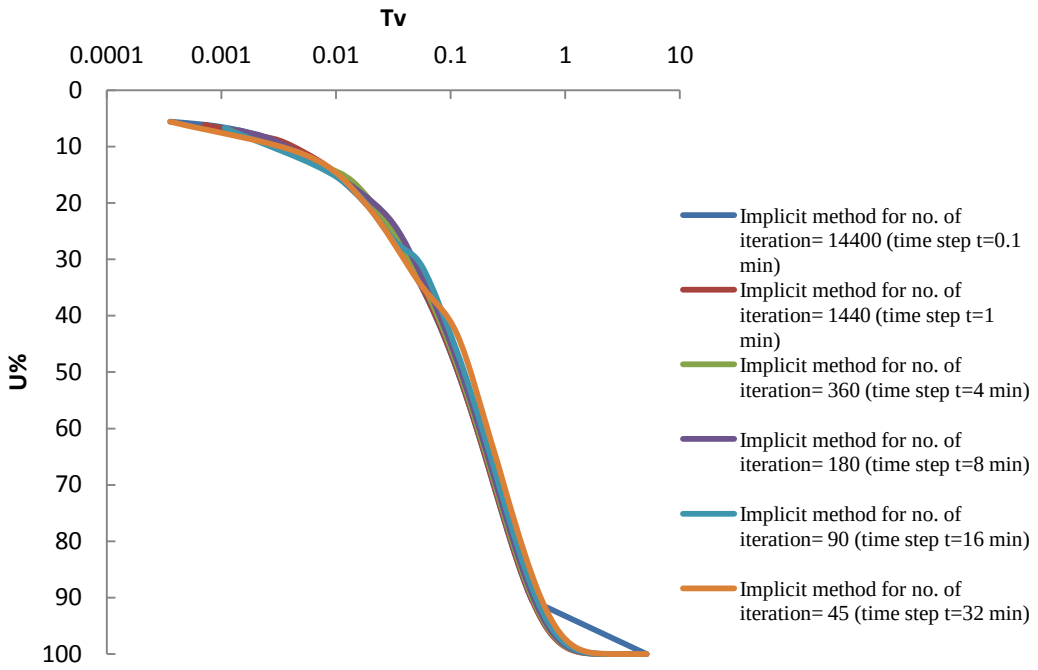

Graph 5.83:- Comparison graph for different no of iteration (by implicit method) for loading 640(kN/m^2) at 100% bentonite.

Chapter 6—Result's Discussion and Conclusion

6.1 Discussion

From the above analysis we can determine various parameters that decides the total degree of settelement in soil sample containing different percentage of bentonite. Different test were carried out and data obtaion corresponds to each test. Specific gravity of sand as well as bentonite is determined. Specific gravity of sand is 2.676 and for bentonite it is comes as 2.318. Specific gravity for different bentonite mix is also determined as the percentage of bentonite increses the specific gravity of sample decreases. The liquid limit of bentonite is 386% and the plastic limit is 111.48%. Thus bentonite is highly platic and can be used as adhesive in some ceramic bodies and formulation of mortars.

In this work void ratio has been estimated for different load conditions for varying bentonite percentages in the bentonite-sand mixture. As observed from the experimental study, void ratio decreases with increasing applied stress. On addition of lower percentages of bentonite to sandy soil namely, 10 % the void ratio of the bentonite-sand mix decreases at higher stress. When the percentage is increased to 15%, the mix shows increased void ratio at lesser stress followed by substantial decrease in void ratio (0.3912) at higher stress (6.4kg/cm^2). On further increse of bentonite in the mix, void ratio increases for lower as well as higher applied stresses.

Settlement and applied loads are related as the loads cause settlement. Settlements in the soil mix on application of loads were observed for different compositions of bentonite and sand. Settlement increases with increasing load for all the samples. Also with increasing percentages of bentonite in the soil the settlement experienced is more. Maximum settlement for the bentonite as observed is 9.36mm in a 20mm thick sample.

Co-efficient of permeability increases initially with load increment for all the samples to some extent and then decresases for higher applied stresses.Average value of co-efficient of permeability increases increases as the bentonite content increases from 10% to 15% in sample. Further increases in bentonite percent cause

decrease in the value of co-efficient of permeability. The maximum average value of co-efficient of permeability is 0.00209(mm/min) for 15% bentonite content and have minimum value 0.0003534(mm/min) for 100% bontonite content in sample.

If the permeability of the material is small, the deformations may be considerably hindered, or at least retarded, by the pore fluid. Thus in this way it is clear that resultant consolidation will not only takes place due to expulsion of pore water & release of stress but also due to restructuring of soil solids. The assumptions that the decrease in permeability is proportional to the decrease in compressibility during the consolidation process or permeability is proportional to the coefficient of consolidation holds good for the experiment being carried out.

Coefficient of consolidation varies in a sinusoidal manner with increasing applied effective stress on a logarithmic plot. With increasing amount of bentonite in the mix the coefficient of consolidation varies in curvilinear manner. Average Coefficient of consolidation is maximum at 15% bentonite in the mix i.e. 2.5643 (mm^2/min) and decreases after further addition of bentonite to the soil.

The Tv-U curve is compared by Numerical analysis (explicit method) and Fourier analysis. Initially there is deviation in solution obtained by both curve but as the time factor increases both curve converges. The deviation increases with the increase in percentage bentonite content as well as increase in loading. There is sudden increase in deviation in the value of U% for incremental loading 160kN/m^2 to 320kN/m^2. For the sample with 100 percent bentonite and applied loading 640kN/m^2 the maximum variation occur in the two solutions.

The Tv-U curve is also compared by Implicit solution for different time step (t=0.1min, 1min, 4min, 8min, 16min and 32min.) All these converge for final consolidation values. But for initial value there is deviation i.e error the solutions. The longer we take the time step more error will occur. Implicit method gives more accurate and reliable result for smaller time step. Like for time step t= 0.1 min time give much more accurate result then time step t= 32 min, but the no of iteration increases. For intermediate time step t= 4 min the result is accurate as iteration is also less.

Initially when the bentonite percentage is less in the sample the primary consolidation completed early. As the bentonite percentage increases in sample the time required for primary consolidation increases. Primary consolidation is assumed to be completed at 90% degree of consolidation. As the load increases the primary consolidation achieve at early stage.

It is clear that decrease in the bentonite percentage in the sand-bentonite mix results in increases of 'rate of consolidation' and consolidation is achieved at a faster rate. 'Rate of consolidation' increases corresponding to the rate of increase of sand in the mix.

6.2 Conclusion

1. The bentonite sand mixture used as lining material for various containment structure. It is also used in earth dam to reduce seepage of water. This mixture is also used as landfill linear.

2. Degree of consolidation is successfully analysed by Fourier transform and numerical method as Explicit method and Implicit method. The predictions about consolidation process for infinitesimal strain problems for a given soil strata can be made.

3. Rate of consolidation obtained by Explicit method is compared with that obtained from Fourier transform.

4. Rate of consolidation obtained by Implicit method is compared for different time step.

5. The Numerical solution is close to obtaining rate of consolidation of soils of low permeability more clearly as compared to Fourier transform.

6. The solution obtained by Numerical solution is convergent with the Fourier for varied sample and pore water pressure converges to a single value.

7. With the help of Numerical solution the process of consolidation can be evaluated at microscopic level and for all kind of soils.

8. Amount of dissipation of pore pressure can be determined at any instant during the process of consolidation using numerical solution.

9. Numerical method is also helpful in determining consolidation of clays and can be applied to secondary consolidation superior to Fourier transform. It can be a source of very useful information like quick determination of consolidation characteristics, time compression data of the present, past and future, type and stage of consolidation, drainage conditions, load increment etc.

10. From the curves of the two respective analysis it can be concluded that with the application of Finite Difference Method

(a) Consolidation of stiff clays can be achieved in faster rate as compare to Fourier series.

(b) For fast decay of soils in terms of pore water pressure Finite difference method will be more reliable.

11. Computer programme can be developed for this technique of finite differences and computation for consolidation characteristics can be simplified.

12. The equation can be solved much faster using an implicit approach, however a minimum time step is required to obtain accurate solutions.

6.3 Future scope

1. Application of Numerical method for 3-Dimensional consolidation can be studied and analysed.

2. The application and validity of the method can be study for multilayered soil.

3. Comparison of rate of consolidation for different kinds of soil had to be done & verified by Numerical method.

4. Degree of consolidation at different time factor is carried out.

5. By combining the explicit and implicit solution approaches into a hybrid solution can be develop, which may gives accurate results quickly.

References

1. Aysen, A 2002. Soil Mechanics basic concepts and engineering applications.

2. Barden L, Berry PL. 1965; 91 Consolidation of normally consolidated clay. *J Soil Mech. Found Div ASCE (SM5):*15–35.

3. Carslaw, H. S.1930. Introduction to the theory of Fourier series and integrals, Dover, New York.

4. Conte, E. and Troncone, A. (2006) "One-Dimensional Consolidation under General Time-Dependent Loading "*Canadian Journal of Geotechnical Engineering*, 43(11), 1107 – 1116.

5. Craig, R. F. (2004). Craig's soil mechanics, *7th edition, Spon Press*,

6. Das, B. M. 2010. Principles of Geotechnical Engineering, *seventh edition.*

7. Davis EH, Raymond GP. 1965; A non-linear theory of consolidation. Geotechnique 15(2):161–73.

8. Davis, E. H. and I. K. Lee (1969), "One Dimensional Consolidation of Layered Soils," *Proc. Seventh Intern. Conf. on Soil Mech. and Found. Engr.*, Mexico City, Vol. 2, pp. 65-72.

9. Evans, L. C. 1997. Partial differential equations, *vol. 19*.

10. Fox, P. J., and Lee, J. 2008. "Model for consolidation-induced solute transport with nonlinear and non equilibrium sorption." *Int. J. Geomech*., 8(3), 188–198.

11. Francesco, R.D. Exact solution to Terzaghi's consolidation equation.Geo & geo instiute, research & development.

12. Gibson RE, England GL, Hussey MJL. 1967; 17. The theory of one dimensional soil consolidation of saturated clays: I. Finite non linear consolidation of thin homogeneous layers. Geotechnique: 261–73.

13. Holtz, R. D., and Kovacs, W. D. 1981.An introduction to geotechnical engineering, Prentice-Hall, Englewood Cliffs, N.J.

14. Hsu, T.W. and Lu, S-C 2006 "Behaviour of One Dimensional Consolidation under Time- Dependent Loading" *The Journal of Engineering Mechanics*, 132(4), 457 – 462.

15. Kim, H.J. and Mission, J.L., 2011. Numerical analysis of one dimensional consolidation in layered clay using interface boundary relations in terms of infinitesimal strain. ASCE, Int. J. Geomech., 11, 72.

16. Li BH, Xie KH, Ying HW, Zeng GX. 1999; 32 Semi-analytical solution of 1-D non linear considering the initial effective stress distribution. *China Civil Eng J* (6):47–52 [in Chinese].

17. Li BH, Xie KH, Ying HW, Zeng GX. 1999; 21. Semi-analytical solution of one dimensional non-linear consolidation of soft clay under time dependent loading. *Chin J Geotech Eng* (3):288–93 [in Chinese].

18. Lovisa, J. and Sivakugan, N., 2010. Consolidation behaviour of soils subjected to asymmetricinitial excess pore pressure distributions. ASCE, Int. J. Geomech. 10:181-189.

19. Maurice A. Biot, February 1941. "General Theory Of Three-Dimensional Consolidation", *Reprinted from JOURNAL OF APPLIED PHYSICS*, Vol. 12, No. 2, pp. 155-164.

20. Mesri G, Rokhsar A 1974. Theory of consolidation for clays. *ASCE*; 100 (GT8):889–903.

21. Mikasa, M. 1963. "The consolidation of soft clay – A new consolidation theory and its application," *Kajima Institution, Tokyo* (in Japanese).

22. Murthy, V. N. S 2002. Geotechnical engineering Principles and Practices of Soil Mechanics and Foundation Engineering

23. NPTEL, Module 5. Advanced Geotechnical Engineering.

24. Robert, P., 2010. Partial differential equation, Tampare university of technology.

25. Roy, E. 1989. Application of finite difference methods to the solution of consolidation problem.

26. Shackelford, C.D. and Lee, J., 2005. Analyzing diffusion by analogy with consolidation.

27. Singh, S. K. 2008. Identifying consolidation coefficient: Linear excess pore-water pressure. J. Geotech. Geoenviron. Eng., 134(8), 1205–1209.

28. Terzaghi, K. V. and O. K. Frohlich (1936), *Theorie der Setzung von Tonschichten*, Franz Deuticke, Leipzig, 166 pp.

29. Tewatia, S. K. and Bose, P. R. 2003. Discussion on A Study on the Beginning of Secondary Compression of Soils by R. G. Robinson, *Journal of Testing and Evaluation,* ASTM, Vol. 34, No. 5.

30. Trivedi, A. and Sud, V. K. 2004. Collapsible Behavior of Coal Ash, *J. Geotech. Geoenviron. Eng*. ASCE 130. Pp 403-415.

31. Trivedi, A. and Banik, T. and Sukumar, T. et al 2014.Consolidation of Clayey Gouge amid Permeating Rock Mass, *Environmental Geotechnics*, ICE.

32. Tveito, A. and Winther, R. 1998. Introduction to partial differential equations A Computational Approach.

33. Tyn, M. U. And Debnath, L. 2007. Linear partial differential equations for scientists and engineers, *fourth edition*.